NASA CONTRACTOR REPORT

NASA CR-1977

TRANSONIC AND SUPERSONIC TEST OF A MACH 2.65 MIXED-COMPRESSION AXISYMMETRIC INTAKE

by J. L. Koncsek and J. Syberg

Prepared by
THE BOEING COMPANY
Seattle, Wash.
for Ames Research Center

NATIONAL AERONAUTICS AND SPACE ADMINISTRATION • WASHINGTON, D. C. • MARCH 1972

1. Report No.	2. Government Accession No.	3. Recipient's Catalog No.
NASA CR-1977		

4. Title and Subtitle	5. Report Date
Transonic and Supersonic Test of a Mach 2.65 Mixed-Compression Axisymmetric Intake	March 1972
	6. Performing Organization Code

7. Author(s)	8. Performing Organization Report No.
J. L. Koncsek and J. Syberg	10. Work Unit No.

9. Performing Organization Name and Address	11. Contract or Grant No.
The Boeing Company Seattle, Washington	NAS 2-6152
	13. Type of Report and Period Covered
12. Sponsoring Agency Name and Address	Contractor Report
National Aeronautics & Space Administration Washington, D.C. 20546	14. Sponsoring Agency Code

15. Supplementary Notes

16. Abstract

The test results describe isolated intake performance between Mach 0.95 and the cruise Mach number of 2.65 at angles of incidence from +5° to -5°. Maximum total pressure recoveries of over 94% with 10% distortion were recorded at the compressor face in the Mach range from 2.65 to 2.4. Typical cruise operating recovery was 91% with 13% distortion, 7% bleed, 5% corrected flow stability margin, and 2.2° angle-of-incidence tolerance without need for control action. In the started range below Mach 2.4, recoveries were 2% to 4% lower than the recoveries above Mach 2.4, and the distortion increased to approximately 20%. At Mach 0.95 the maximum measured capture flow was 99.4% of the theoretical choked value. The recovery was 97.1% with less than 10% distortion.

17. Key Words (Suggested by Author(s))	18. Distribution Statement
Intakes, Inlets, Propulsion Systems, Supersonic Transport, Boundary Layers, Supersonic, Transonic, Axisymmetric	UNCLASSIFIED-UNLIMITED

19. Security Classif. (of this report)	20. Security Classif. (of this page)	21. No. of Pages	22. Price*
UNCLASSIFIED	UNCLASSIFIED	88	$3.00

*For sale by the National Technical Information Service, Springfield, Virginia 22151

TRANSONIC AND SUPERSONIC TEST OF A MACH 2.65 MIXED-COMPRESSION AXISYMMETRIC INTAKE

By J. L. Koncsek and J. Syberg
The Boeing Company

SUMMARY

An analysis of data obtained during wind tunnel testing of a supersonic intake is presented. Included is an outline of the analytical procedure used in designing the intake, with special attention given to boundary layer control.

Major objectives of the test were to obtain supersonic and transonic intake performance data, to determine the transonic flow capacity of the intake, to verify the analytical procedures used in designing the intake, and to gain a better understanding of intake boundary layer development as influenced by bleed and surface roughness.

The test results describe isolated intake performance between Mach 0.95 and the cruise Mach number of 2.65 at angles of incidence from +5° to -5°. Started performance was tested with 0.05 freestream Mach tolerance. Maximum total pressure recoveries of over 94% with 10% distortion were recorded at the compressor face in the Mach range from 2.65 to 2.4. Typical cruise operating recovery was 91% with 13% distortion, 7% bleed, 5% corrected flow stability margin, and 2.2° angle-of-incidence tolerance without need for control action. In the started range below Mach 2.4, recoveries were 2% to 4% lower than the recoveries above Mach 2.4, and the distortion increased to approximately 20%. The off-design performance losses were associated with the centerbody bleed system.

Based on the information obtained during this test, a new centerbody system can be designed that will improve off-design performance.

The model was tested up to 5° angle of incidence with simulated centerbody control. No major operational problems were encountered at these extreme conditions. Buzz suppression capability (stable unstarted operation) was demonstrated up to the cruise Mach number.

The transonic performance design goal was met. The maximum measured capture flow at Mach 0.95 was 99.4% of the theoretical choked value. The intake must be oversized by 8% at cruise to match the GE4 engine transonically and meet the Boeing SST design recovery goal of 97.1%. This goal is met at a throat Mach number of 0.82, which is safe for engine operation, since the intake can be operated with a throat Mach number of 0.85 without exceeding 10% distortion.

Experimental boundary layer profiles agreed well with theoretical predictions. Bleed flow rates were calculated, prior to the test, using theoretical surface pressures and empirical discharge coefficients. These calculations were confirmed by the data.

INTRODUCTION

The need for efficient propulsion of increasingly faster supersonic airplanes has prompted considerable activity in the development of mixed-compression air intakes during the past decade. Research and development work on the prototype U.S. supersonic transport intake contributed to the advancement of this technology. The program resulted in the design of a variable-cowl axisymmetric intake. As a simplified production alternate, NASA Ames proposed the fixed-cowl intake described in this report. The test article was a 1/3-scale model of this simplified intake. The diffuser contours were developed by the NASA Ames Aerodynamics staff. Other design details, as well as fabrication and testing, were carried out by The Boeing Company.

The purpose of the test was to obtain performance data for a Mach 2.65 mixed-compression intake. The test results were used to substantiate and improve the analytical methods employed in the design of high-speed supersonic intakes.

Testing was conducted at the NASA Ames Research Center's unitary plan wind tunnel facilities under contract NAS2-6152. The 8- by 7-ft tunnel was used for testing in the cruise range of Mach 2.5 to 2.65; the 9- by 7-ft tunnel in the started off-design range, Mach 1.6 to 2.4; and the 11- by 11-ft tunnel in the transonic range, Mach 0.8 to 1.4. Testing started on April 15, 1971 and was completed on May 14, 1971.

The subjects of primary interest were: efficient control of the internal boundary layers, the use of bleed holes to obtain stability against downstream flow transients, and the design requirement for transonic flow matching. In addition, studies were made of other factors influencing performance.

The methods used in predicting boundary layer growth and bleed flow rates, as well as the overall bleed system design procedure, were to be evaluated. Cruise design performance goals of the prototype Boeing SST intake were to be attained. Off-design performance problems were anticipated due to centerbody bleed system constraints. These were primarily caused by the requirements of obtaining stability through an increase in throat bleed, the large centerbody translation resulting from designing for maximum transonic flow capacity with a fixed cowl geometry, and the isentropic cruise supersonic diffuser design. Information was to be obtained for improving the bleed system if performance degradations or operating problems were found.

The test was structured to give an added insight into boundary layer behavior (from boundary layer profile measurements) in a mixed-compression intake, including the dangers of bleed recirculation. Improved criteria for bleed system design can thus be established. The relationship between stability margin and operating recovery was to be identified. The transonic flow capacity of the intake was to be determined to provide improved design information concerning maximum capture capabilities at transonic speeds.

SYMBOLS

A	area
A_L, A_{LIP}	cowl lip area
A_{TH}	intake throat area
CRIT	conditions at critical normal shock position, i.e., immediately before intake unstart
CWE	engine weight flow corrected to standard sea level conditions
d	bleed hole diameter
DIST	distortion, $(P_{TMAX} - P_{TMIN})/P_{TAV}$
ℓ	bleed hole length
M	freestream Mach number
M_{TH}	intake throat Mach number
NDI	General Electric distortion index
N_i	equivalent incompressible boundary layer power law exponent
OP	intake operating point
P, P_S	static pressure
P_P	pitot pressure
P_{PL}	bleed plenum pressure
P_T	total pressure
P_{TAV}	area weighted average total pressure at compressor face
P_{TMAX}	maximum total pressure at compressor face
P_{TMIN}	minimum total pressure at compressor face
P_{TO}	freestream total pressure
P_{TSEC}	average total pressure in secondary air duct

R	intake radius
R_L	cowl lip radius
R_o	compressor face hub radius
STA	normalized intake station
VG	vortex generator
W	weight flow
W_{BL}	intake bleed flow
W_{BT}	total intake bleed flow
W_C	intake capture flow
W_E	engine flow
W_L	theoretical freestream airflow through an area equal to the cowl lip area
W_{SBL}	low-pressure centerbody forward bleed flow
W_{SEC}	secondary airflow
X	intake station(X = 0 at theoretical centerbody tip station with centerbody in cruise position)
Y	distance from surface in boundary layer profile measurements
β	intake yaw angle
ΔX	centerbody forward translation from theoretical cruise position
ΔM	change in freestream Mach number
θ_{BY}	bypass door opening angle

TEST APPARATUS

Model Description

The test model is a mixed-compression intake designed for a cruise Mach number of 2.65. It is an axisymmetric, translating centerbody design with a cowl lip diameter of 19.576 in. (49.723 cm). Both internal and external contours are representative of flight hardware. The model has a remotely operable centerbody, bypass doors, secondary air valves, and engine flow plug valve. Boundary layer bleed hole patterns can be changed by filling or reopening rows of holes drilled on the cowl and centerbody. Bleed exit areas are manually adjustable. Rectangular and triangular vortex generators are available for installation in the subsonic diffuser. The aft section of the subsonic diffuser cowl can be changed (with inserts) to vary the diffuser area distribution just ahead of the bypass gap.

Model size is approximately 1/3 scale of an intake suitable for application on a supersonic transport. Figures 1 and 2 are photographs of the model. A schematic representation of the intake is shown in figure 3.

The available cowl bleed holes are listed in table I. As noted above, some rows of bleed holes were filled during the test. The cowl contains three plenums for collecting the bleed

Table I.—Cowl Bleed Holes

Row	Plenum 1 station X/R_L [a]	Plenum 2 station X/R_L [b]	Plenum 3 station X/R_L [c]
1	3.600	4.000	4.150
2	3.632	4.010	4.160
3	3.664	4.040	4.170
4	3.696	4.050	4.180
5	3.728	4.080	4.190
6	3.760	4.090	4.200
7	3.792	---	4.210
8	3.824	---	4.220
9	3.856	---	4.230
10	3.888	---	4.240
11	3.920	---	4.250
12	---	---	4.260
13	---	---	4.270
14	---	---	4.280
15	---	---	4.290

[a]Hole spacing 1.32°; hole angle to surface 20°

[b]Hole spacing 1°; hole angle to surface 40°

[c]Hole spacing 0.90°; hole angle to surface 90°

Hole diameter, plenums 1, 2, and 3 = 0.0625 in.

Maximum bleed exit throat area/A_L, plenums 1, 2, and 3, = 0.030

flow before it is discharged overboard through calibrated exit louvers. The plenums are isolated from one another, and each plenum is split into quadrants with longitudinal dividers at 0° and 90° to the model pitch axis. The louver exit areas are manually adjustable and are calibrated versus plenum-to-exit pressure ratio allowing measurement of the discharge flow. Due to variations in the cowl skin thickness and the bleed hole slant angle, the holes have varying aspect ratios (i.e., length/diameter). The aspect ratios are 5, 3, and 1.8 for plenums 1, 2, and 3, respectively.

The available centerbody bleed holes are listed in table II. As with the cowl, some rows of holes were filled during the test. The centerbody bleed system is shown schematically in figure 4. Flow from the bleed holes is collected into several plenums separated by bulkheads, as shown. The inner edges of the bulkheads are attached to a sleeve (slider) that rides over the centerbody support tube. Part of the slider is cut away to provide an exit from each plenum. The interior of the support tube is partitioned into longitudinal ducts. Slots are cut in the tube to provide a separate entry into each duct. When the opening in the slider for a given plenum is positioned over one of the support tube slots, flow passes through the bleed holes into the plenum and then exhausts into the support tube. (If the slider opening is not aligned with one of the support tube slots, then the plenum is sealed from the support tube and there is no flow.) Bleed flow from the support tube is channeled through the centerbody support struts into exit plenums. From the exit plenums, the bleed is discharged overboard through louvers. As on the cowl, the louvers are calibrated and the exit areas are manually adjustable. The covers, shown with dashed lines on figure 4, are used to change the centerbody ducting. Two or three plenum systems can be set up as indicated in the table at right center on the figure.

Model Control System

Four model systems are positioned with electrohydraulic servo control valves, namely: centerbody, primary engine flow plug valve, secondary air butterfly valves, and the bypass doors. The compressor face rotating total-pressure rake is positioned by an electrical servo system. All systems are operated closed loop with the position signal as the negative feedback (see fig. 5).

Instrumentation and Data Systems

Compressor face total-pressure recovery is measured with an eight arm, seven-probes-per-arm, rotating rake. Low-blockage boundary layer rakes can be installed at any of four stations on the cowl and four stations on the centerbody. Normally, only two rakes are used at a time on each surface to minimize disturbances to the flow. Each rake has six total-pressure probes. The outer probe is 0.3 in. (7.6 mm) from the surface. Transonic mass flow is measured with two total-pressure rakes located 2.4 in. (6.1 cm) downstream of the cowl lip. Each rake has eight total-pressure probes and a Prandtl static tap at mid-area. These rakes were installed only during capture flow calibration.

The steady-state data are recorded on 378 channels. The sources are model wall static pressure taps, total-pressure rakes, thermocouples, and potentiometers. Pneumatic signals

Table II.—Centerbody Bleed Holes

Bleed region	Row	Station X/R_L	Hole slope, deg	No. of holes per row	Hole diameter, in.
		Forward bleed			
	1	3.700			
	2	3.732			
1	3	3.764	20	213	.0625
	4	3.796			
	5	3.828			
	6	3.860			
	7	3.920			
	8	3.934			
2	9	3.948	40	219	.0625
	10	3.976			
	11	3.990			
	12	4.004			
	13	4.048			
	14	4.062			
3	15	4.076	40	220	.0625
	16	4.112			
	17	4.126			
	18	4.140			
		Throat bleed			
	19	4.200			
1	20	4.216	90	300	.0625
	21	4.232			
	22	4.248			
	23	4.300			
2	24	4.316	90	300	.0625
	25	4.332			
	26	4.348			
	27	4.390			
3	28	4.406	90	296	.0625
	29	4.422			
	30	4.438			
	31	4.490			
4	32	4.506	90	292	.0625
	33	4.522			
	34	4.538			
	35	4.580			
5	36	4.596	90	286	.0625
	37	4.612			
	38	4.628			
	39	4.680			
6	40	4.696	90	282	.0625
	41	4.712			
	42	4.728			
	43	4.770			
7	44	4.786	90	276	.0625
	45	4.802			
	46	4.818			
	47	4.860			
8	48	4.876	90	268	.0625
	49	4.892			
	50	4.908			
	51	4.950			
9	52	4.966	90	262	.0625
	53	4.982			
	54	4.998			
	55	5.040			
10	56	5.056	90	256	.0625
	57	5.072			
	58	5.088			
	59	5.130			
11	60	5.146	90	247	.0625
	61	5.162			
	62	5.178			
	63	5.220			
12	64	5.236	90	237	.0625
	65	5.252			
	66	5.268			
	67	5.310			
13	68	5.326	90	226	.0625
	69	5.342			
	70	5.358			
	71	5.390			
14	72	5.406	90	211	.0625
	73	5.422			
	74	5.438			

are conveyed to scanivalves located within the centerbody and intake diverter. The scanivalves are equipped with pressure transducers. The data acquisition system accepts the analog signals from the pressure transducers, thermocouples, and position sensors for analog-to-digital conversion in the Beckman 210 and storage on punched paper tape. These data are also relayed to the central Honeywell 800 computer for reduction into on-line and off-line outputs. The data system block diagram is shown in figure 5.

Pressure data acquisition and position measurement accuracies were determined to be ±1/2% of the full-scale reading.

THEORETICAL ANALYSIS

Intake Sizing and Mass Flow Characteristics

Supersonic intakes are usually sized to match cruise engine airflow demand with a flow capture ratio of unity (shock on lip). The large transonic flow capacity of current turbojets makes it difficult to satisfy the engine demand near Mach 1 with a translating centerbody intake sized for a high cruise Mach number.

For transonic operation (centerbody extended), the maximum throat area of the model is 58.9% of the lip area. In this configuration, the throat is near the cowl lip, and the flow area is restricted by the maximum diameter of the centerbody. If the centerbody contours were designed with a reduced maximum diameter, then the minimum cowl diameter would also need to be reduced to achieve the area contraction required at the cruise Mach number. This reduced cowl diameter would then form an internal throat when the centerbody is extended. For this reason, 58.9% capture area ratio at Mach 1 is about the highest that can be obtained with a fixed-cowl design. One means of eliminating the second-throat problem is to provide movable cowl surfaces that expand when the centerbody is translated for maximum throat area, as was to be done on the intake for the Boeing SST prototype. This adds complexity to the intake, so the NASA design was generated in an attempt to simplify the intake and provide design guidelines for future high-speed airplanes with regard to engine-cycle/intake-design trades.

During transonic operation, the throat is nearly choked to capture the maximum flow. Supercritical operation should be avoided since an internal normal shock and/or reverse bleed could cause flow separation and excessive distortion at the compressor face. To prevent internal choking resulting from boundary layer growth, the intake is designed for a gradually increasing area profile downstream of the throat (see fig. 6). On a fixed-cowl design, the increasing area profile implies a relatively long centerbody travel, as on the present model, due to diffusion limitations at cruise. The long travel complicates the centerbody bleed system design, as described later. Due to the high external pressure, the bleed holes may be relatively ineffective in this condition, or the bleed flow may even reverse.

Inviscid Analysis

After the intake type and basic performance requirements are defined, the first step in the analytical design procedure is an inviscid analysis of the intake flow fields. Supersonic diffuser contours were developed by the NASA Ames Aerodynamics staff, with the help of a computer program using the supersonic method of characteristics. The subsonic diffuser was designed using potential flow analysis and results of previous subsonic diffuser tests. This design was coupled to the aft cowl assembly, which consisted of a diffuser bellmouth, bypass, and secondary air system simulating the Boeing SST prototype intake.

Supersonic diffusion.—At the cruise design point (Mach 2.65), the centerbody is retracted, and the conical shock is located near the cowl lip, giving a capture flow ratio of 0.9977. The supersonic diffuser is designed to isentropically compress the flow to a Mach number of 1.25 at the throat. The normal shock is positioned slightly aft of the throat providing stability (preventing intake unstart) against minor flow transients. The theoretical cruise static pressure profiles and characteristics net are shown on figure 7. The area contraction required for a Mach 1.25 throat at off-design flight Mach numbers is obtained by translating the centerbody forward. This increases the throat area and, at the same time, reduces the capture flow since the cone shock is located upstream of the cowl lip. In these conditions, the supersonic diffusion is no longer isentropic. Oblique shocks and severe compression gradients can be seen on the samples of static pressure profiles shown on figures 8 and 9. (The flow fields on figs. 7 through 9 were calculated with the MOCHA computer program. MOCHA is a Boeing program. It uses the method of characteristics for calculation of complex two-dimensional or axisymmetric flow fields.) Using similar calculations, the cowl and centerbody surface static pressure contour maps shown on figures 10 and 11 were constructed. These maps were used in the design of the bleed system as discussed under "Boundary Layer Control."

The maximum centerbody travel is 1.55 cowl lip radii. Figure 6 shows duct area profiles at various centerbody positions. During transonic speeds, the intake is operated in the external compression mode with the centerbody fully extended.

Subsonic diffusion.—During mixed-compression operation, the intake normal shock is positioned just downstream of the throat with an approach Mach number slightly over 1.25. The subsonic diffuser has an area distribution providing an approximately linear rate of change of Mach number from the throat to the bypass gap. Rapid area expansion is used in the forward part of the diffuser. This is done to avoid second-throat problems when the centerbody is extended during transonic operation. Prior test experience has shown that this rate of diffusion is acceptable when the throat boundary layers have nearly full velocity profiles. As the centerbody is translated for off-design operation, the throat area increases; this reduces the subsonic diffuser ratio and provides a range of compressor face Mach numbers from about 0.3 at cruise to about 0.5 at a freestream Mach number of 1.0.

Excess capture airflow (bypass flow) and engine cooling airflow (secondary airflow) are removed from the subsonic diffuser through the bypass gap. Previous testing conducted by NASA Ames, on a 1/4-scale model of this intake design, indicated that the pressure recovery of the secondary air during transonic operation was not sufficient to satisfy the cooling air

requirements of an afterburning engine. Should this be the case with the improved 1/3-scale model, a set of alternate aft-cowl contours was designed to provide increased diffusion just ahead of the bypass gap, thereby increasing the potential secondary air recovery (see fig. 6).

Boundary Layer Control

Most performance problems encountered in the operation of supersonic intakes are due to boundary layer separation. Separation in the subsonic diffuser results in reduced total-pressure recovery and increased distortion at the compressor face; separation in the supersonic diffuser causes flow instability and premature intake unstart. An intake cannot be considered optimized unless it has efficient boundary layer control. Bleed holes are used in the supersonic diffuser and throat region and vortex generators in the subsonic diffuser to stabilize the boundary layers in the present intake.

Bleed requirements.—Supersonic diffuser cowl and centerbody boundary layer profiles were calculated with the Boeing compressible boundary layer computer program described in Boeing document D6-23236, "A Computer Program for Finite Difference Calculations of Compressible Turbulent Boundary Layers," by T. A. Reyhner. Inputs for the program include surface Mach number (or static pressure) distributions (figures 10 and 11) and mass flow removal (bleed location and flow rate) specified by the designer. Bleed requirements were determined from the contour maps of the equivalent incompressible boundary layer power law exponents N_j, shown on figures 12 and 13. These maps were developed from the computer calculations. Test experience has shown that when N_j drops below approximately 3, bleed must be provided to prevent flow separation. In addition, boundary layer control is used to "arrive" in the throat with N_j close to 7 to tolerate the strong pressure gradient from the normal shock.

The theoretical predictions are refined as follows. The boundary layer program is rerun incorporating bleed flow at likely locations to prevent N_j from becoming less than 3. A new set of exponents is thus generated. Concurrently, the MOCHA program is also rerun to determine the effects of mass flow removal on the surface Mach number distribution. This process is iterated until good boundary layer characteristics are obtained throughout the diffuser. Only the first iteration of the bleed system design procedure was completed for the present intake.

Bleed system design.—Boundary layer bleed in a supersonic intake is very costly in terms of drag. Since some of the flow is bled from the intake, more flow must be captured than required by the engine. Bleed is removed at relatively low recovery, and drag is incurred when this flow is discharged overboard, which is a significant detriment to the overall performance of the intake.

Cowl bleed system: The cowl boundary layer is bled over three regions (see "Model Description"). The regions are identified, for convenience, by pressure level (low-pressure forward, high-pressure forward, and throat). These locations were determined from the static pressure and power law exponent plots, figures 10 and 12. The forward bleed was designed to provide adequate boundary layer control throughout the started regime. The throat bleed performs the added function of stabilizing the normal shock during engine flow transients.

The bleed hole slant angles (i.e., the included angle between the hole centerline and the local surface) selected for the intake represent a compromise between two conflicting requirements. First, to minimize bleed drag, the bleed plenum should be operated at the highest pressure possible. This requirement calls for holes with the minimum slant angles practicable because bleed hole pressure recovery improves with decreasing angle. Second, to obtain adequate stability margin against engine airflow fluctuations, with minimum recovery penalty, the increase in bleed flow rate should be maximized as the normal shock moves toward critical position. This requirement calls for 90° bleed holes because such holes provide the highest change of flow rate with local Mach number.

Based on the above, 20° holes were selected for the first forward plenum, 40° holes for the second forward plenum, and normal holes for the throat plenum.

The first plenum divider separates the low- and high-pressure forward bleeds. By adjusting the exit areas, each plenum is pressurized to the maximum level compatible with local surface conditions at the cruise point. As a result, cruise bleed drag is minimized without danger of region-to-region recirculation.

The second plenum divider separates the high-pressure forward bleed and the throat bleed. If the normal shock moves to critical position, the throat plenum pressure increases by a factor of about two. The divider prevents this pressure rise from influencing (decreasing) the forward bleed.

Each plenum is split into quadrants by longitudinal dividers at 0° and 90° to the intake pitch axis. These dividers prevent crossflow within the plenums when the intake is operated at angle of incidence.

Centerbody bleed system: Boundary layer control on the centerbody is conceptually similar to that on the cowl, but, due to the motion of the centerbody, this bleed system is mechanically more complex. The centerbody moves through a range of 1.55 lip radii. It is translated with Mach number and with angle of incidence. Referenced to the centerbody, the locations where bleed is required shift with these parameters. Bleed locations for cruise and off-design Mach numbers were determined from figures 11 and 13, and a traveling bleed system was designed to provide bleed in these regions.

During cruise, the bleed hole slant angle arrangement is the same as on the cowl, see table II. Note on figure 4, that the option is available to mix or separate the low- and high-pressure forward bleeds. When the forward bleeds are mixed, the system has two centertube plenums (forward and throat bleed); when they are separated, a three-plenum system is obtained (low-pressure forward, high-pressure forward, and throat). With either type of centertube plenum arrangement, the third forward bleed plenum can be active or inactive. The plenum is made inactive by installing an insert in the forward centertube slot, as shown in figure 4. The insert can be used to reduce cruise bleed while maintaining forward bleed through this plenum up to $\Delta X/R_L = 0.6$, as required, when the centerbody is translated for off-design operation. The centertube plenum options provide flexibility in the optimization of off-design bleed.

When the centerbody is translated beyond $\Delta X/R_L = 1.1$, the first and second forward plenums communicate through a common volume forward of the centertube passage cover, figure 4. Thus, a potential path for bleed recirculation exists. The possibility of recirculation increases beyond $\Delta X/R_L = 1.2$ when the throat plenums begin to bleed into the same volume. For the two-plenum system, the centertube passage cover is installed, sealing this volume from the bleed exit, see figure 4. For the three-plenum system, the passage is open allowing some flow to be discharged overboard. Different recirculation characteristics can be expected with the two- and three-plenum systems. The support tube configuration required for the three-plenum system, combined with the necessity of locating forward bleed in the strong positive-pressure gradients at off-design Mach numbers, did not allow a bleed system design without the potential recirculation problems described above.

As shown in Table II, the centerbody throat bleed holes are normal to the surface. This is done to obtain maximum stability from the bleed increase as the normal shock moves from the operating point toward critical. At off-design Mach numbers, the throat plenums move in front of the throat and into the forward bleed slot region on the support tube. Forward centerbody bleed is thus removed through the 90° holes in the throat plenums. The flow coefficient for 90° holes is a strong function of local Mach number. If the bleed holes are sized to provide minimum bleed when acting as throat bleed holes in the throat Mach number environment, then only a small amount of bleed can be removed through the same holes when they are located in the supersonic diffuser in a Mach number environment of, say, 1.5 to 1.8. At the same time, the centerbody vortex generators are translated into the supersonic diffuser, further aggravating the situation. Therefore, off-design performance problems were anticipated.

The total impact of the individual weaknesses of the bleed system on the intake performance was not known. A major objective of the test was to explore the problems with the system as described and to obtain experimental data to aid in future refinements of the bleed system, if required.

TEST RESULTS

Intake Performance

Started mode.—Critical started intake performance with 0.05 freestream Mach tolerance is summarized on figure 14. Data are shown for three configurations. The difference among the three is in the centertube slot arrangement for the forward bleed. The bleed schedules for these configurations are shown on figures 15 through 17. Configuration 18 is a two-plenum system, i.e., the low-pressure and high-pressure forward bleeds are mixed in one set of centertube ducting separated from the throat bleed ducts. Configurations 20 and 26 are three-plenum systems. Here the low-pressure and high-pressure forward bleeds are isolated from one another as well as from the throat bleed. The difference in bleed schedule between configurations 20 and 26 results from an insert in the forward bleed slot used with configuration 26. The support tube changes involved in setting up these systems are shown on figure 4.

Peak (critical) recoveries of over 94% with distortion at or below 0.10, were recorded the Mach range from 2.4 to 2.65. Below Mach 2.4, the critical recoveries are about 2% to % less and distortion increases to approximately 20%. The causes of this performance loss e insufficient forward centerbody bleed, bleed recirculation, and poor bleed distribution lative to the centerbody vortex generators. The problem is discussed in detail under "Data nalysis."

Critical centerbody positions (i.e., positions just prior to unstart) are shown as funcons of Mach number and yaw angle in figure 18. Also shown are the theoretical positions or the zero-yaw case. Predicted centerbody translation is achieved at all Mach numbers xcept 1.8. The translation determines the supersonic diffuser area contraction; therefore, iroat blockage due to boundary layer buildup was correctly predicted, except for the case oted. The excess throat blockage near Mach 1.8 is due to bleed recirculation. A well-ehaved supersonic diffuser for a mixed-compression, axisymmetric intake is usually charac-rized by a linear change in critical centerbody position with flow angle of incidence. In ddition, the translation required to maintain started operation for a given flow angle hange should decrease with Mach number. The test data shown in figure 18 indicate that iese conditons are satisfied except at 5° yaw angle in the Mach range of 2.2 to 2.4.

Simulated controlled intake performance up to 5° yaw angle (design limit) is shown in gure 19. The distortion increases with yaw angle but stays below 25%, except at Mach 2.65 nd 5°. The data shown were obtained by increasing the corrected engine flow until stable tarted operation was achieved. This simulation is not completely valid because, under flight onditions, the corrected engine flow would remain constant at the zero-yaw value and the ypass doors would be opened to stabilize the normal shock. In the test, the engine face lach numbers were unrealistically high at the larger yaw angles (e.g., 0.55 rather than 0.30 t Mach 2.65, 5°). At high angles of incidence, very little flow passes through the engine face n the windward side. As a result, the total pressure is only slightly higher than the static ressure in this region. It follows then that the distortion increases with engine face Mach umber. With the proper simulation, the excessive distortion at 5° yaw and Mach 2.65, night not have been present. Theoretical calculations (assuming no change in peak recovery n leeward side and in average recovery) indicate that the distortion would be approxinately 27% rather than the 43% shown in figure 19. The data taken at this condition, using he bypass doors for normal shock control, were lost in the computer.

External compression mode.—Below Mach 1.6, the intake is operated in the unstarted external compression) mode. In this mode, the centerbody is fully extended ($\Delta X/R_L$ = .55) to maximize the throat area (i.e., the capture capacity), as required, for engine lemand matching. The geometric throat area is 58.9% of the lip area and is located 0.12 lip adius downstream of the cowl lip station. Testing was conducted in the transonic wind unnel from Mach 0.7 to 1.4. The intake throat could not be choked below Mach 0.9 due to ack of flow capacity in the plug valve. Between Mach 1 and 1.2 the model presented excesive tunnel blockage (i.e. the tunnel normal shock was riding over the cowl, thus influencing he bleed exits). Therefore, test results are shown only for Mach 0.95 and 1.4. An intake izing study to match the prototype GE4 engine airflow demand schedule at these Mach umbers is summarized in figure 20. Transonic intake performance and excess cruise airflow re shown as functions of intake lip area. The intake must be oversized by 8% at cruise to ring transonic performance up to the Boeing SST design goals. Maximum measured capture

flow at Mach 0.95 was 99.4% of the theoretical choked value. Intake operation with up to 0.85 throat Mach number was possible without exceeding 10% total-pressure distortion, as shown under "Data Analysis."

Data Analysis

Cruise.—Cruise intake performance is presented in figure 21 for configurations 18, 20, and 22. Configurations 18 and 20 are described under "Intake Performance." Configuration 22 is identical to configuration 20 with the exception that, on the former, the bleed holes over centerbody throat plenum 2 are closed. The bleed schedule for configuration 22 is shown on figure 22.

The operating point of the intake is defined by a ±5% stability margin at 0.05 Mach tolerance, i.e., the intake must remain started, without control action, if a 5% step decrease in engine corrected flow or a 0.05 decrease in freestream Mach number occurs. (Note that the intake has inherent stability against sudden increases in corrected engine flow or freestream Mach number since both of these conditions tend to drive the normal shock downstream in the subsonic diffuser, thereby reducing the likelihood of intake unstart.) Significant performance parameters at the cruise operating point are listed in table III for the three configurations noted.

Table III. Cruise Performance

Configuration	Critical point			Operating point				
	Recovery, $\frac{P_{TAV}}{P_{TO}}$	Distortion, $\frac{P_{TMAX}-P_{TMIN}}{P_{TAV}}$	Total bleed, $\frac{WBT}{WL}$	Recovery, $\frac{P_{TAV}}{P_{TO}}$	Distortion, $\frac{P_{TMAX}-P_{TMIN}}{P_{TAV}}$	Total bleed, $\frac{WBT}{WL}$	Yaw tolerance, deg	Corrected engine flow, lb/sec
18	0.937	0.093	0.081	0.905	0.143	0.064	2.0	365
22	0.941	0.074	0.089	0.910	0.131	0.071	2.20	365
20	0.943	0.070	0.094	0.913	0.124	0.077	2.15	361

The important conclusion to be drawn from this table is that the system that is superior in terms of critical performance is not necessarily superior at the operating point. If configuration 18 is used as the baseline, then, to gain 0.5% operating recovery, the operating bleed is increased by 0.7% (configuration 22). An additional 0.3% recovery costs another 0.6% bleed (configuration 20). Since, typically, airplane range loss due to a 1% increase in operating bleed is offset by approximately 2% increase in operating recovery, the higher recoveries of configurations 20 and 22 are more than offset by the higher bleed. However, in the final bleed selection, the better yaw tolerances of configurations 20 and 22 may be a determining factor, even though the range factor for configuration 18 is the best. Also, the performance penalty resulting from the higher compressor face distortion for configuration 18 must be established for the particular engine to be used with the intake.

These data were obtained without cowl vortex generators. Analysis, under "Vortex generator evaluation" below, indicates that this allows slightly higher critical recovery;

however, at the operating point, the intake performance improved (i.e., recovery increased and distortion decreased) when generators were used on the cowl.

Boundary layer bleed versus intake recovery is shown in figure 23. Forward bleed remains constant up to the critical point, at the levels tabulated in figure 23, indicating no influence from the normal shock. Cowl throat bleed rise begins at 90% recovery for all three systems. Centerbody throat bleed pressure rise also begins at 90% recovery for configuration 22; but, for the other two systems, the centerbody throat plenums are already partially pressurized at a recovery of 88%. The cause of this difference is illustrated on the throat static pressure profiles, figures 24 through 26. Note that the bleed holes over centerbody throat plenum 2 are open on configurations 18 and 20 but are closed on configuration 22. The normal shock is already forward of plenum 2 at 88% recovery but does not reach plenum 1 until 90% recovery. Closing plenum 2 allows the normal shock to move into the geometric throat before the centerbody throat bleed rise begins. Also, due to the decreased bleed area, configuration 22 has less centerbody throat bleed than the other systems. It is concluded that the centerbody throat bleed should be moved forward to delay the throat bleed rise and thereby reduce the operating bleed while maintaining stability.

For centerbody translations ($\Delta X/R_L$) from zero to 0.06, the bleed is shut off in centerbody forward bleed plenum 3 on configuration 18 (see fig. 15). This bleed deficiency causes flow separation on the centerbody from approximately 1% supercritical to critical normal shock positions, as illustrated by the static pressure profiles of figure 24. Clean normal shocks, indicating attached flow, are seen all the way to the critical point in figures 25 and 26 where forward plenum 3 is bleeding. The effects of the separation can be seen on the compressor face profiles (figure 27). For configuration 18, the innermost total-pressure probe reaches a maximum of 0.916 P_{TO} at an average recovery of 0.902 and drops to 0.900 P_{TO} at the critical point. At the same time, the core flow shifts toward the cowl. This effect is less pronounced for configurations 20 and 22 where no centerbody flow separation is present in the throat.

Another point of interest on the throat static profiles, figures 24 through 26, is the change in normal shock pressure gradient on the cowl just prior to unstart, indicating boundary layer separation. This apparent separation feeds forward to the last row of the cowl forward bleed.

Experimental supersonic diffuser static pressure profiles at Mach 2.65 are compared with theoretical predictions in figures 28 and 29. Experimental bleed hole locations are indicated by hash marks along the boundaries of the characteristics nets. The decrease in surface pressure over the bleed regions is considered to be localized near the bleed holes without influencing the core flow. The experimental profiles show good agreement with theory up to station 4.0. Further downstream, the experimental gradients are strongly influenced by the throat bleed and therefore deviate from the predicted pressure profiles.

Boundary layer profiles: Experimental boundary layer pitot pressure profiles are compared with theoretical predictions in figure 30. For the theoretical calculations (see "Boundary Layer Control"), the normal shock was assumed to be far downstream of the throat (the geometric throat is at station 4.22 during cruise). Good agreement is seen between theory and experiment for this case. As the normal shock moves into the throat

(increasing recovery), the throat boundary layer profiles tend toward separation. The cowl throat boundary layer remains attached up to the critical point. On the centerbody, a small separation appears just downstream of the throat at 87% recovery. As the recovery is further increased, the normal shock influence feeds forward to station 4.15, and the throat boundary layer is reattached. The cowl separation indicated by the throat static pressure gradients does not appear on the boundary layer profiles measured downstream of the throat bleed. The flow is evidently reattached as a result of the throat bleed.

Prediction of bleed rates: The intake bleed rates for various bleed patterns were predicted prior to the test from empirical bleed hole flow characteristics for 20°, 40°, and 90° holes. These predictions make it possible to adjust the exit area for any hole pattern such that the bleed holes are pressurized close to the unchoking point, thereby maximizing the exit plenum pressure. Comparisons of the predicted and experimental bleed flow rates for the forward cowl and centerbody bleed plenums are shown in figures 31 and 32. Excellent agreement is obtained for the 40° bleed holes, while it appears that the 20° bleed hole coefficients are slightly below predictions.

Figure 33 shows the predicted and experimental cowl throat bleed rates for high supercritical (normal shock downstream of bleed holes) and critical operation. The predictions were based on local average Mach numbers of 1.25 and 0.80 across the bleed holes at supercritical and critical operation, respectively. The experimental surface static pressures indicate that the average Mach numbers for both conditions are slightly higher than predicted. The fact that the experimental bleed flow rates also are slightly lower than predicted indicates that the bleed hole characteristics used in the predictions for the 90° throat bleed holes are fairly accurate.

Vortex generator evaluation: Optimization of subsonic diffuser performance included an evaluation of the effects of various vortex generator installations. The results of this study are summarized in table IV. Performance parameters are listed at the operating point for each configuration. Figure 34 shows compressor face recovery as a function of normal shock position for the various generator configurations. With the small cowl vortex generators, the critical recovery is 0.5% higher than with the large generators. Operating recovery is also 0.5% higher. No changes in distortion or bleed are observed, figure 35. With the small generators, the normal shock is further downstream for a given recovery, indicating cleaner flow in the subsonic diffuser.

When the cowl vortex generators are removed, the critical recovery and normal shock position are slightly improved. However, at supercritical operation, the throat bleed increase occurs at a lower recovery (see fig. 35). This is also illustrated in figure 34, which shows that the recovery for the same normal shock position is lower without cowl vortex generators. Consequently, the operating point (i.e., 5% stability margin) for this configuration has lower recovery and more bleed than the configuration with vortex generators installed. The distortion is also significantly higher, as seen on figure 35.

Moving the centerbody generators forward increases the cruise operating recovery by 0.4%. No significant change occurs in critical recovery or normal shock position. The difference in supercritical bleed, figure 35, is due to a small difference in centerbody position for the two configurations.

Table IV.—Vortex Generator Evaluation

	Configuration	Station, X/R_L	Size, in.		Number of vortex generator pairs	Spacing, a/b	Recovery, P_{TAV}/P_{TO}	Distortion, $\frac{P_{TMAX} - P_{TMIN}}{P_{TAV}}$	Distortion index, NDI	Total bleed, W_{BT}/W_L
			h	ℓ						
Cowl vortex generators	9	4.64	0.3	0.6	32	2/1	0.907	0.087	0.075	0.056
	10	4.64	0.5	1.0	24	5/3	0.902	0.086	0.074	0.055
	15	4.64	0.5	1.0	24	5/3	0.906	0.089	0.101	0.059
	16	—	—	—	None	— —	0.900	0.142	0.143	0.066
Centerbody vortex generators	10	4.77	0.5	1.0	12	2.3/1	0.902	0.086	0.074	0.055
	15	4.62	0.5	1.0	12	2.3/1	0.906	0.089	0.101	0.059

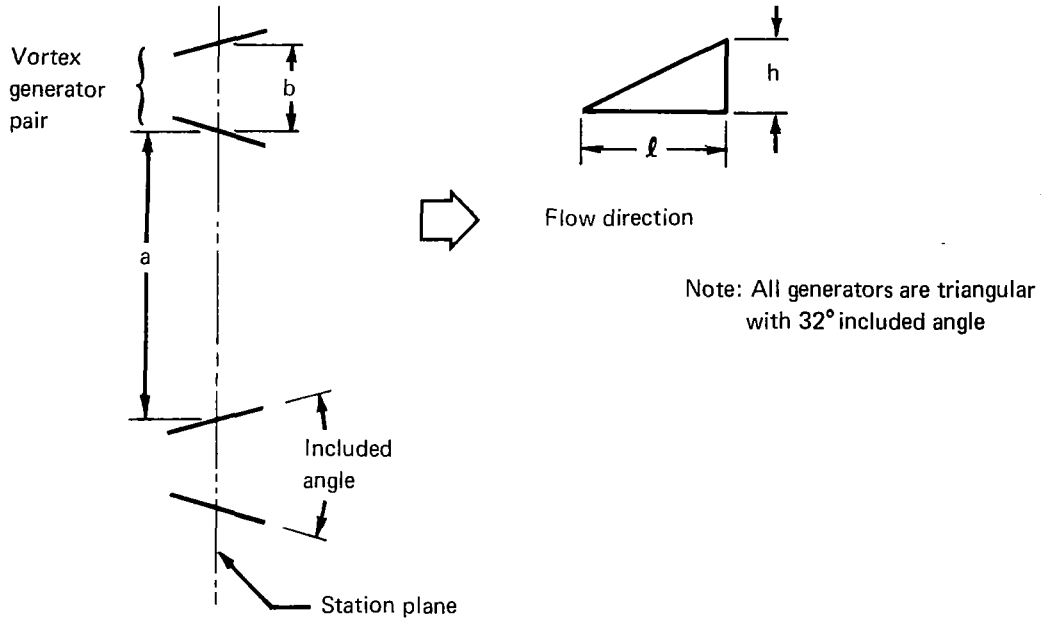

Note: All generators are triangular with 32° included angle

Compressor face profiles corresponding to the conditions discussed above are shown on figures 36 through 38. Figure 37 indicates that the cowl generators maintain good recovery near the cowl to a higher supercritical margin, but this occurs basically at the expense of recovery near the centerbody. This effect is greater with the large cowl generators, figure 36. The centerbody boundary layer becomes increasingly weaker as the normal shock approaches the throat, causing a pressure deficiency near the hub at the engine face. Placing the centerbody vortex generators further forward reduces the radial distortion, as shown in figure 38.

Diffuser insert evaluation: As noted under "Model Description," inserts are available to alter the subsonic diffuser cowl contours between station $X/R_L = 5.8$ and the bypass gap ($X/R_L = 6.32$). This provision is made to increase the secondary air pressure recovery if this recovery is found to be too low during transonic operation. Figure 39 shows the "cruise" and "transonic" insert lines. The transonic insert provides more diffusion and, therefore, higher secondary air recovery potential. Should a need for the extra diffusion be demonstrated during transonic operation, the cruise performance associated with this diffuser must be evaluated if it is to be a permanent contour. If there is an unacceptable penalty, then a variable (trim door) surface should be provided at the aft of the subsonic diffuser cowl. This surface would be in the "cruise" position during normal started operation and in the "transonic" position during operation at transonic speeds or with high bypass flow rates.

A comparison of intake cruise performance with the two inserts at various bypass door opening angles is shown on figure 40. From 0.5% to 2% total pressure recovery is lost at the engine face with the transonic insert. Distortion also increases, although not with the bypass doors closed. Figure 41 shows the corresponding engine face total-pressure profiles near the operating points. As expected, the loss occurs near the cowl. This implies that the flow on the cowl separates due to the higher rate of diffusion. Similar losses occur when the diffuser inserts are completely removed (data not presented). The performance penalty with the transonic diffuser is less at off-design Mach numbers. At Mach 2.4, no loss was observed (data not presented). Performance below Mach 2.4 is not good enough to conclusively establish the losses resulting from the increased diffuser ratio.

Started–off-design.–Operating performance for the two basic centerbody bleed configurations is shown in figure 42. (The operating point is defined at an engine-corrected flow of 5% above the critical value.) The two systems shown have identical bleed hole patterns on both cowl and centerbody. Configuration 18 is a two-plenum system and configuration 26 is a three-plenum system. The corresponding bleed schedules are shown in figures 15 and 17, respectively. Performance, as a function of corrected engine flow, is shown for the individual Mach numbers in figures 43 and 44. A severe performance degradation is indicated at Mach numbers below 2.4. This performance penalty is associated with the centerbody bleed system. Recirculation in the forward bleed region is a problem at large centerbody translations, and the throat plenums, now acting as forward bleed plenums, do not provide good bleed distribution relative to the vortex generators. Since the 90° holes are sized to operate in the throat region, they do not provide enough bleed in the high Mach number environment of the forward bleed region. These problems are discussed further below.

The surface static pressures and the bleed plenum pressures (figures 45 and 46) indicate recirculation through centerbody forward plenum 1 at Mach 1.8. Recirculation is possible

because, at centerbody translations greater than $\Delta X/R_L = 1.2$, the first and second forward plenums and the first throat plenum communicate through a common volume. This volume is located in front of the centertube passage cover (see fig. 4) and is isolated from the bleed exits (cover installed) for configuration 18, while, for configuration 26 (cover removed), 0.0005 W_L bleed flow is discharged through the low-pressure forward bleed duct. The bleed flow rate with the three-plenum system is small, but its effect is significant because otherwise this flow would recirculate. The recirculating flow is bled from the surface slightly downstream of the predicted location of the first centerbody shock reflection and is reinjected just ahead of the shock reflection. The mass injection distorts and, possibly, separates the boundary layer approaching the shock. The cowl lip shock imposed on this boundary layer produces a separation bubble as indicated in figures 45 and 46 by the gradual pressure rise on the centerbody at station $X/R_L = 2.7$ and the lack of a reflected shock on the cowl at station $X/R_L = 3.25$. The three-plenum system has a smaller separation (i.e., steeper pressure gradient at centerbody station $X/R_L = 2.7$), as expected.

The bleed configurations are the same for the two systems downstream of the separation. This bleed is aft of the vortex generators, which have been translated far into the supersonic diffuser, see figures 45 and 46. The boundary layer approaching the generators is thick and highly distorted, if not separated. The interaction between the three-dimensional shock system from the vortex generators and the boundary layer probably further distorts the profile. The downstream bleed is quite limited and is not likely to provide significant profile improvement. The adverse pressure gradient from the normal shock could readily force separation all the way forward of the vortex generators. This would not allow positioning of the normal shock for high recovery. The higher recovery of the three-plenum system (see fig. 42) is probably due to the better boundary layer profile ahead of the vortex generators, which allows a greater normal shock gradient without massive separation (leading to unstart) with this system.

The recirculation problem is eliminated as the centerbody is retracted for higher Mach number operation. At Mach 2.2, the possibility of recirculation no longer exists, but the vortex generators are still positioned in the supersonic diffuser, see figures 47 and 48. The three-plenum system has a potential advantage over the two-plenum system since the former has forward plenum 1 open (compare figs. 17 and 15). However, at Mach 2.2, this plenum is ahead of the first centerbody shock (see fig. 48), and the surface pressure across the bleed holes is lower than freestream static pressure. Consequently, no bleed is removed from the plenum, so the advantage noted above is not realized. The two-plenum system has bleed at the vortex generator station (fig. 47) while the three-plenum system does not (fig. 48). Therefore, the two-plenum (configuration 18) system has more forward bleed (0.0135 W_L) than the three-plenum (configuration 26) system (0.0122 W_L). As a result of this higher forward bleed, the two-plenum system has a higher operating recovery at Mach 2.2, as shown in figure 42. Both systems show higher than predicted compression downstream of the first centerbody shock (figs. 47 and 48), indicating excessive boundary layer growth. Bleed needed to improve the boundary layer at this location is not available with either system.

As the Mach number is increased further, the vortex generators move aft, and both systems provide bleed forward of the generators as well as near them. At Mach 2.3, the slanted holes are active for the three-plenum configuration, and, while both systems show

improved recovery (fig. 42), the improvement is greater with the three-plenum system. At Mach 2.4, the vortex generators are positioned in the geometric throat. The supercritical surface pressures closely folllow theoretical pressures, as shown in figure 49. The critical recovery is high—near 94%. The three-plenum system with bleed from forward plenum 1 has a higher recovery (see fig. 42). As the Mach number increases above 2.4, performance remains at a high level up to the cruise point, as shown in figure 43.

Figure 50 illustrates the performance problem at the low Mach numbers. The critical normal shock position based on the surface static pressures is shown versus freestream Mach number. Above Mach 2.4, the normal shock is located slightly ahead of the geometric throat and the vortex generators are downstream of the throat. At Mach 2.4, the generators are positioned in the throat and the critical shock moves further upstream in the intake. Below Mach 2.4, the normal shock, as indicated by the cowl static pressures, seems to break into a multiple shock system, probably as a result of the centerbody boundary layer separation described above. The normal shock pressure rise on the centerbody tends to follow the vortex generators as the Mach number is decreased from 2.4.

Buzz suppression.—Normally, the intake is operated in the mixed-compression mode above Mach 1.6. If a control failure makes this mode unavailable, then unstarted operation must be maintained. For structural reasons, it is necessary to operate without buzz. This can be done with proper position of the centerbody and bypass doors, called the buzz-suppression mode. At the higher Mach numbers, the unstarted intake recovery is significantly lower than the started recovery because of the total-pressure loss through the external normal shock. Compressor face total-pressure distortion must be kept low enough to avoid engine stall. (Note that thrust is reduced because of the low recovery.) In the buzz-suppression mode, the centerbody should preferably be extended fully because natural forces tend to drive it to this position. Then, even if centerbody actuation power is lost, the intake could be operated without buzz.

External compression performance data for engine corrected airflow at climb power setting and normal shock positioned at the threshold of buzz (by means of the bypass doors) are shown in figure 51. Test results are presented for two centerbody positions ($\Delta X/R_L$ = 1.55 and 1.25) with two configurations, 18 and 22, which are two- and three-plenum systems, respectively (see "Started—off-design"). As shown in figure 51, the recovery is higher and distortion significantly lower when the centerbody is retracted to $\Delta X/R_L$ = 1.25 from the fully extended position ($\Delta X/R_L$ = 1.55). At $\Delta X/R_L$ = 1.25, the distortion is lower with the three-plenum system, probably as a result of the less severe recirculation problem of the forward centerbody bleed, see "Started—off-design." These data indicate that a buzz-suppression mode with fixed centerbody position is feasible with the existing bleed system but that some improvements can be expected if the centerbody bleed recirculation problem is eliminated.

Transonic operation.—Intake capture flow was measured with two lip rakes located at station X/R_L = 2.565. Figure 52 shows the capture calibration of configuration 26 at Mach 0.95. The capture flow is plotted versus cowl static pressure PC601 located at station X/R_L = 2.415, (i.e., 1.5 in. (3.81 cm) upstream of the rake and 0.3 in. (0.76 cm) upstream of the throat). This pressure tap is, therefore, not influenced by the rake for choked or nearly choked conditions. The intake recovery obtained after removal of the lip rakes is also

plotted in figure 52. The capture flow for data recorded without the lip rakes can be obtained by means of this calibration curve as indicated.

The above procedure was used to develop the performance curves shown in figure 53. Intake recovery, distortion, ND_I, and bleed are plotted versus capture flow at Mach 0.95 for the cruise subsonic diffuser configuration. Compressor face rake profiles for throat Mach numbers between 0.77 and 0.90 are shown in figure 54. The flow is fully attached to the surfaces at all throat Mach numbers.

An important objective of the test was to determine the transonic flow capacity of the intake. The maximum measured capture flow ratio W_C/W_L at Mach 0.95 was 0.584, or 99.4% of the theoretical choked value (see fig. 52). Compressor face distortion of 10% is considered acceptable for steady-state engine operation. This limit is reached at a one-dimensional theoretical throat Mach number of slightly over 0.85 in figure 53. Recovery at this point is 0.968, the bleed rate is approximately 0.01 W_L or 0.018 W_E.

It is concluded that, in transonic sizing studies, the intake can be safely designed for 0.85 throat Mach number if a gradually increasing diffuser area profile is provided downstream of the throat.

Diffuser insert and secondary air evaluation: The effect of the transonic diffuser insert on compressor face and secondary air recovery was evaluated at Mach 0.95. Approximately 1.7% of the lip flow (0.017 W_L or 0.03 W_E) was removed through the secondary air system. Figure 55 shows that the compressor face recovery is approximately 0.6% lower at a throat Mach number of 0.85 with the transonic diffuser insert. Schematics of the cruise and the transonic diffuser inserts are shown in figure 56. The theoretical static pressure at the trailing edge of the diffuser for a throat Mach number of 0.85 is 0.796 for the cruise insert and 0.862 for the transonic insert, with an assumed recovery of 0.970 at the trailing edge. As shown in figure 56, the increase in secondary air recovery with the transonic diffuser insert exceeds the increase in theoretical static pressure at the trailing edge of the diffuser due to additional ram recovery obtained with this configuration.

At Mach 0.95, the secondary air recovery obtained with the cruise insert just matches the maximum afterburning requirement of the GE4 engine. The transonic insert is not needed down to Mach 0.9. As the freestream Mach number decreases, the recovery requirement increases. It was not possible to determine whether matching can be obtained at lower Mach numbers with the cruise diffuser because of the flow plug valve problems (see "External compression mode").

The effect of secondary air on intake performance was evaluated at Mach 0.95 with the cruise diffuser insert. Figure 57 shows that the intake recovery increases by 0.5% when the secondary air flow rate is 0.016 W_L. This increase in recovery is caused by removal of the boundary layer on the cowl wall as illustrated in figure 58, which shows compressor face rake profiles with and without secondary air.

Figure 59 indicates that the secondary air flow improves intake performance only when the primary engine airflow is lower than 0.55 W_L.

Intake performance–Mach 1.40: Intake recovery, distortion, and bleed, versus capture flow are shown in figure 60 for a freestream Mach number of 1.40. The normal shock is inside the cowl lip at the highest capture flow but is external (spilling) for all other points. The intake bleed increases with decreasing capture flow due to the increasing duct pressures. Bleed flow rate is 0.05 W_L at the threshold of buzz.

Figure 61 shows compressor face profiles at Mach 1.40. The recovery is low near the centerbody, but the flow appears to be fully attached for all data points. The low recovery near the centerbody is caused by a boundary layer separation on the centerbody near the cowl lip. Figure 62 shows total-pressure profiles measured with the lip rake in a different run. Separation is clearly indicated in the entire capture flow range from normal shock on lip to buzz threshold. The separation is associated with the normal shock and is probably aggravated by recirculation through the forward centerbody bleed holes, as indicated on figure 63. This figure shows centerbody static pressure profiles and bleed and plenum pressure for the capture flows and recoveries shown in figures 60 and 62. The bleed plenum pressure is considerably higher than the surface static pressure across the bleed holes in forward plenums 1 and 2 for the lowest recovery shown. As the normal shock moves forward, this pressure differential decreases and, at buzz threshold, all bleed holes are probably bleeding. It appears that the centerbody forward and throat bleed holes leading into the low-pressure duct in the support tube have an adverse effect on intake performance when the normal shock is close to the lip but improve the performance when the shock is near the buzz threshold. The magnitude of these effects is not known, but, based on the overall performance, it is probably acceptable at this freestream Mach number.

NASA Ames intake/GE4 engine matching: The transonic engine airflow demand, in terms of capture area, for the prototype GE4 engine is shown in figure 64. This airflow demand is based on the prototype design intake recovery also shown. To meet the recovery goal of 0.971 at Mach 0.95, the intake must operate with a throat Mach number of 0.82 (see figure 53) or a capture flow area of $0.571A_L$. At this point, the bleed rate is $0.013A_L$ and the engine flow is $0.558A_L$. Since the engine demand capture area is 13.35 sq ft (1.240 m^2) the lip area must be 23.92 sq ft (2.222 m^2). Using this lip area, the engine demand and the recovery curve (figure 60), the intake recovery for matched engine flow at Mach 1.40 is found to be only slightly lower than the design goal (figure 64). The GE4 engine airflow demand at cruise (including minimum secondary air) is 20.25 sq ft (1.881 m^2), with an assumed operating recovery of 91%. For a lip area of 23.92 sq ft (2.222 m^2), the engine demand is 84.7% of the lip flow. Therefore, with 7% bleed at cruise, the intake is supplying 8.3% excess air that must be bypassed through the secondary air system and/or the bypass doors. The excess cruise airflow can be reduced by reducing the intake lip size, but this would result in lower recovery and higher distortion in the transonic range (see fig. 20).*

*If efficient trim (reduced compressor rpm) can be incorporated in the engine control system the transonic engine airflow demand can be met with less excess cruise airflow. Feasibility of transonic engine rpm trim depends on airplane flight placard and engine cycle. On the GE4 afterburning engine, transonic trim could only be used on standard atmospheric day flights. On a cold day this engine was already operating at the minimum rpm limit, dictated by afterburner requirements.

CONCLUDING REMARKS

Good cruise performance was obtained, indicating the soundness of the bleed system at the design point. Operating recovery must be set approximately 3% below the critical value to obtain stability against a 5% step decrease in corrected engine flow.

Cruise operating performance can be improved by locating the centerbody throat bleed farther forward. This will delay the centerbody throat bleed rise as the normal shock moves toward the operating point and, therefore, reduce the bleed at the operating point.

Intake performance was good down to Mach 2.4. Started performance deteriorated below this Mach number, as anticipated. The normal centerbody throat bleed holes, required to obtain maximum stability margin through an increase in bleed flow rate, did not provide sufficient forward bleed at these conditions. At the lower Mach numbers (e.g., Mach 1.8), bleed recirculation between some of the front centerbody plenums further degraded the intake performance.

The test results verified the procedures used for predicting boundary layer growth and bleed flow rates. Near-optimum bleed configurations and plenum exit areas can be predicted thereby reducing testing time significantly.

Transonic flow capacity of the intake was determined. The maximum measured capture flow at Mach 0.95 was 99.4% of the theoretical choked value. Operation with up to 0.85 throat Mach number was possible without exceeding 10% distortion. The intake must be oversized by 8% at cruise to match the GE4 engine with the transonic recovery goal of the prototype Boeing SST intake.

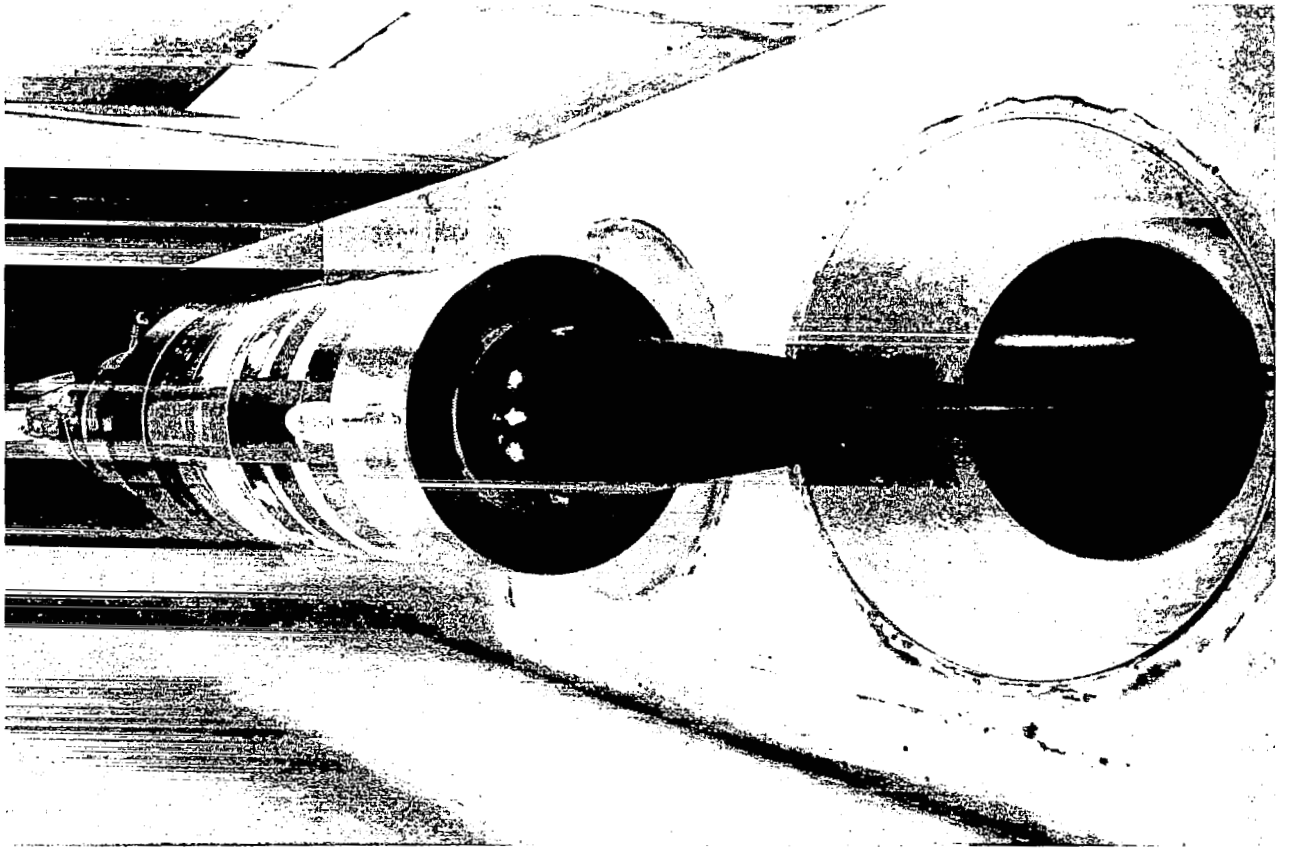

Figure 1.—1/3 Scale NASA Ames Intake Model Installed in 9- by 7-Ft Tunnel

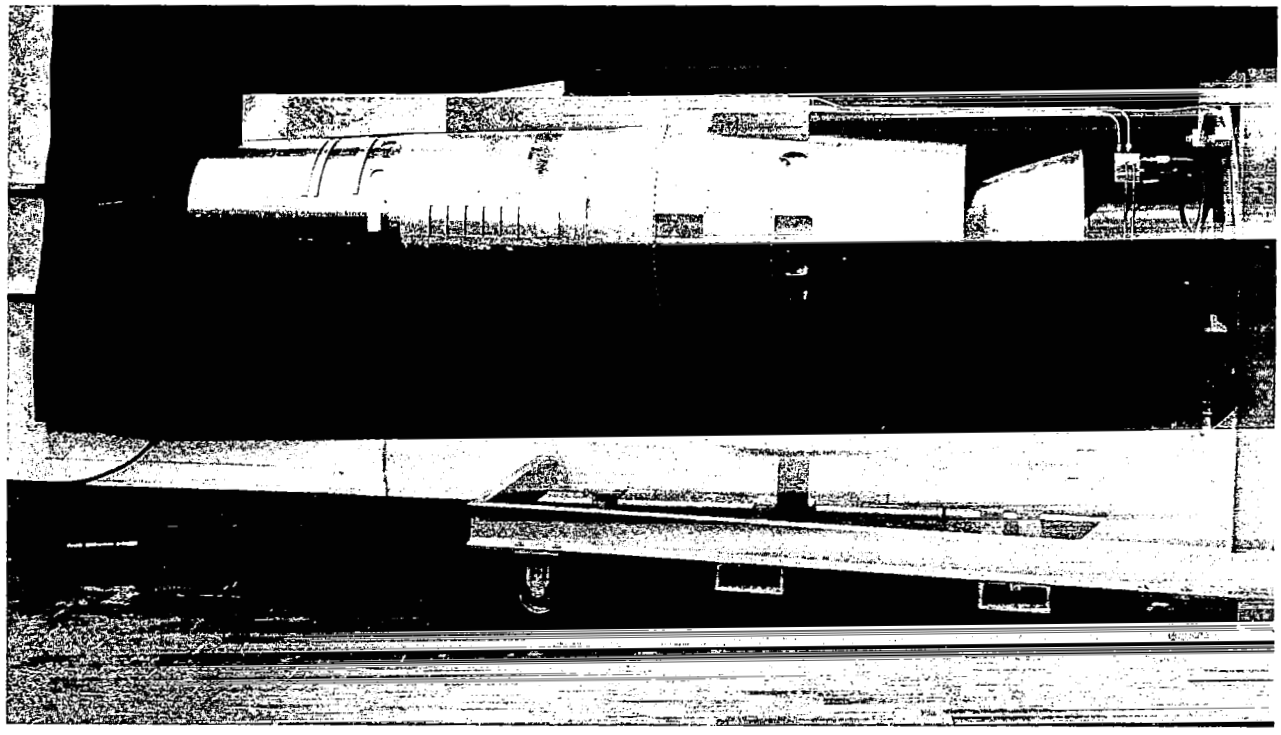

a) Centerbody Retracted

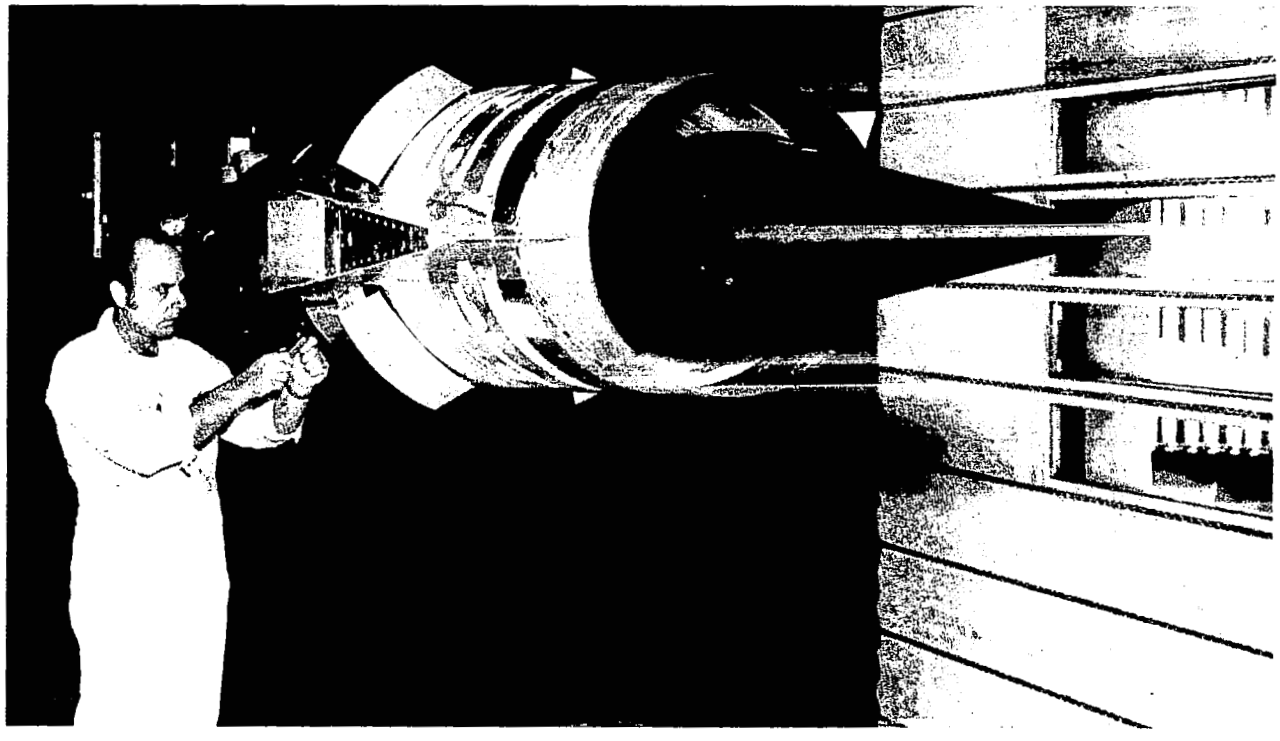

b) Centerbody Extended, Bypass Doors Open

Figure 2.—1/3-Scale NASA Ames Intake Model

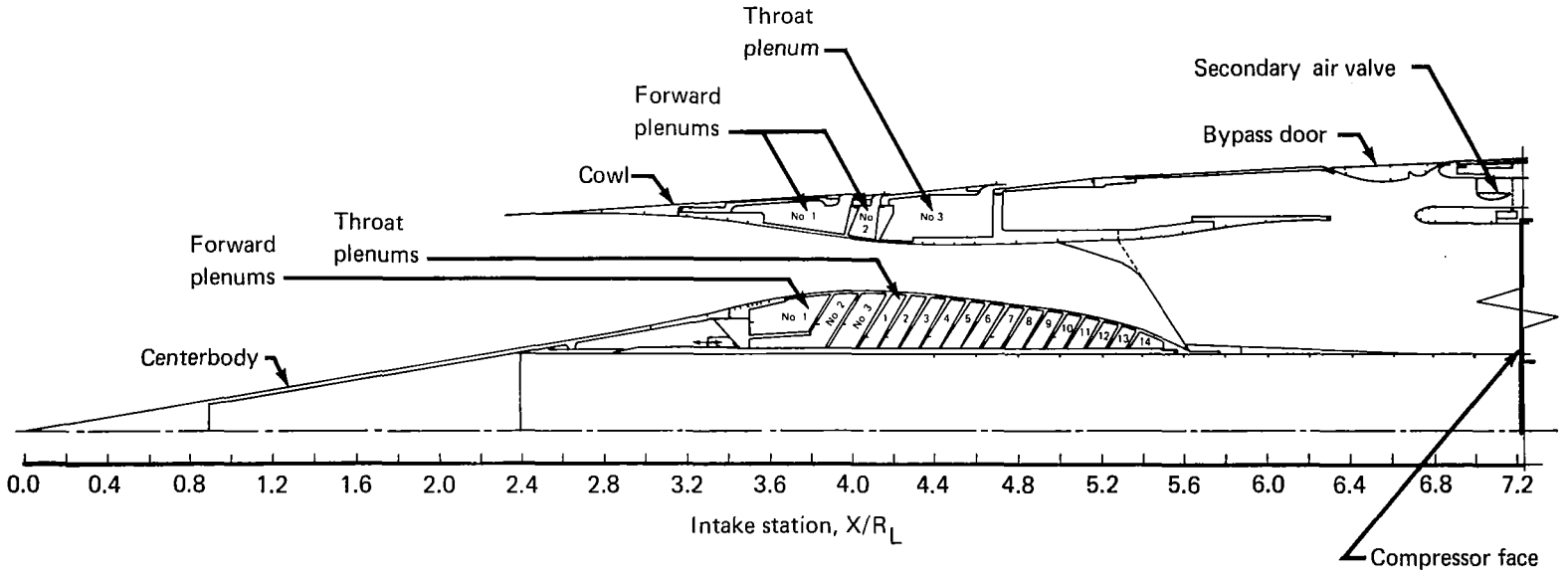

Figure 3.—Intake Schematic

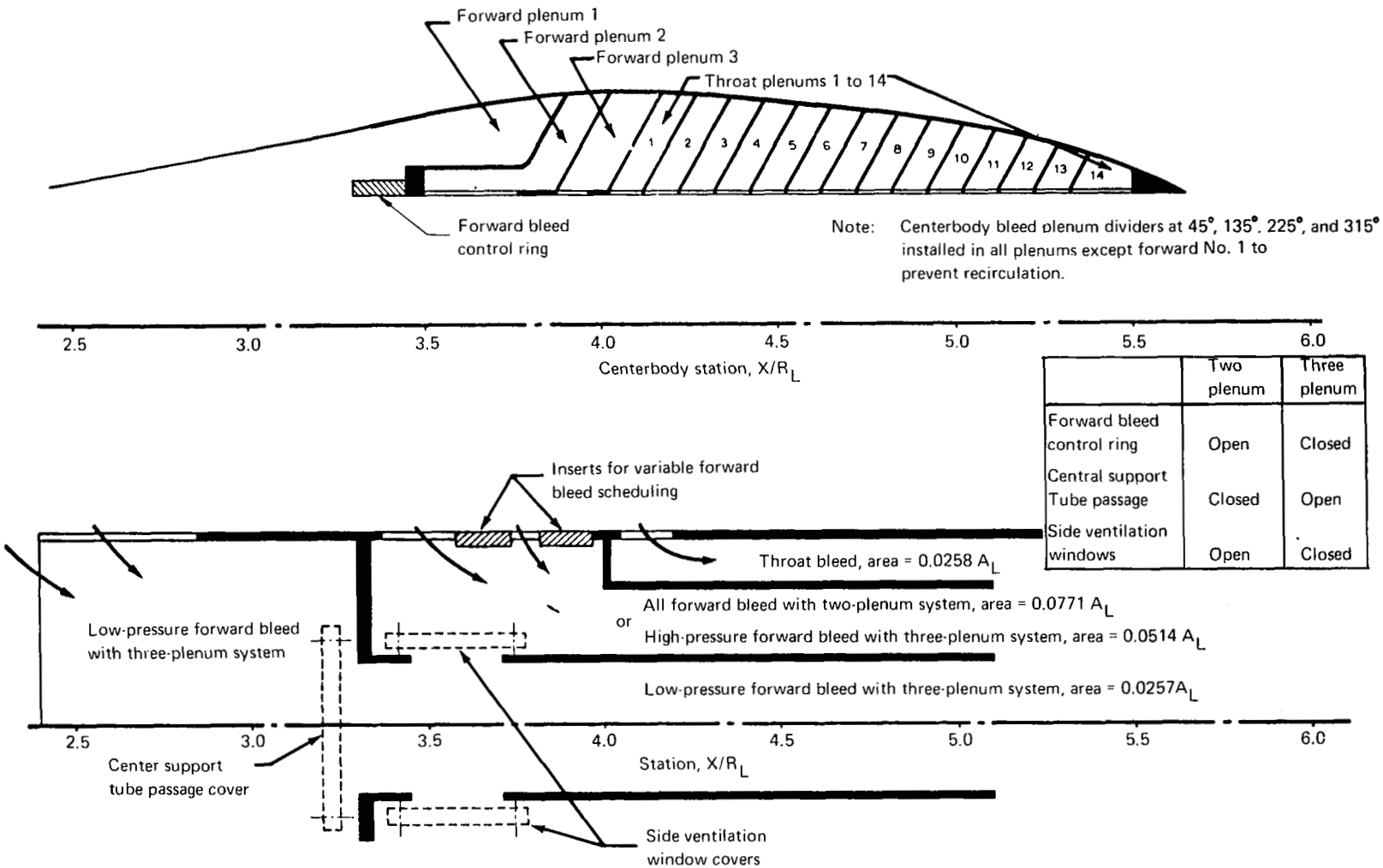

Figure 4.—Centerbody Bleed System

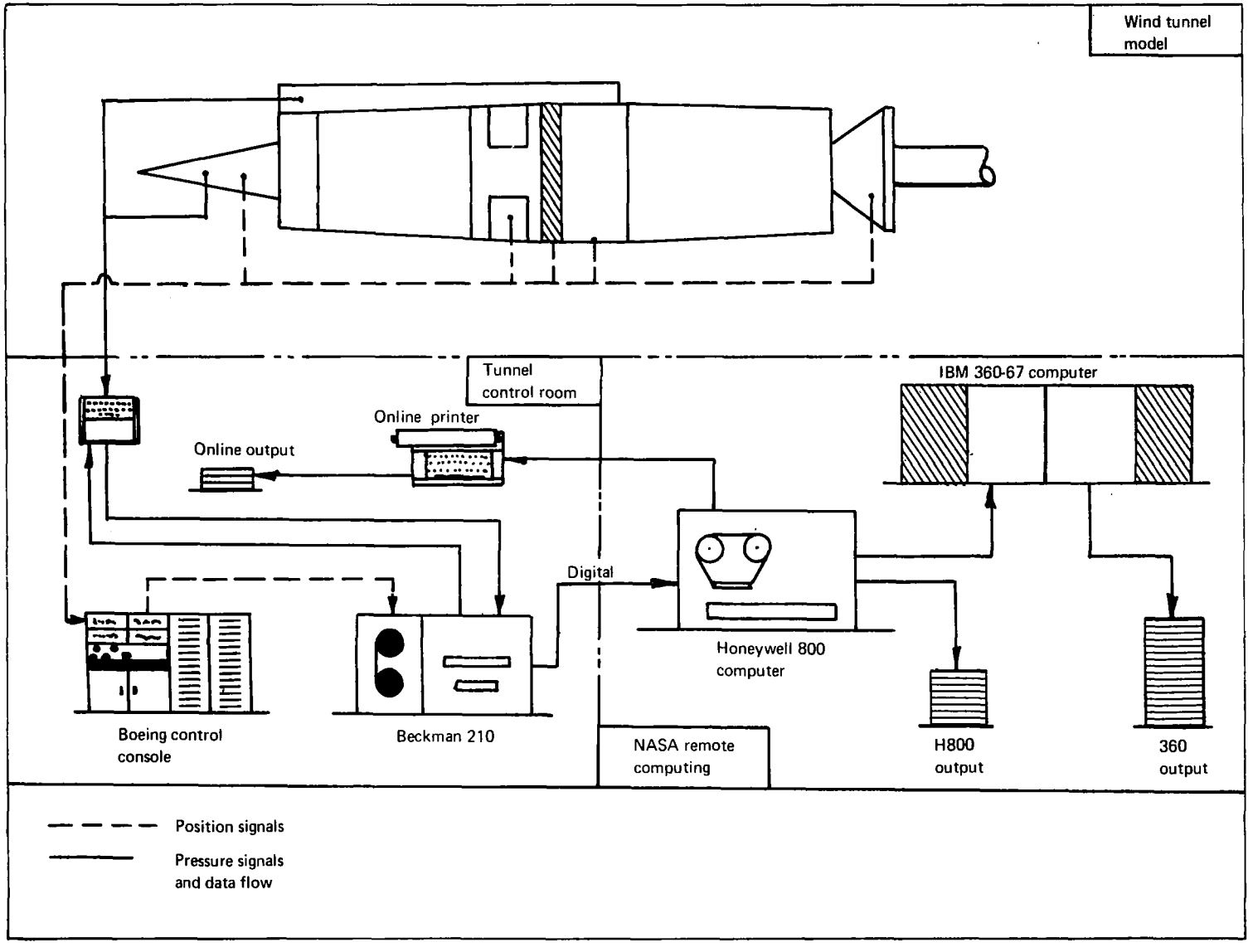

Figure 5.—Data System Block Diagram

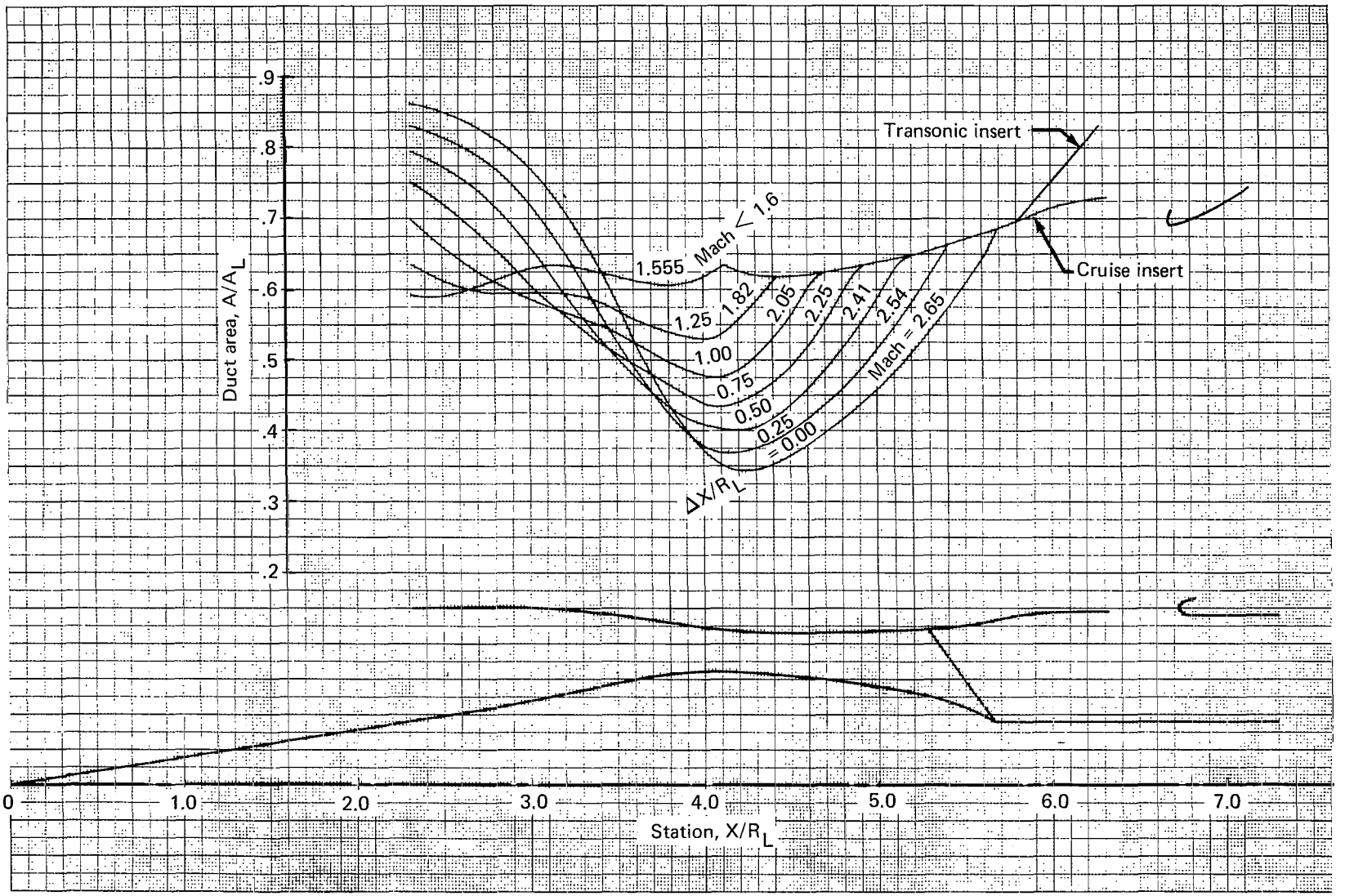

Figure 6.—Intake Area Profiles

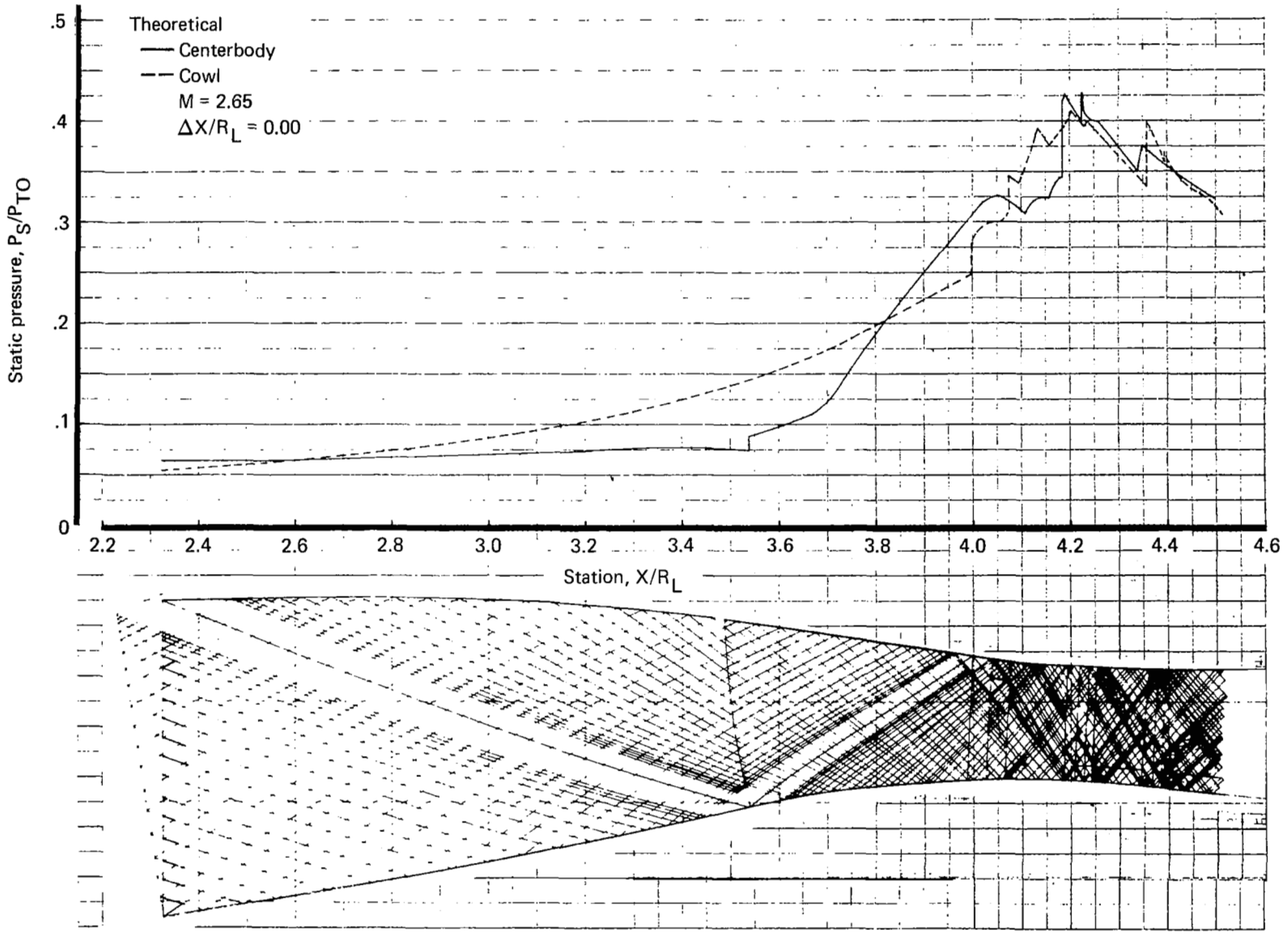

Figure 7.—Supersonic Diffuser Profile—Mach 2.65

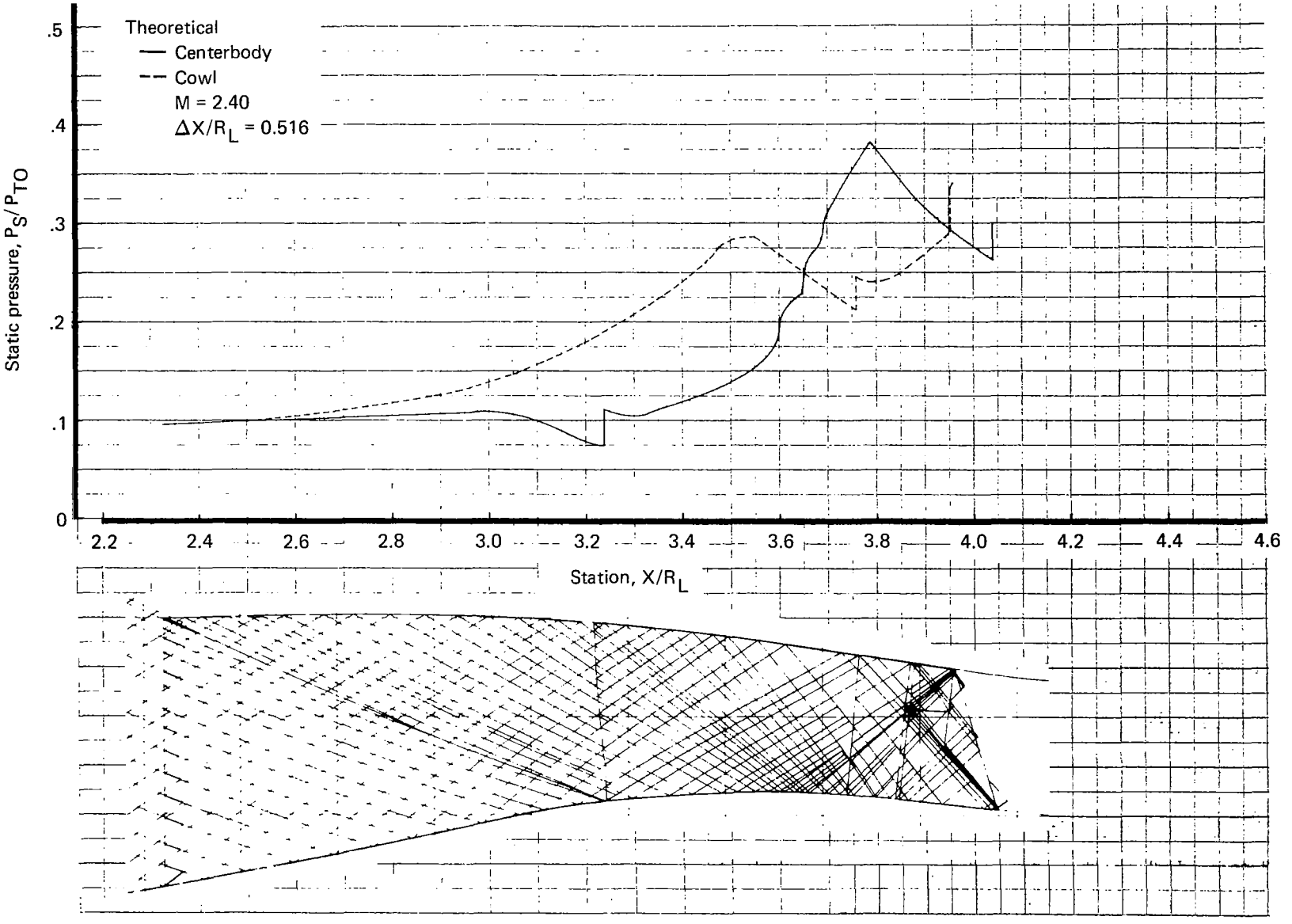

Figure 8.—Supersonic Diffuser Profile—Mach 2.40

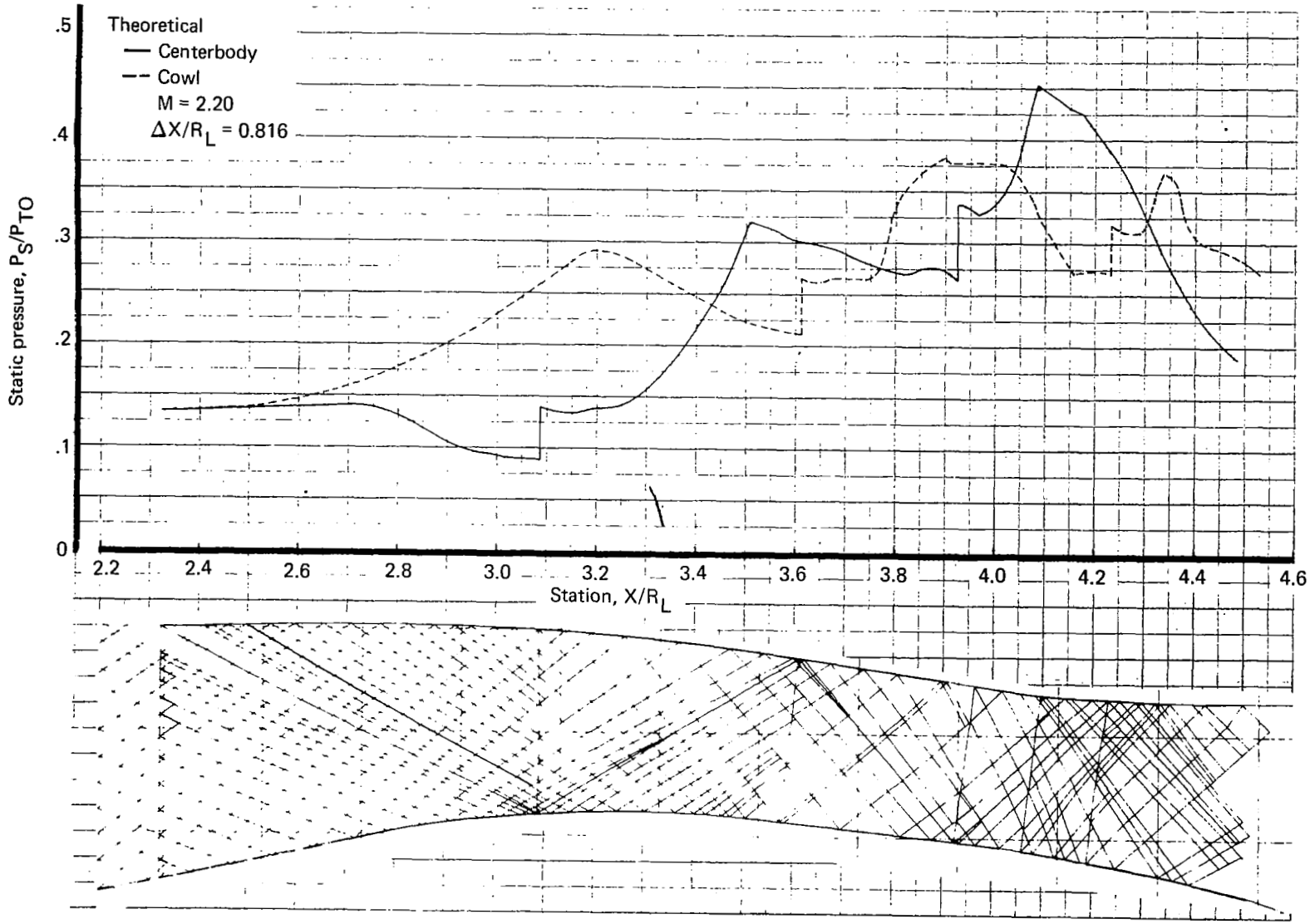

Figure 9.—Supersonic Diffuser Profile—Mach 2.20

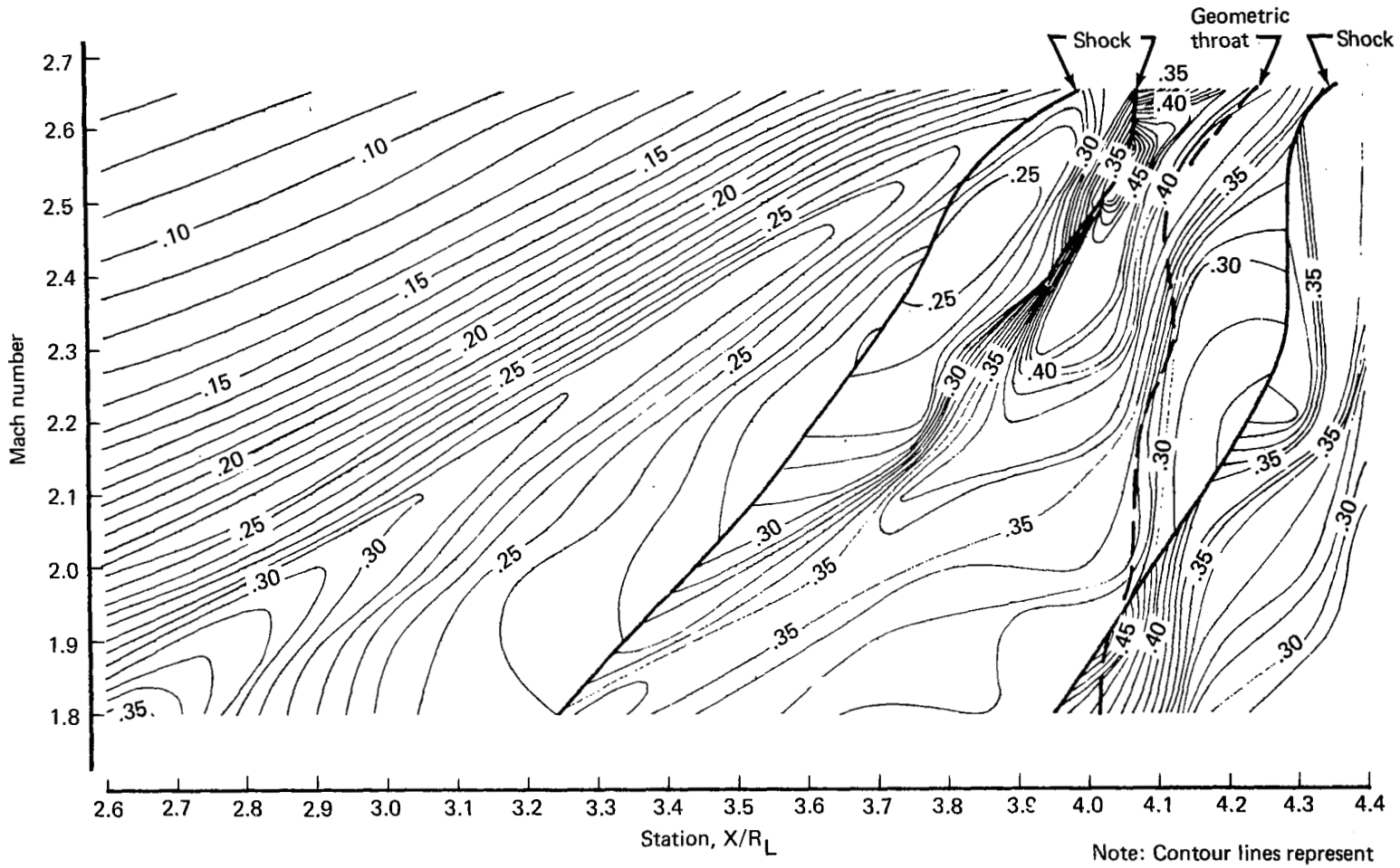

Figure 10.—Cowl Surface Static Pressures—Mach 1.80 to 2.65

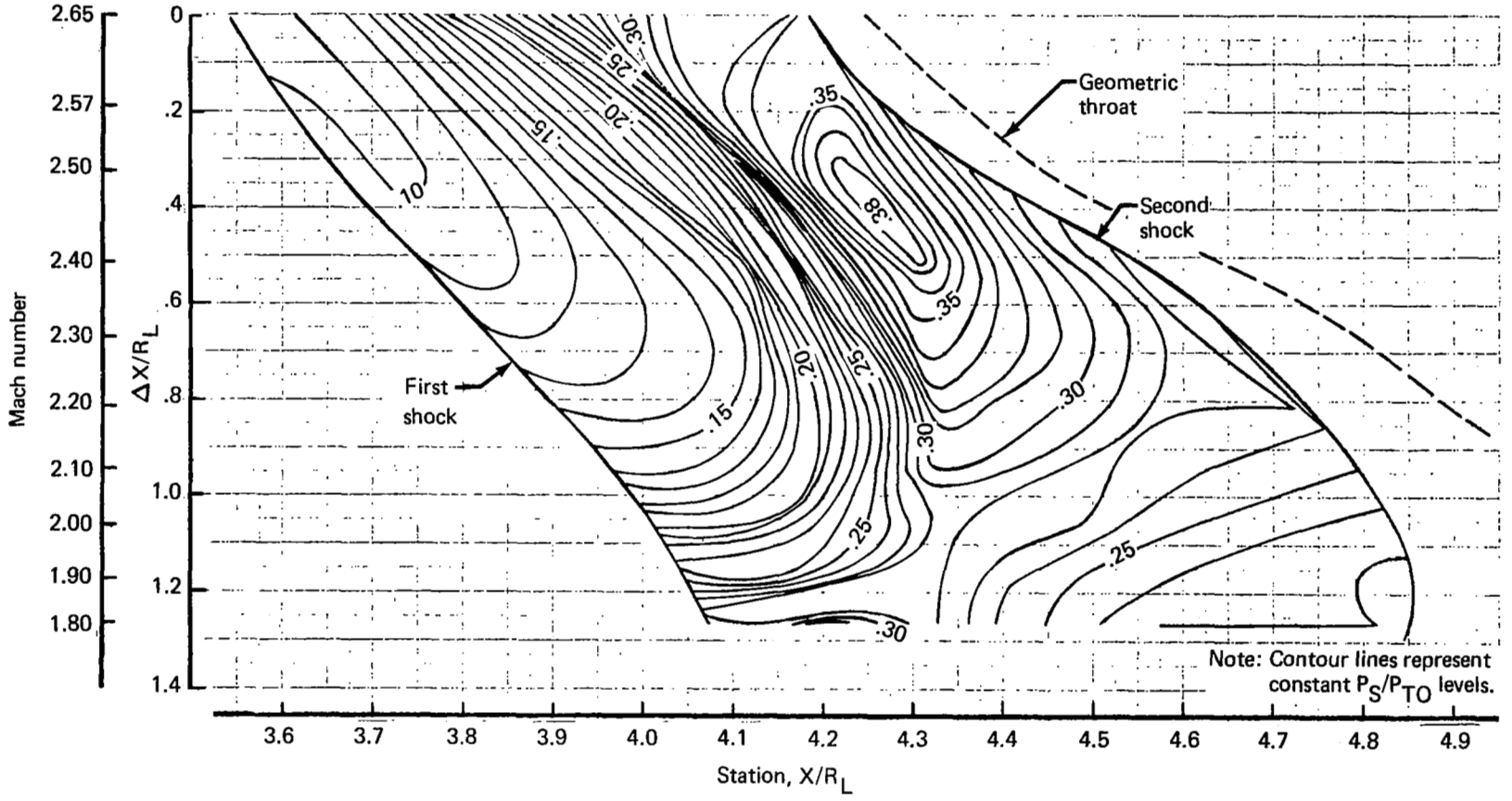

Figure 11.—Centerbody Surface Static Pressures—Mach 1.80 to 2.65

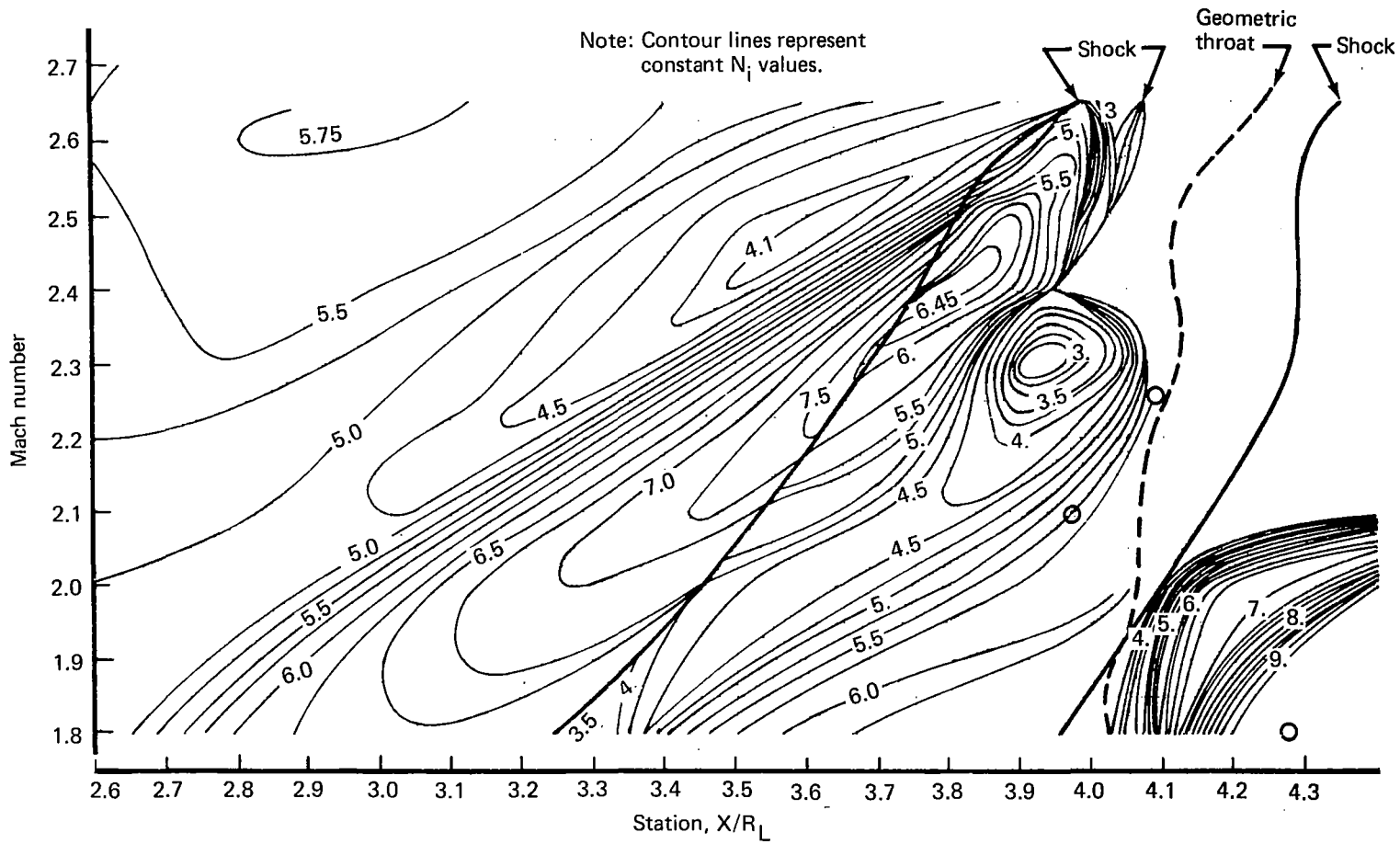

Figure 12.—Cowl Boundary Layer Power Law Exponent N_i—Mach 1.80 to 2.65

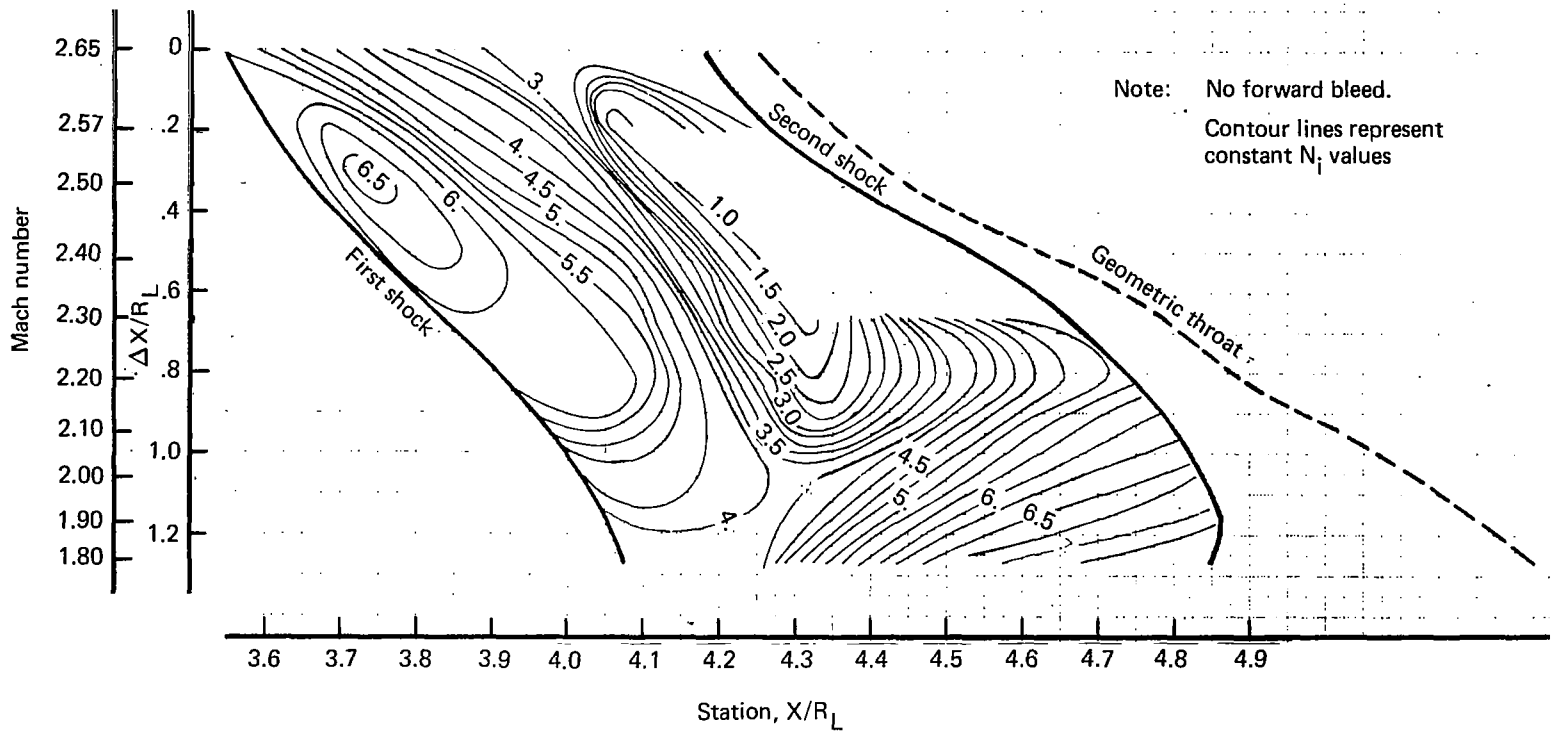

Figure 13.—Centerbody Boundary Layer Power Law Exponent N_i—Mach 1.80 to 2.65

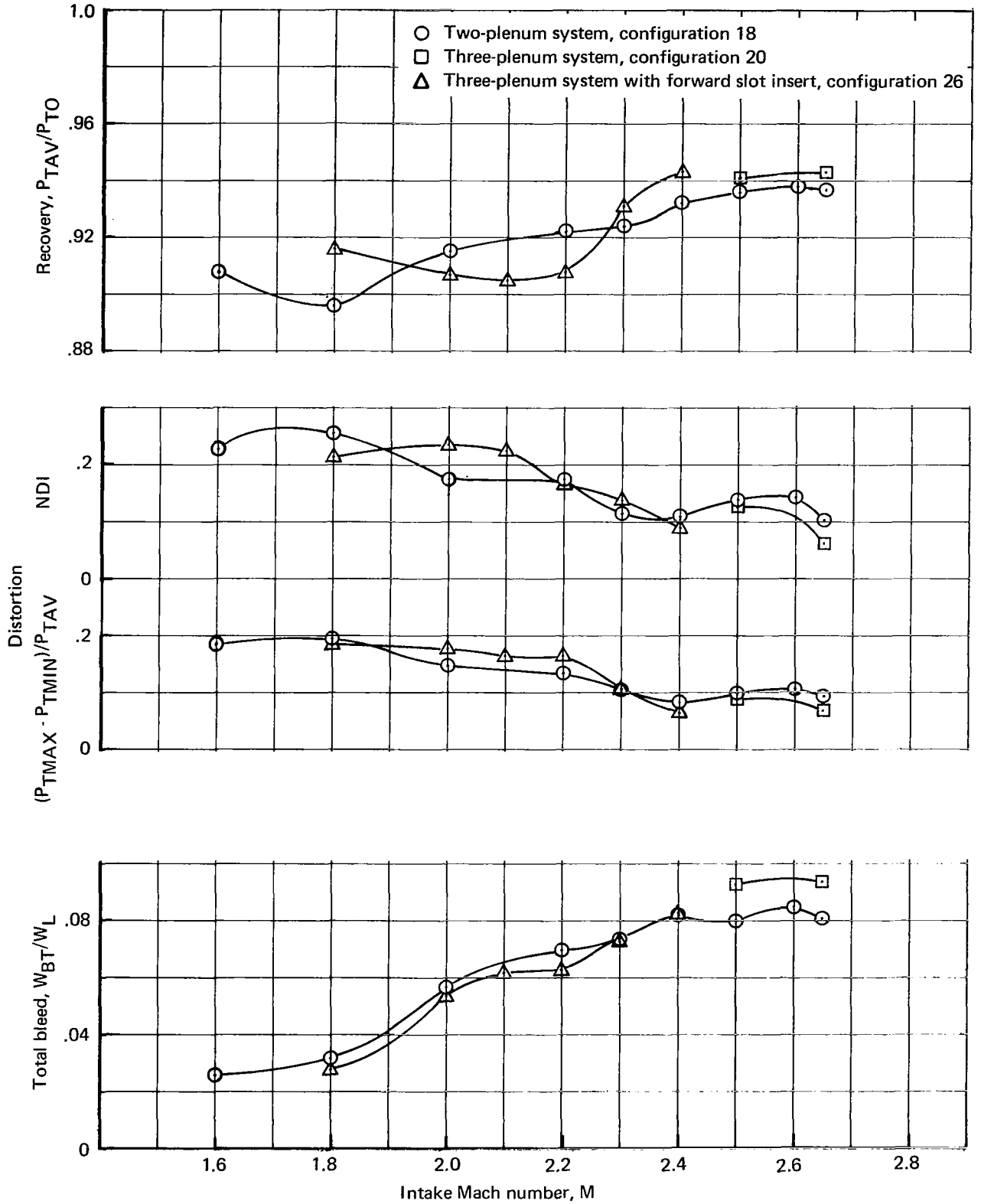

Figure 14.—Critical Started Intake Performance With 0.05 Mach Tolerance

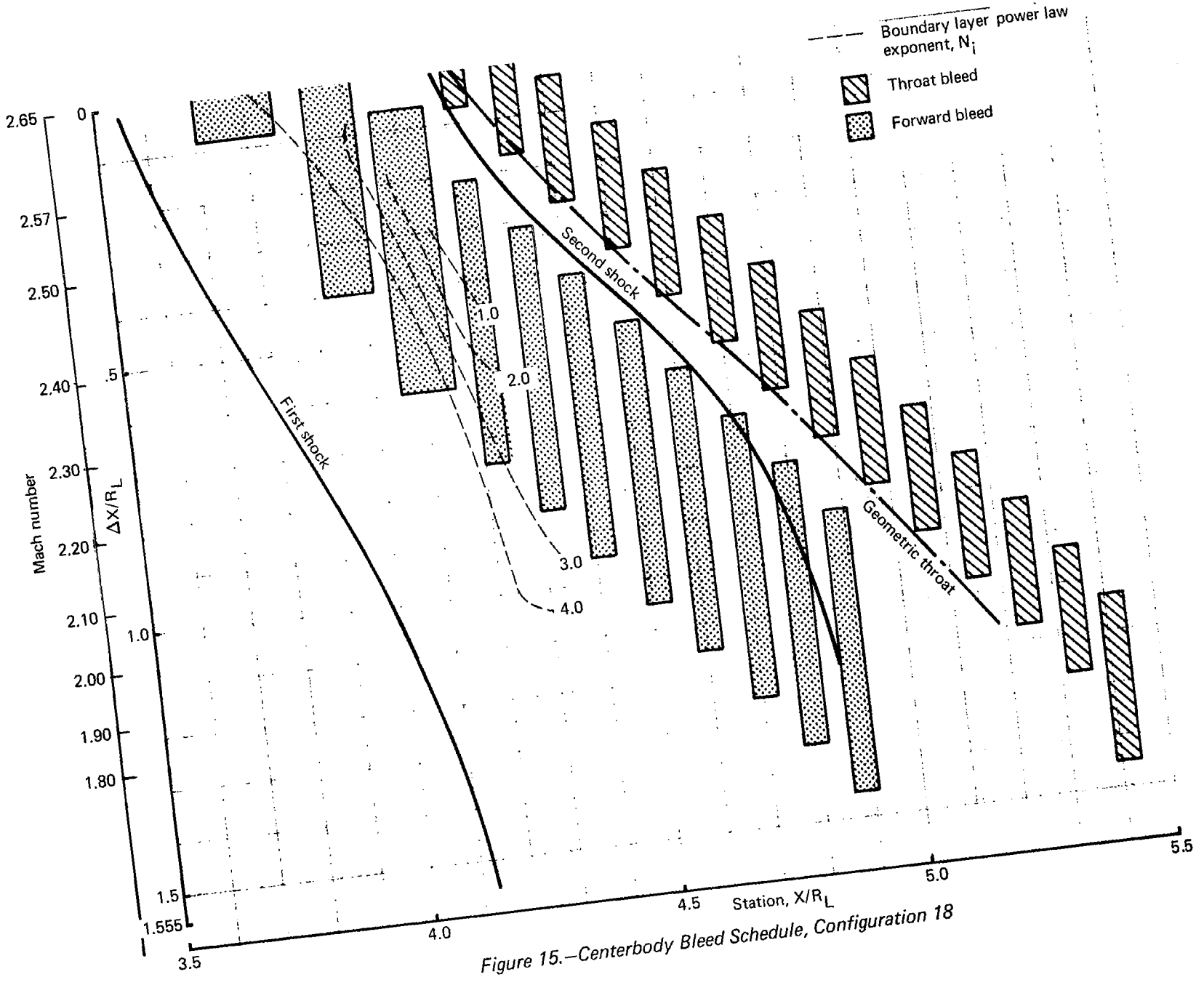

Figure 15.—Centerbody Bleed Schedule, Configuration 18

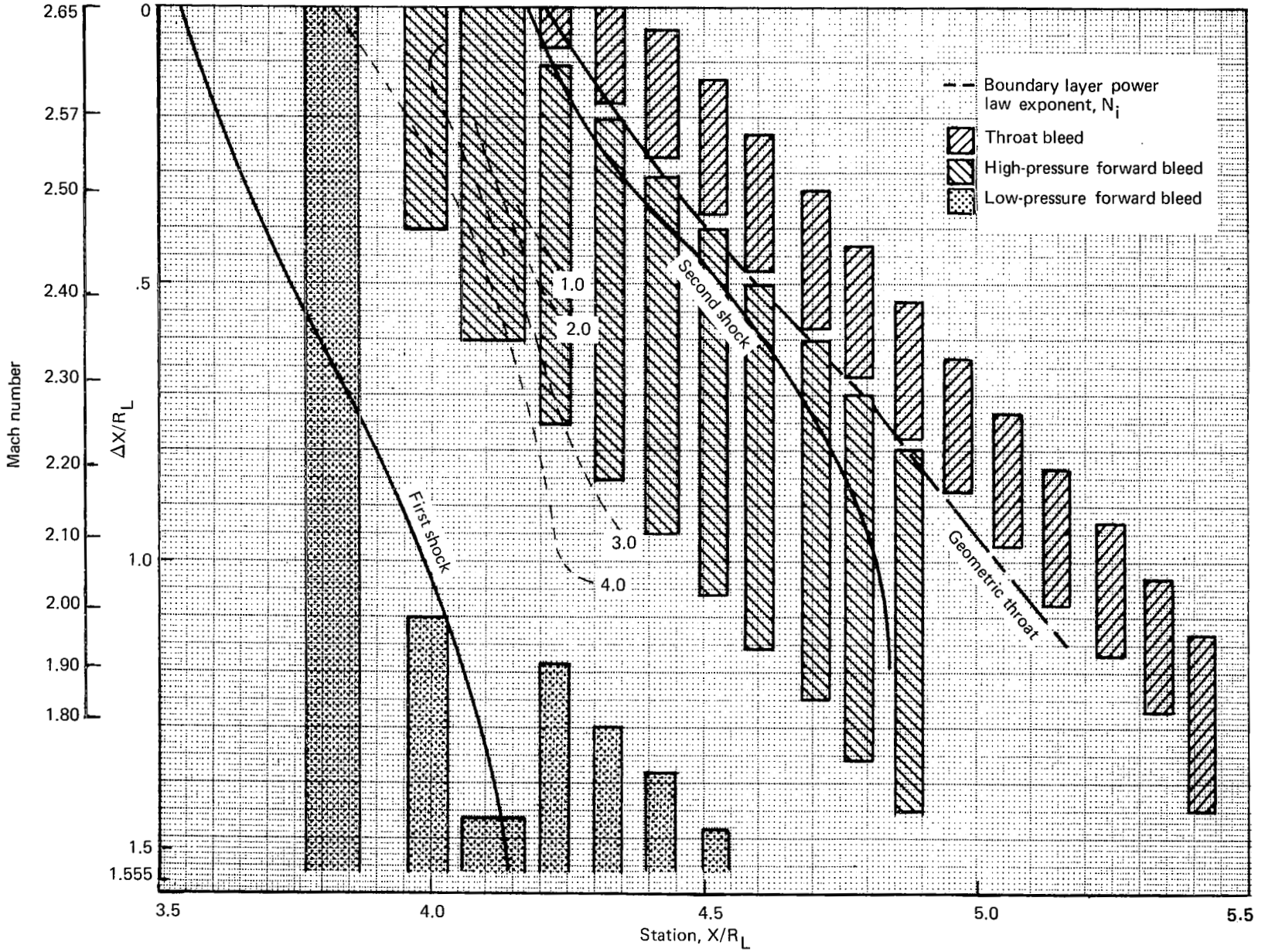

Figure 16.—Centerbody Bleed Schedule, Configuration 20

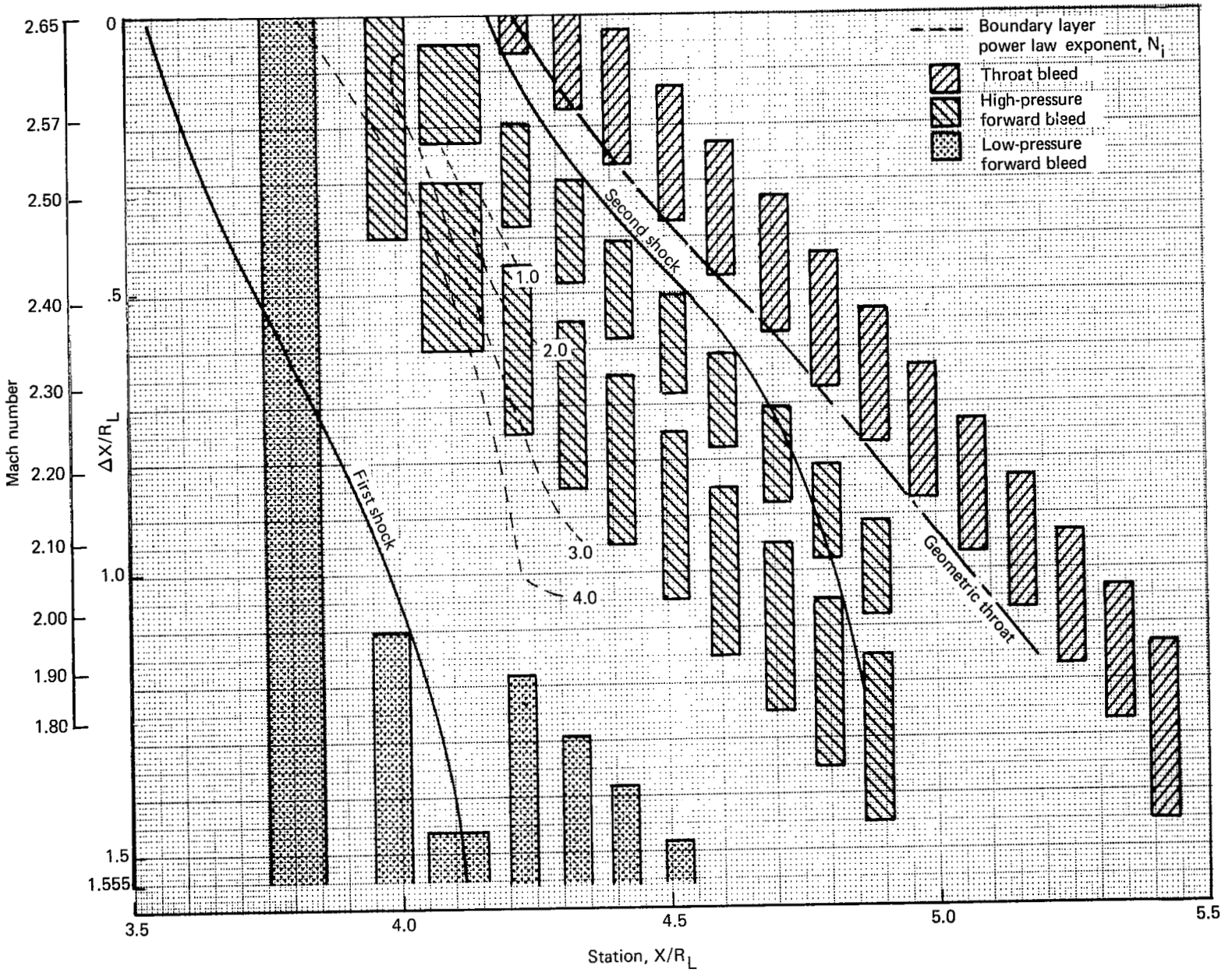

Figure 17.—Centerbody Bleed Schedule—Configuration 26

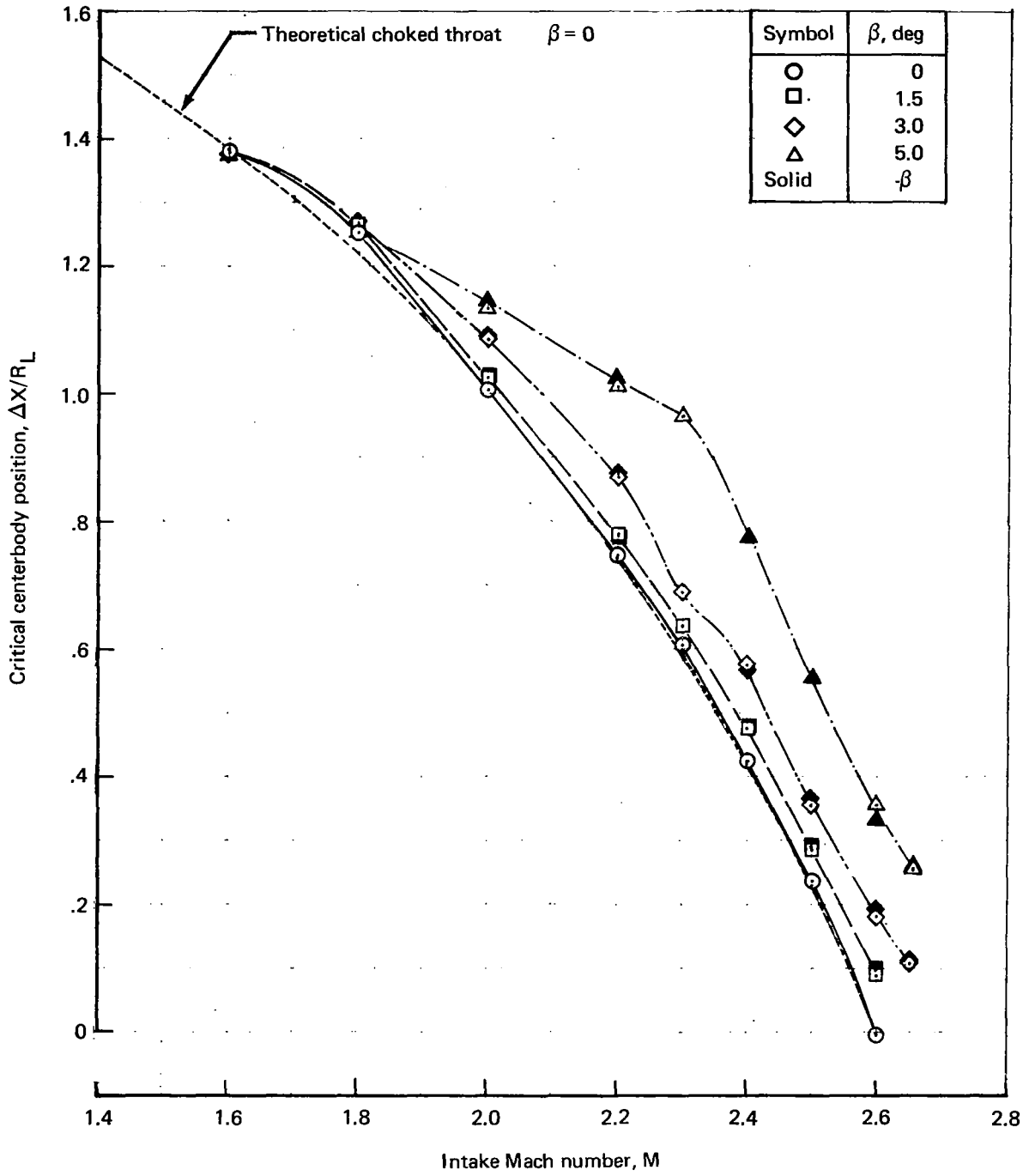

Figure 18.—Critical Centerbody Positions, Configuration 18

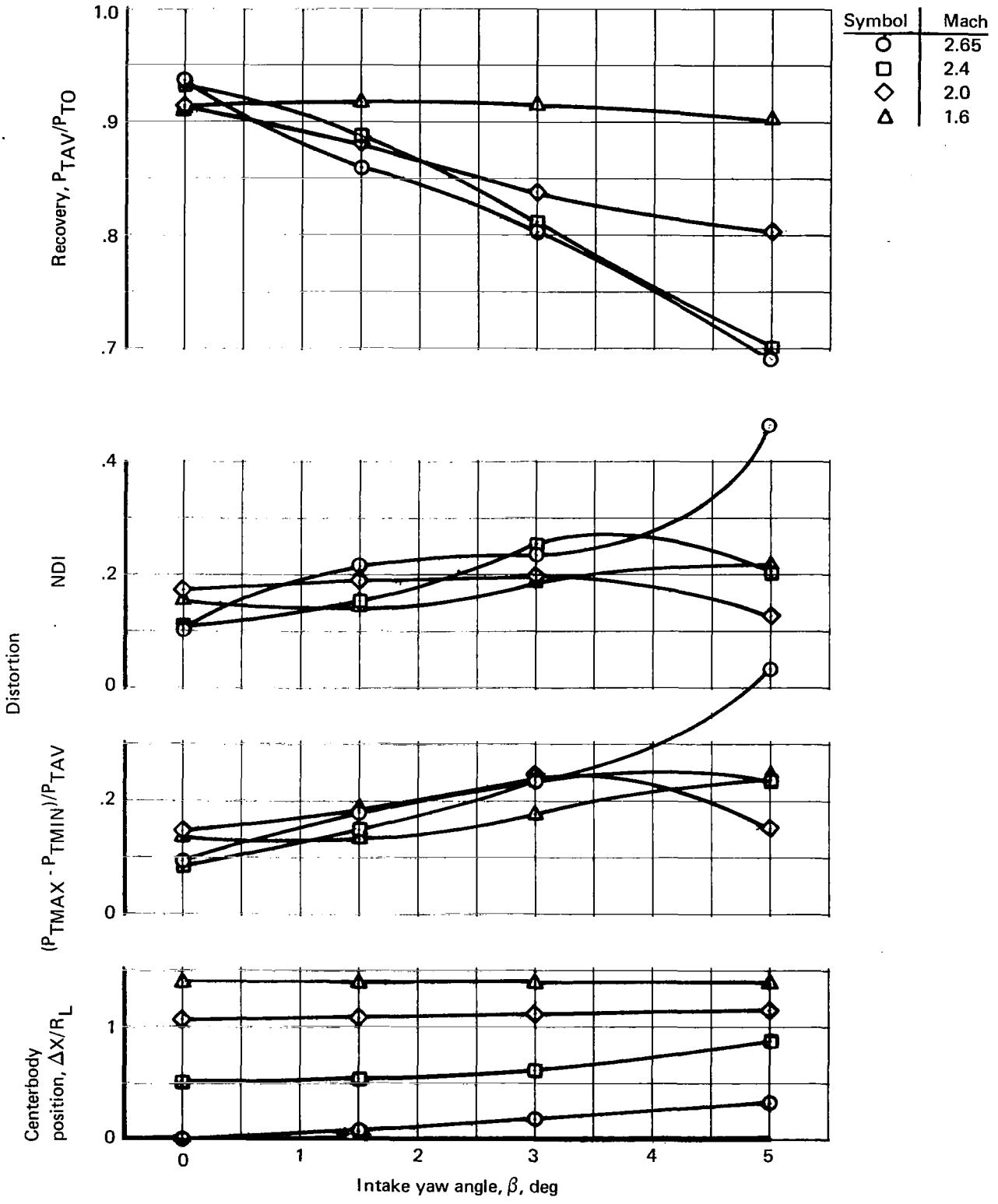

Figure 19.—Intake Performance at Angle of Incidence, Configuration 18

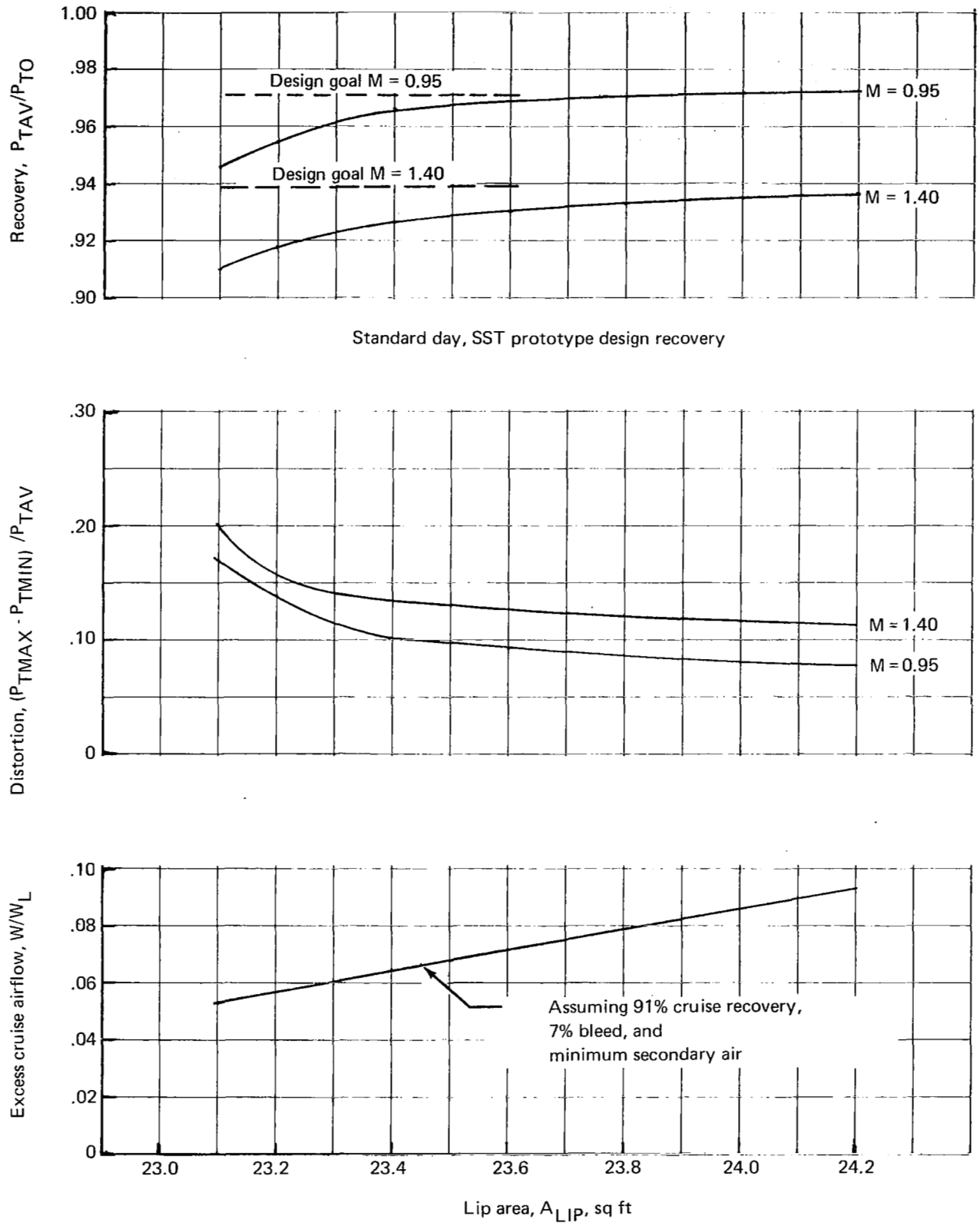

Figure 20.—NASA Ames Intake/GE4 Engine Matching

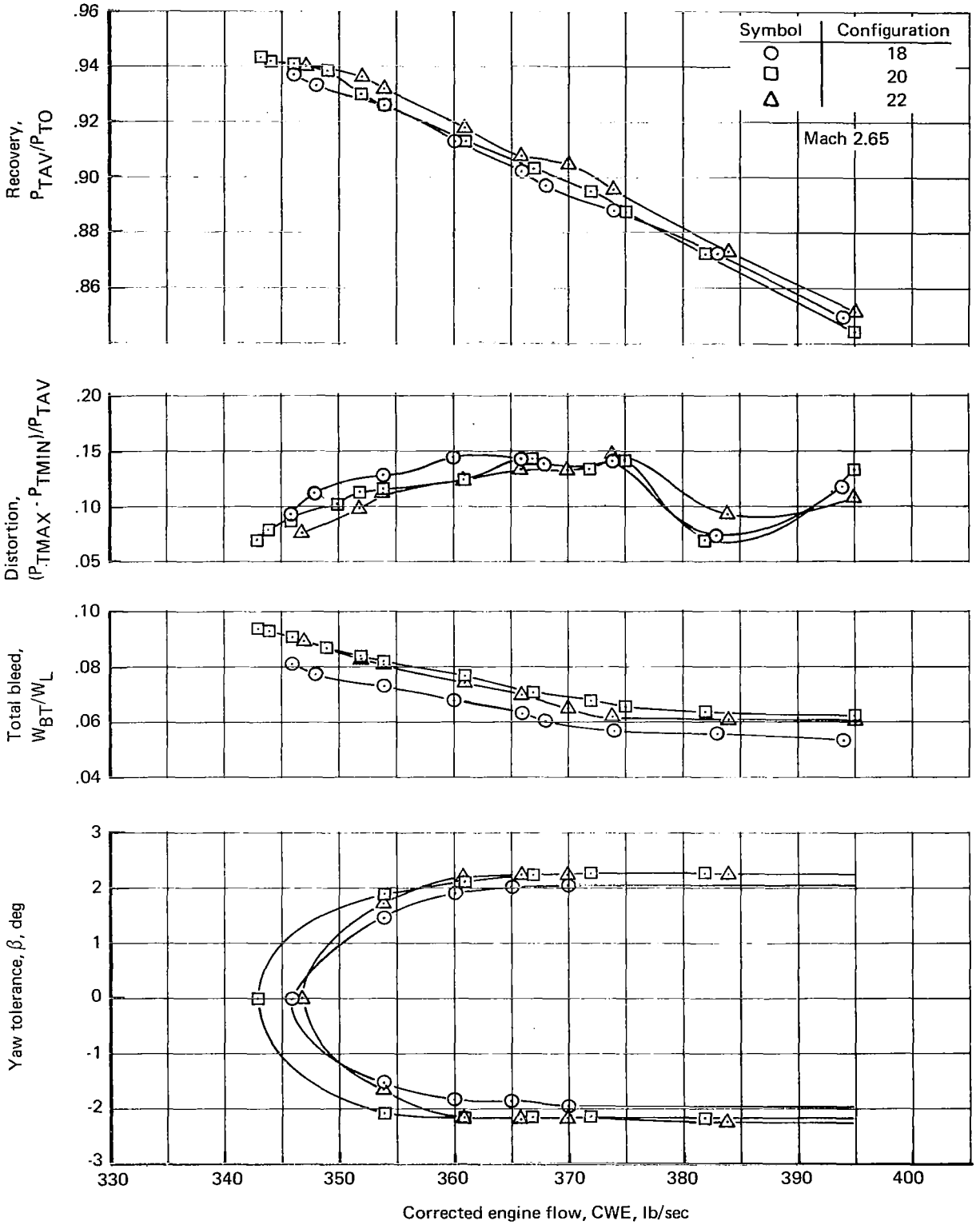

Figure 21.—Intake Cruise Performance

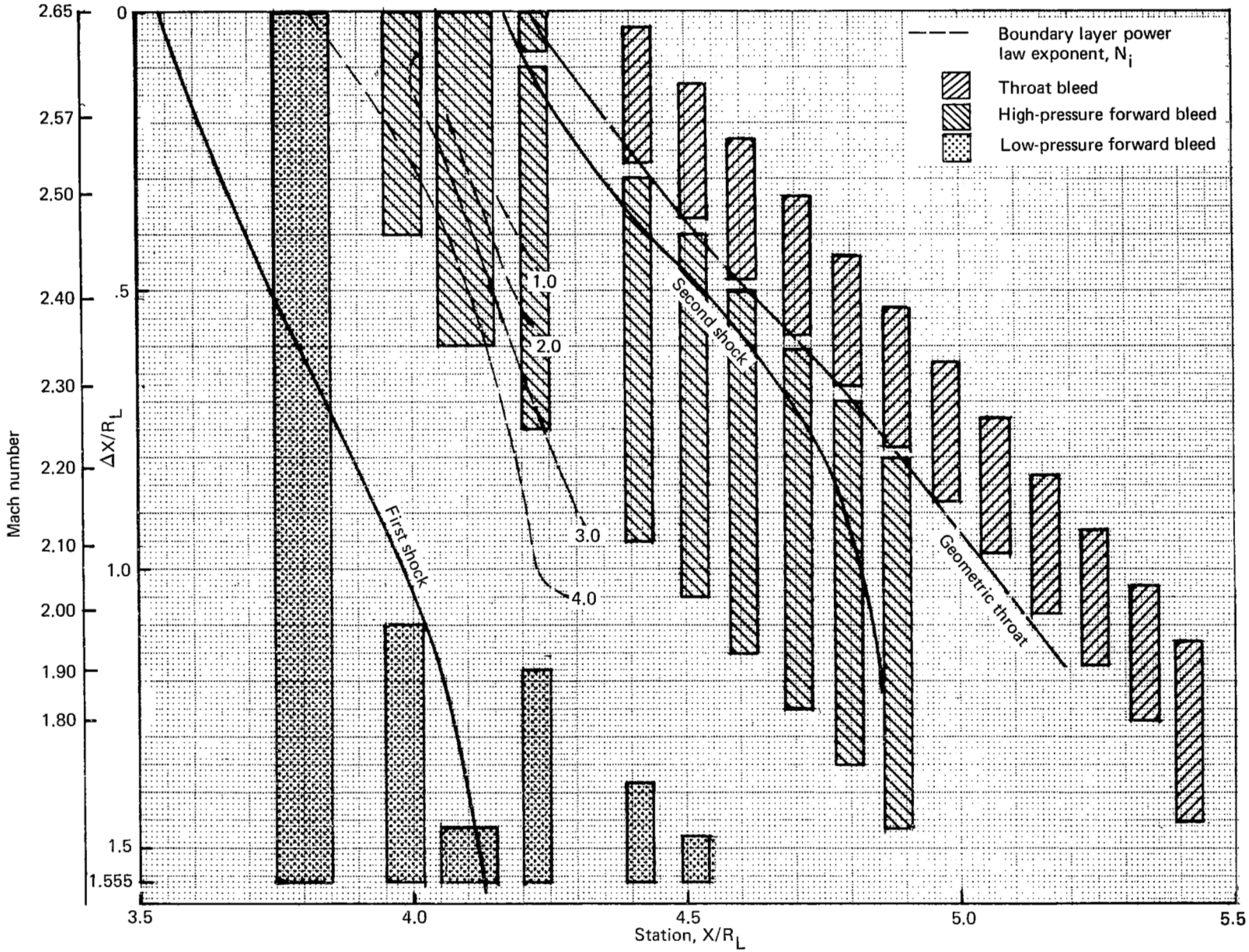

Figure 22.—Centerbody Bleed Schedule, Configuration 22

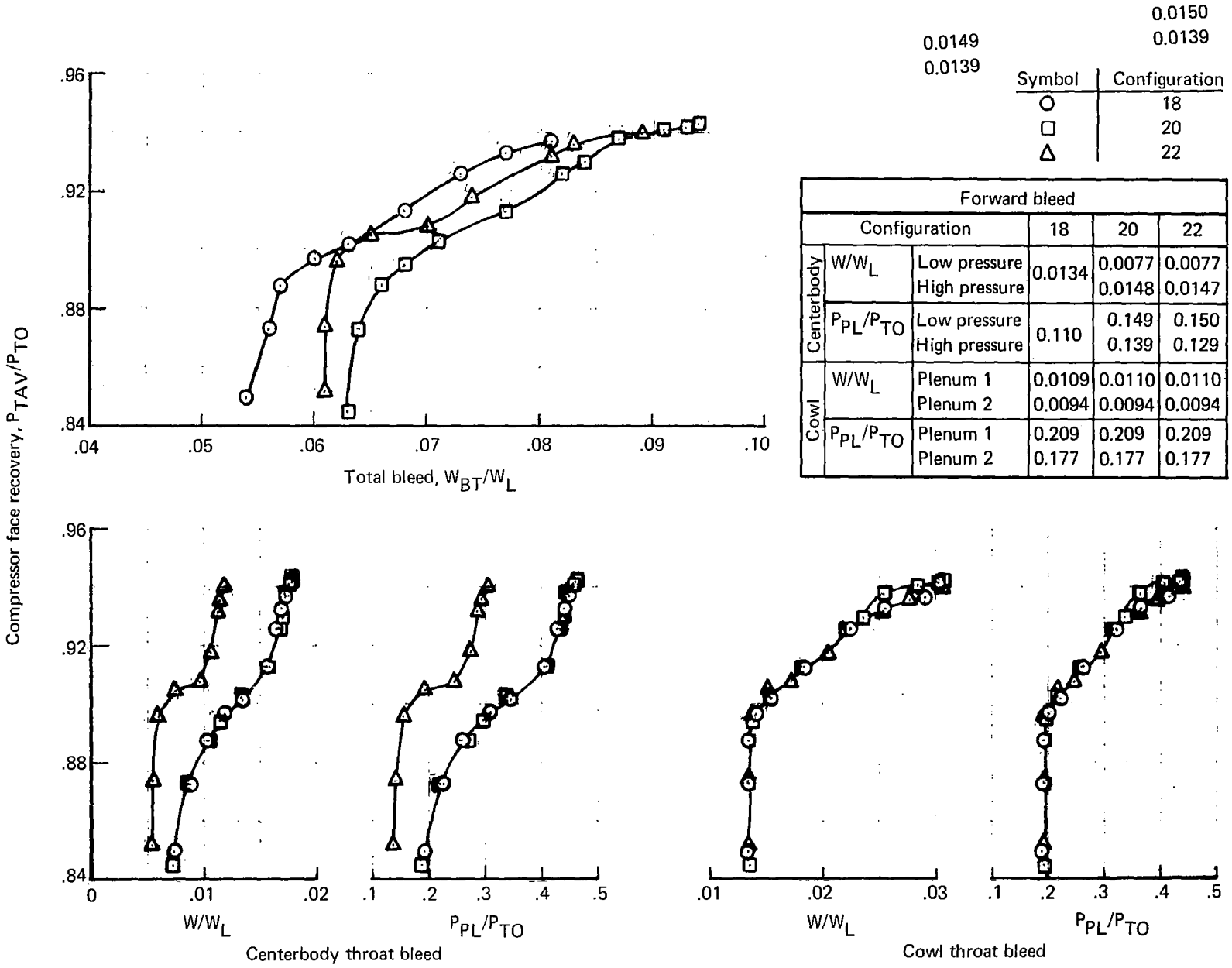

Figure 23.—Intake Bleed Flow Characteristics, Mach 2.65

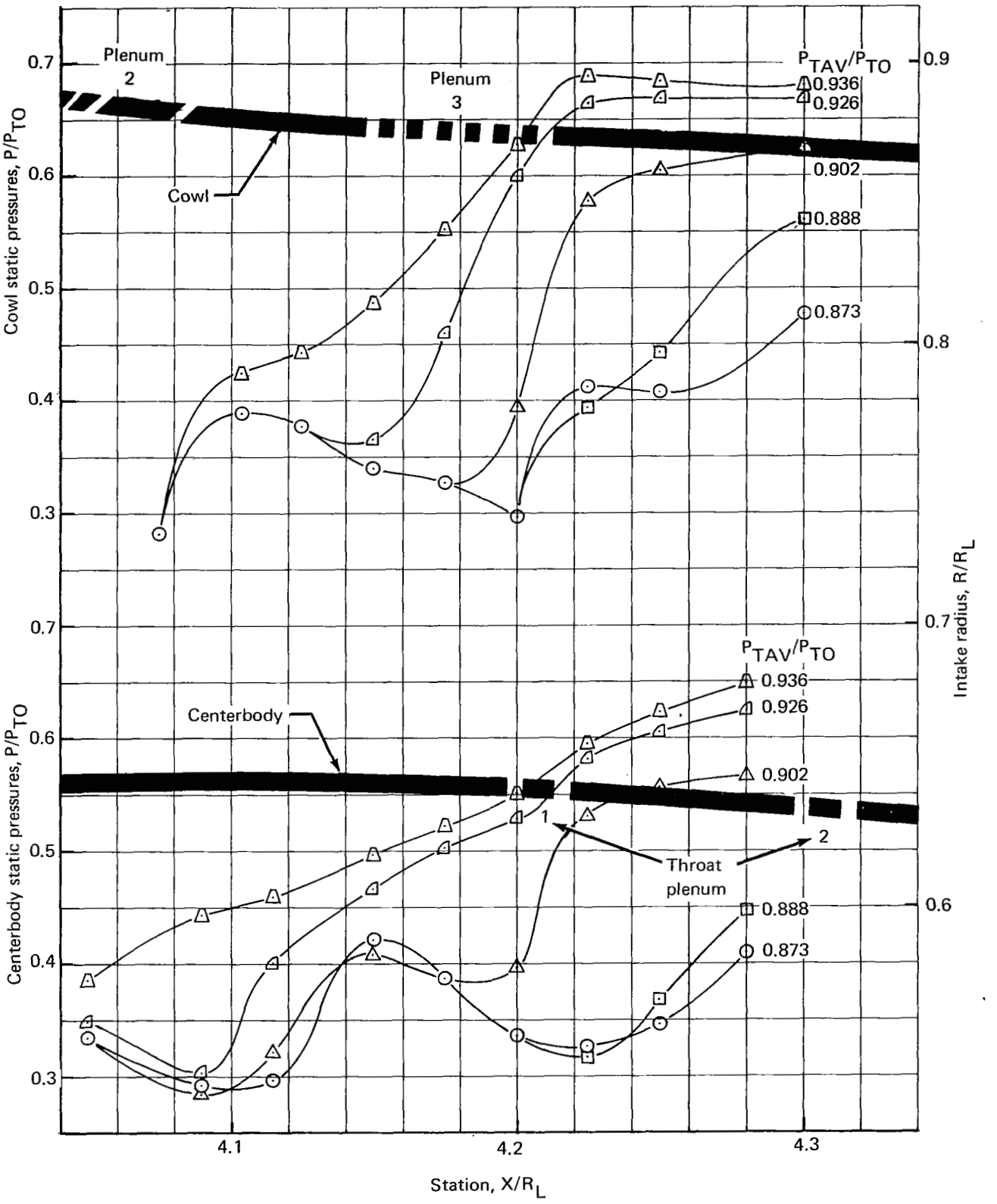

Figure 24.—Throat Static Pressure Profiles, Mach 2.65, Configuration 18

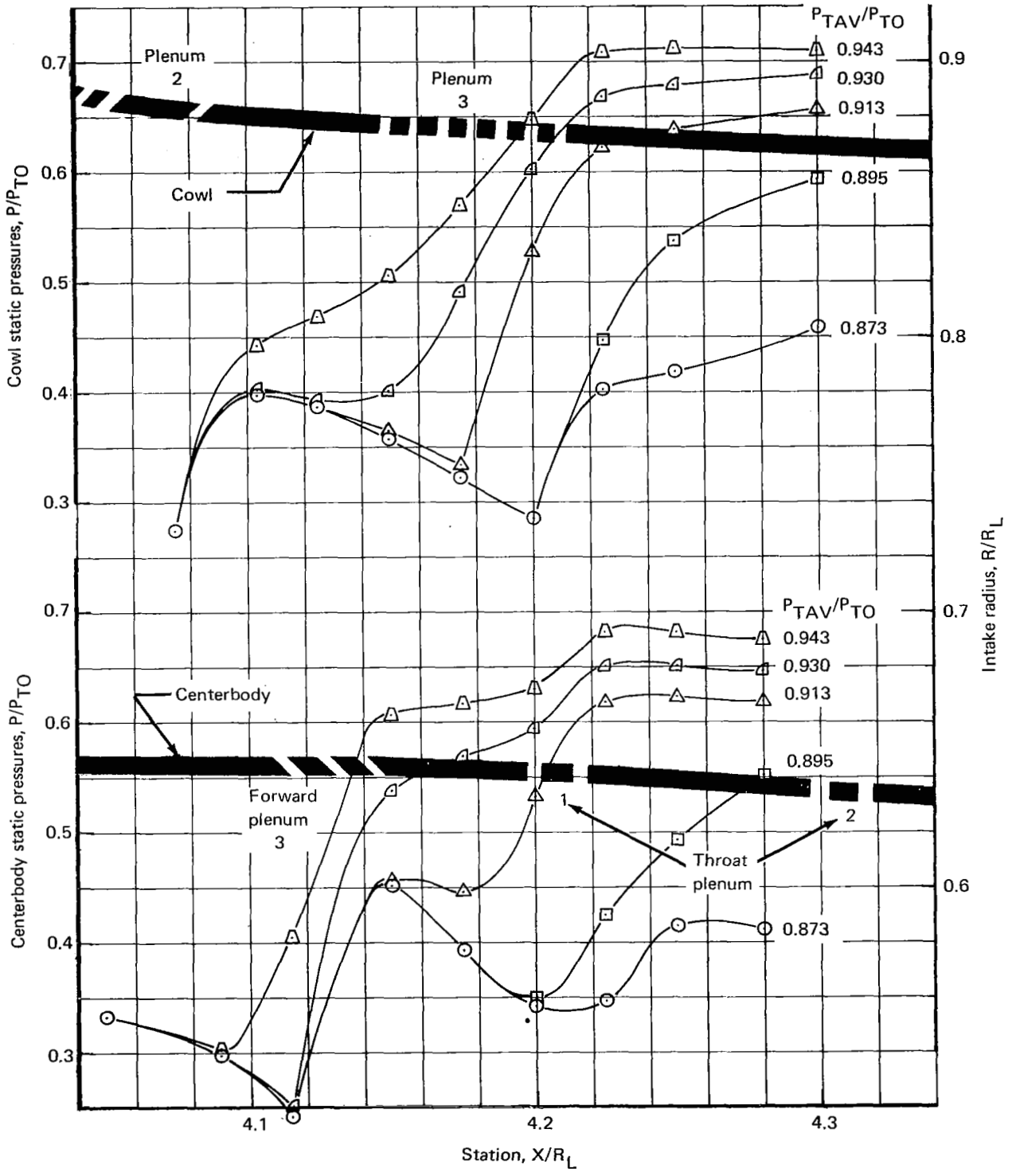

Figure 25.—Throat Static Pressure Profiles, Mach 2.65, Configuration 20

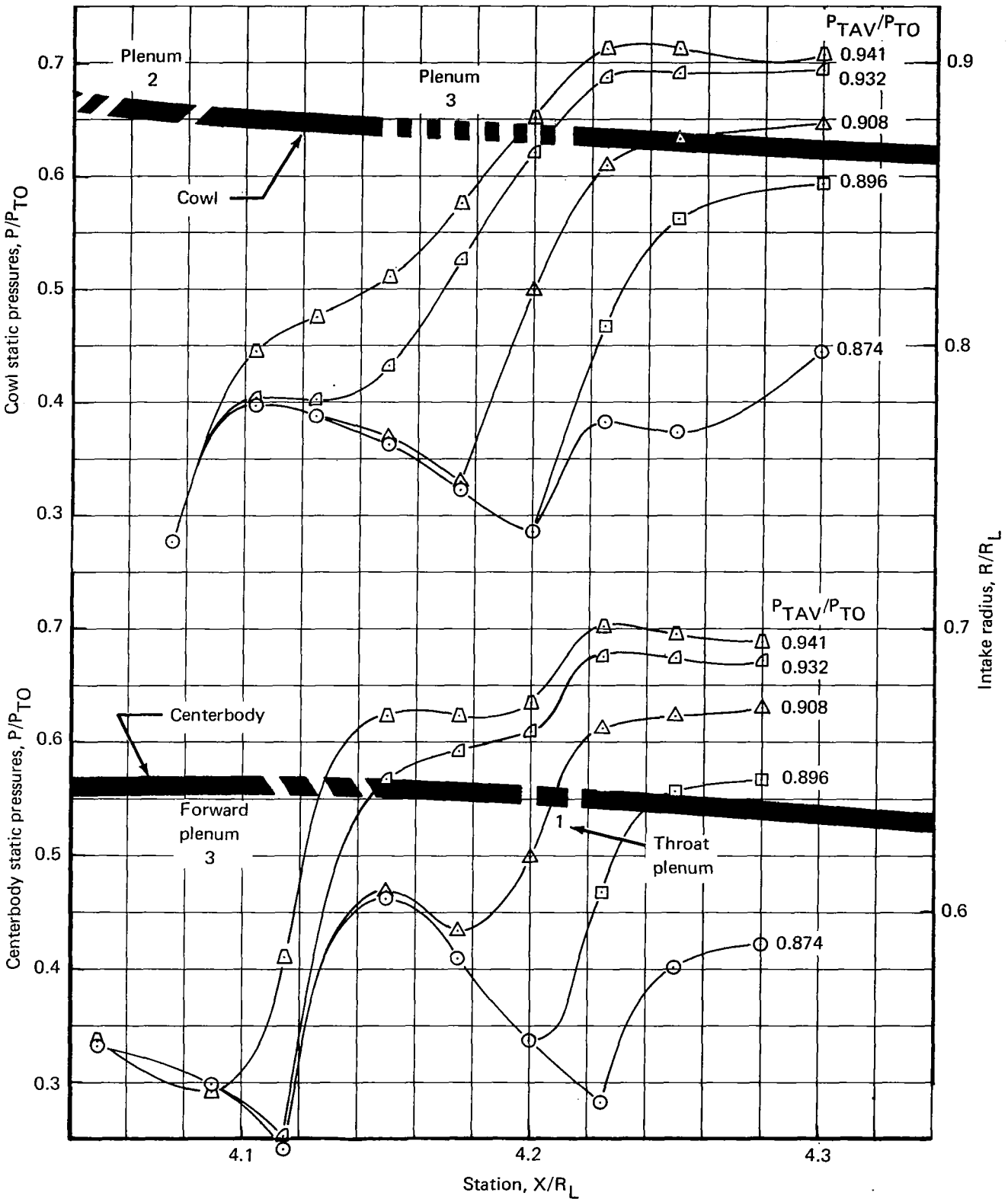

Figure 26.—Throat Static Pressure Profiles, Mach 2.65, Configuration 22

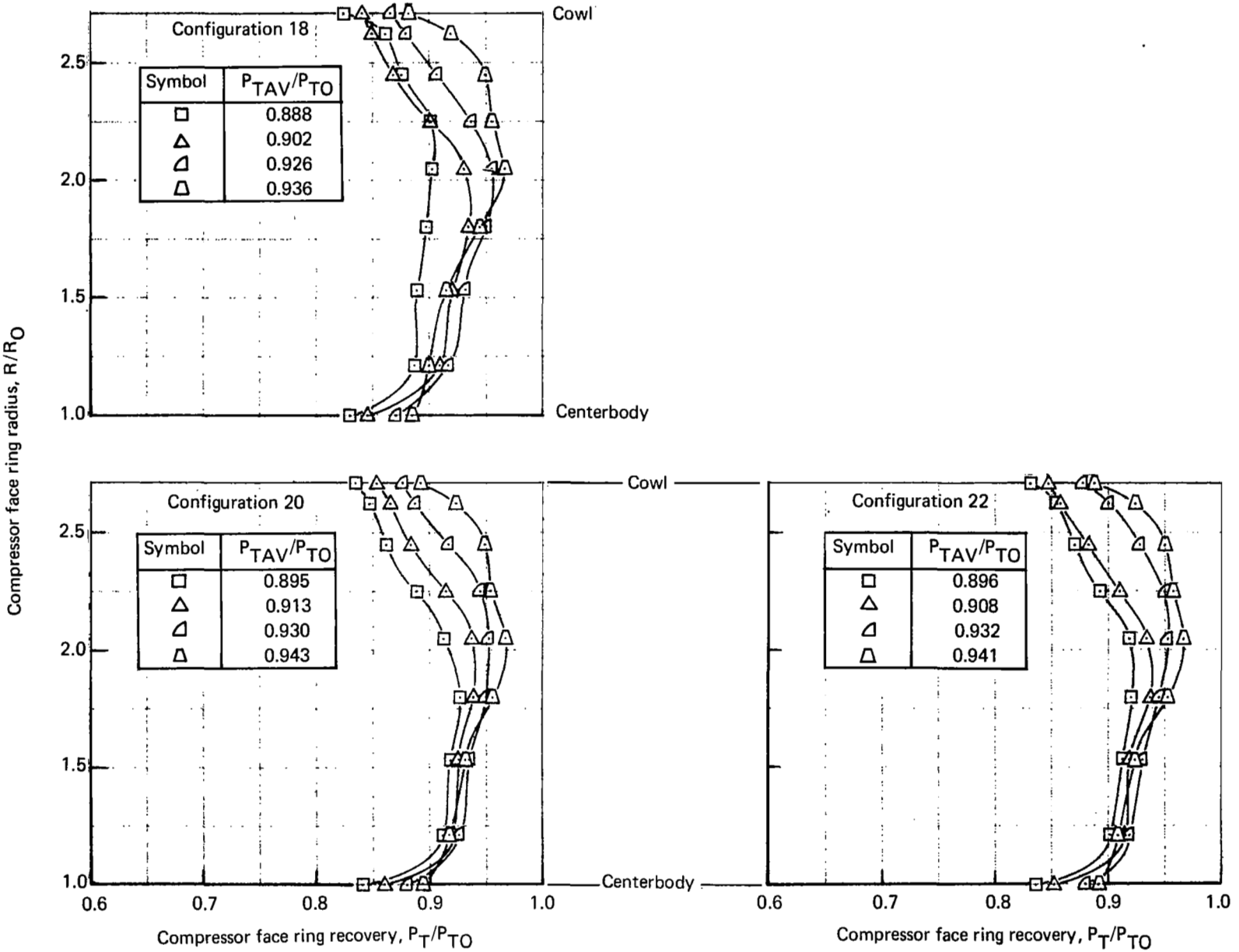

Figure 27.—Compressor Face Average Rake Profiles, Mach 2.65

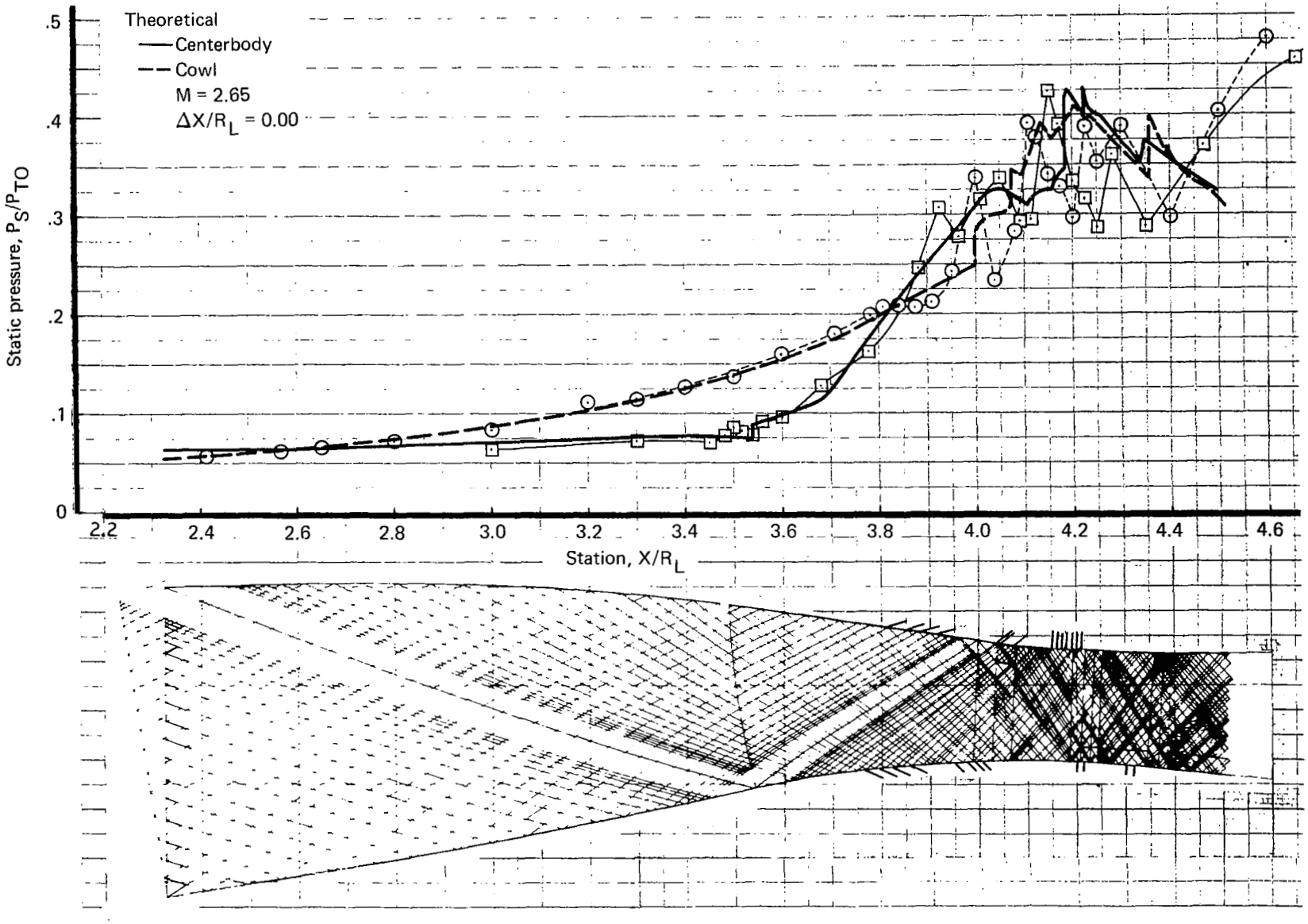

Figure 28.—Supersonic Diffuser Profile—Mach 2.65, Configuration 18

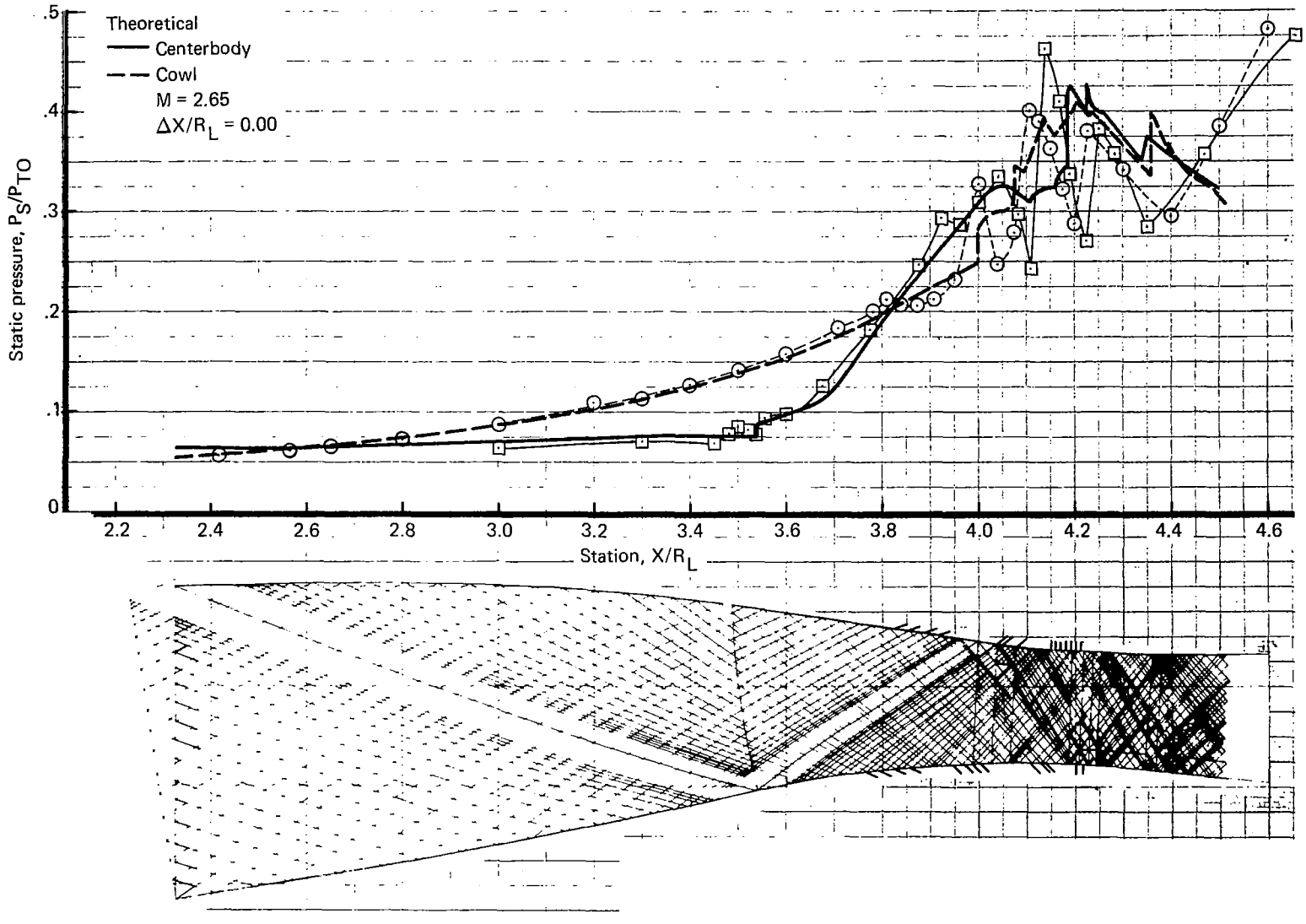

Figure 29.–Supersonic Diffuser Profile–Mach 2.65 Configuration 22

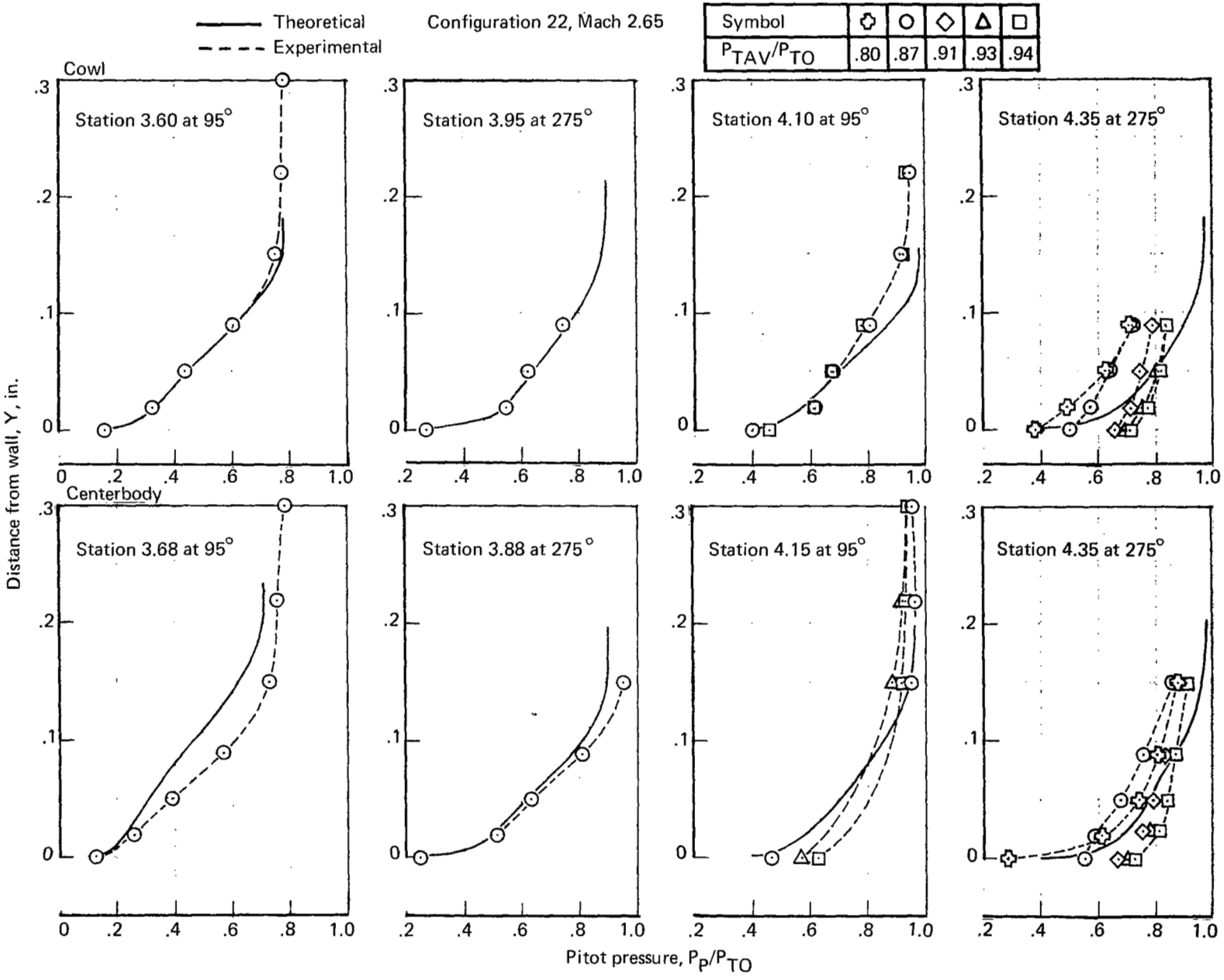

Figure 30.—Boundary Layer Pitot Pressure Profiles

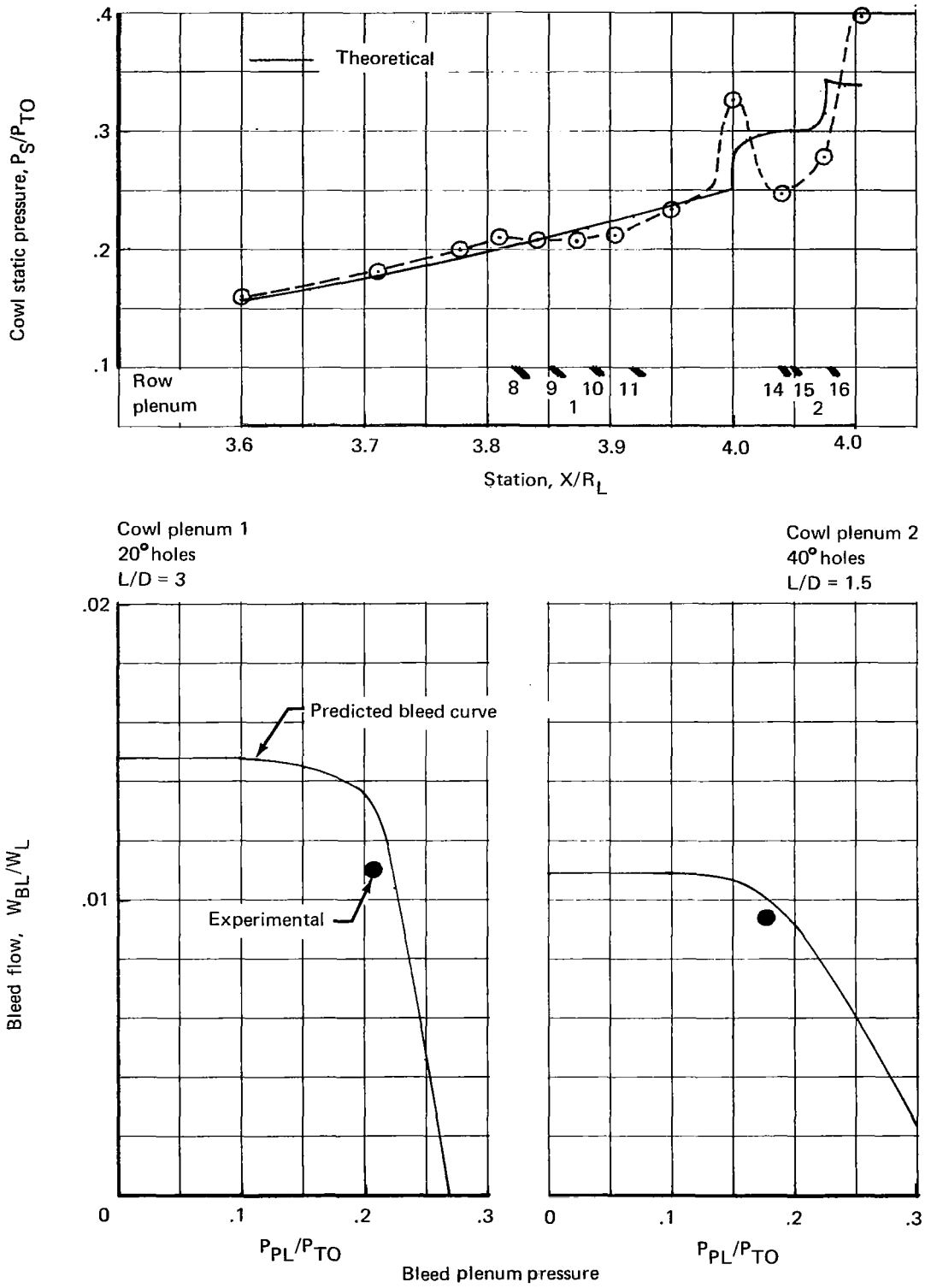

Figure 31.—Predicted and Experimental Forward Cowl Bleed Rates, Mach 2.65

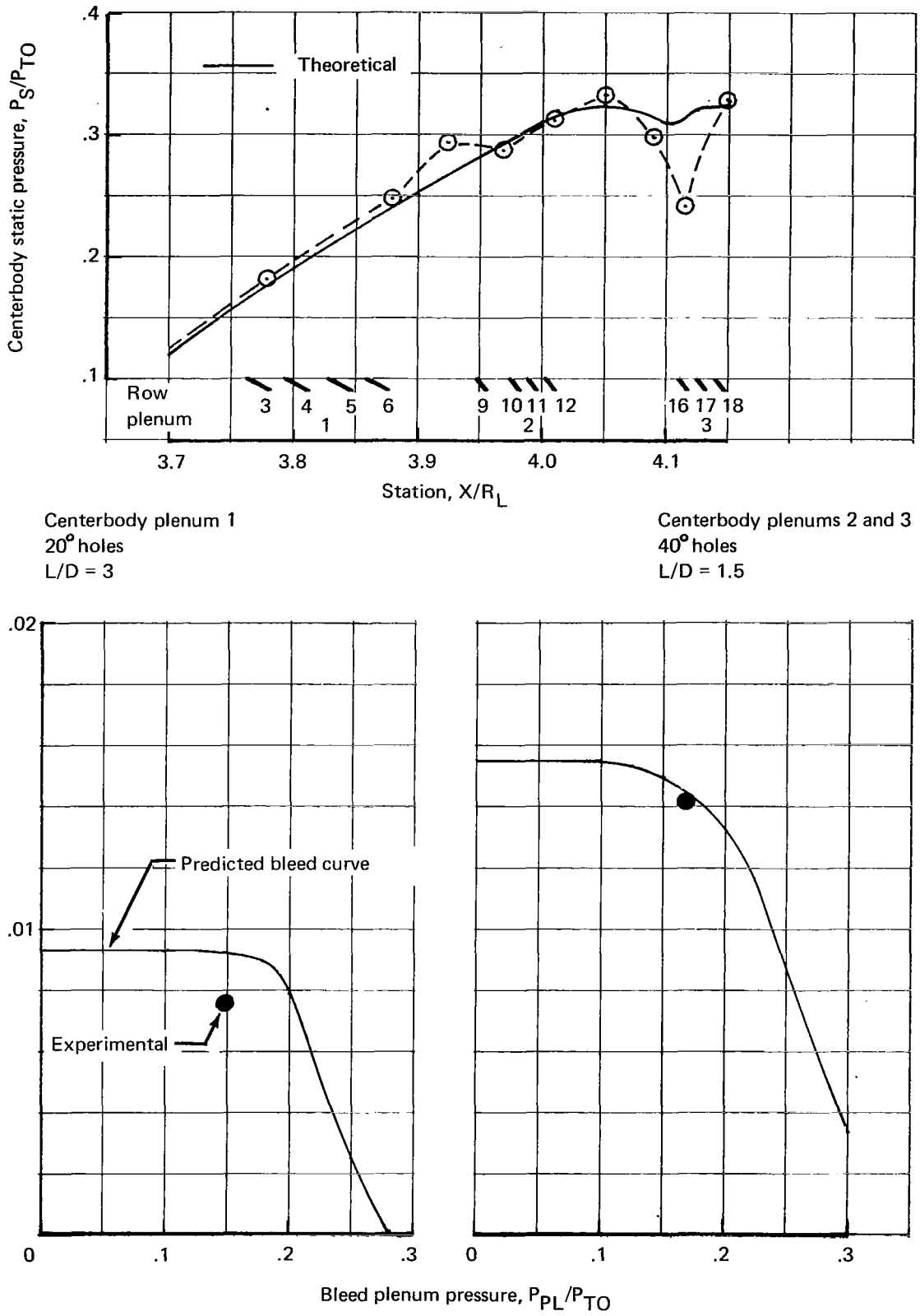

Figure 32.—Predicted and Experimental Forward Centerbody Bleed Rates, Mach 2.65

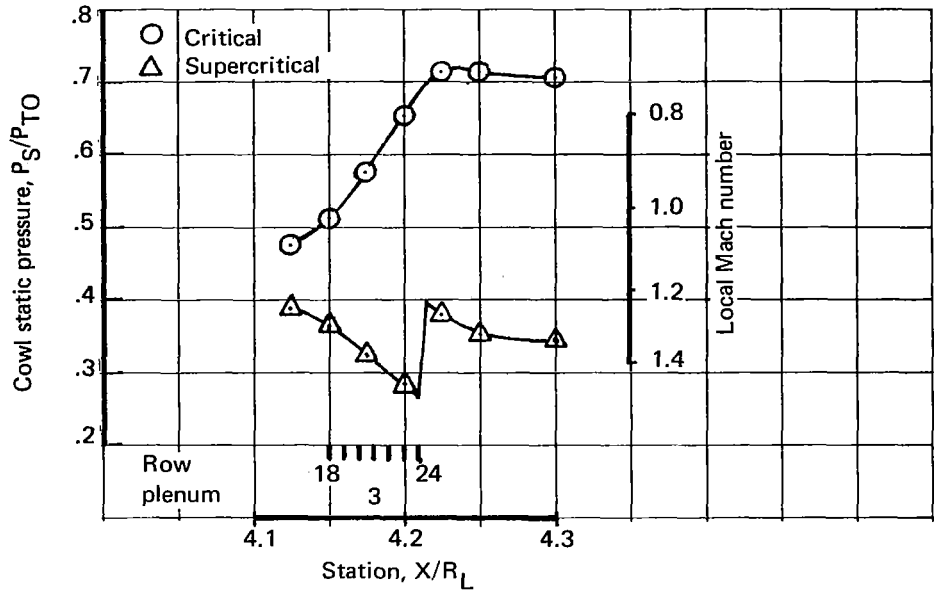

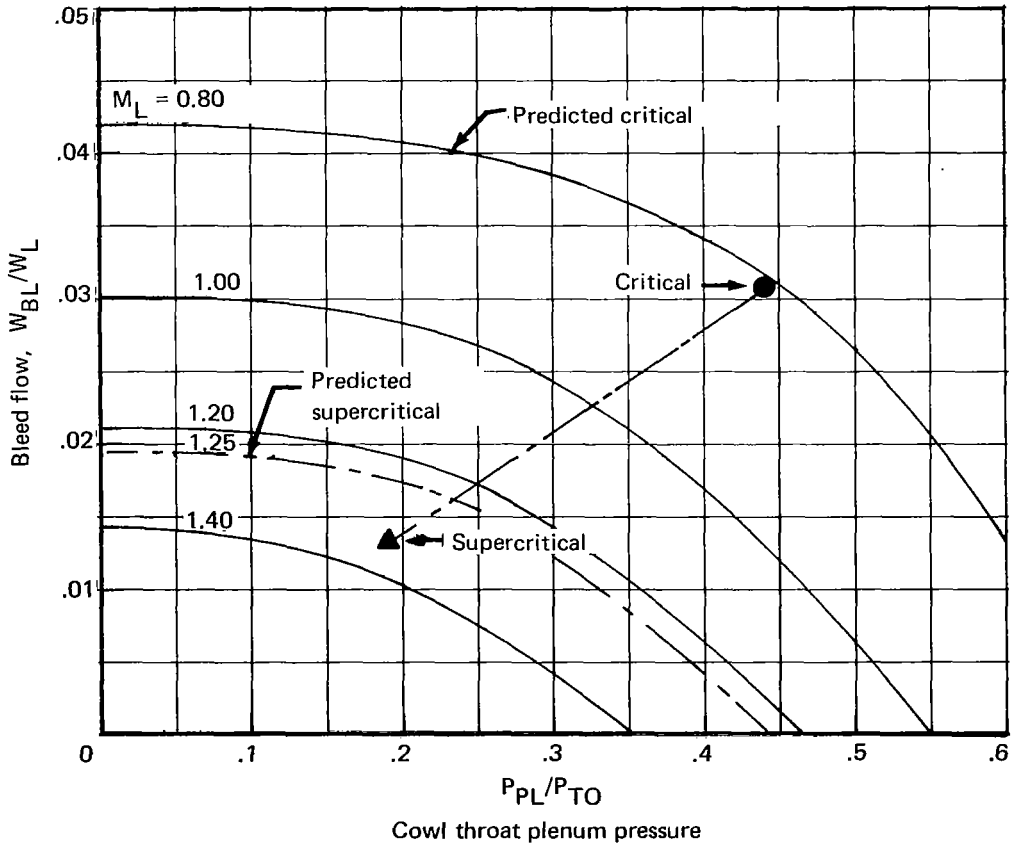

Figure 33.—Predicted and Experimental Cowl Throat Bleed, Mach 2.65

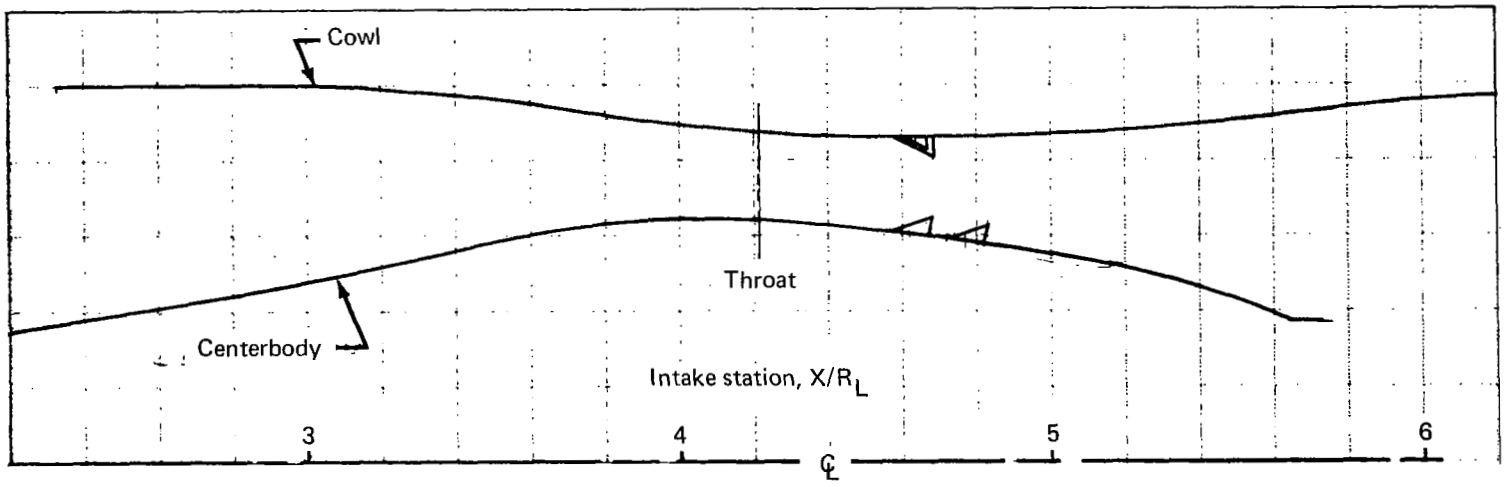

Note: Plots show 0.5 P_{TO} static pressure level locations on cowl and centerbody, respectively
Geometric throat is at station 4.22

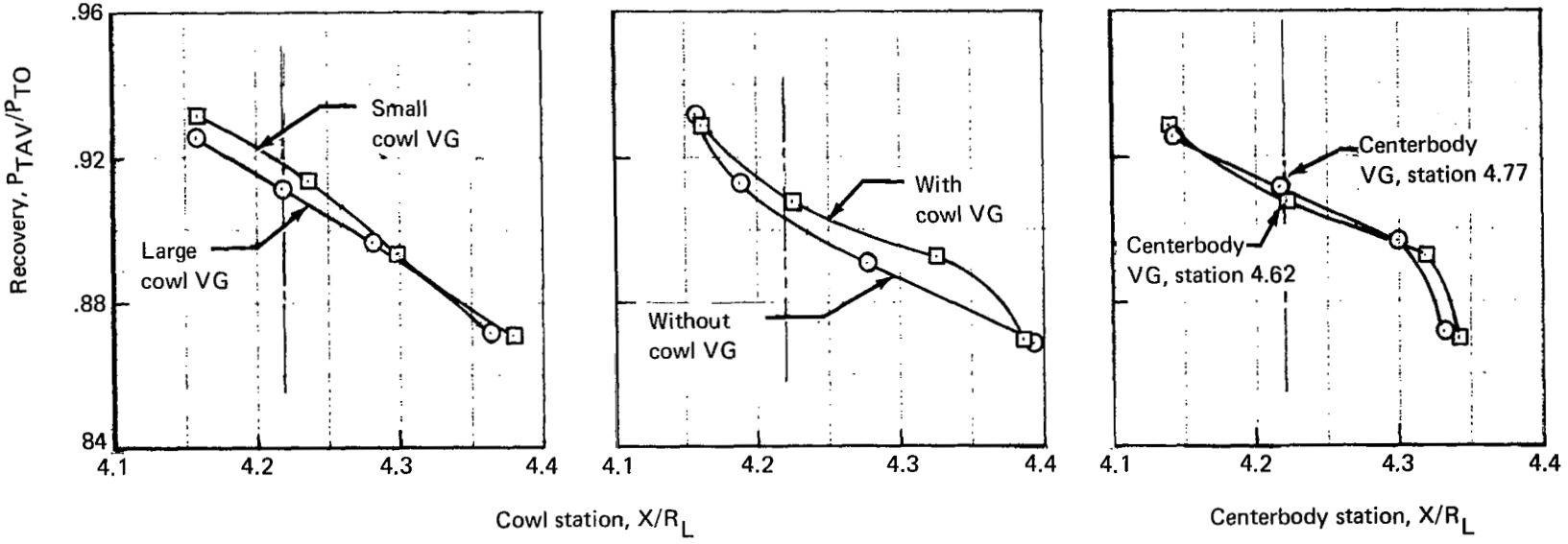

Figure 34.—Normal Shock Positions, Mach 2.65

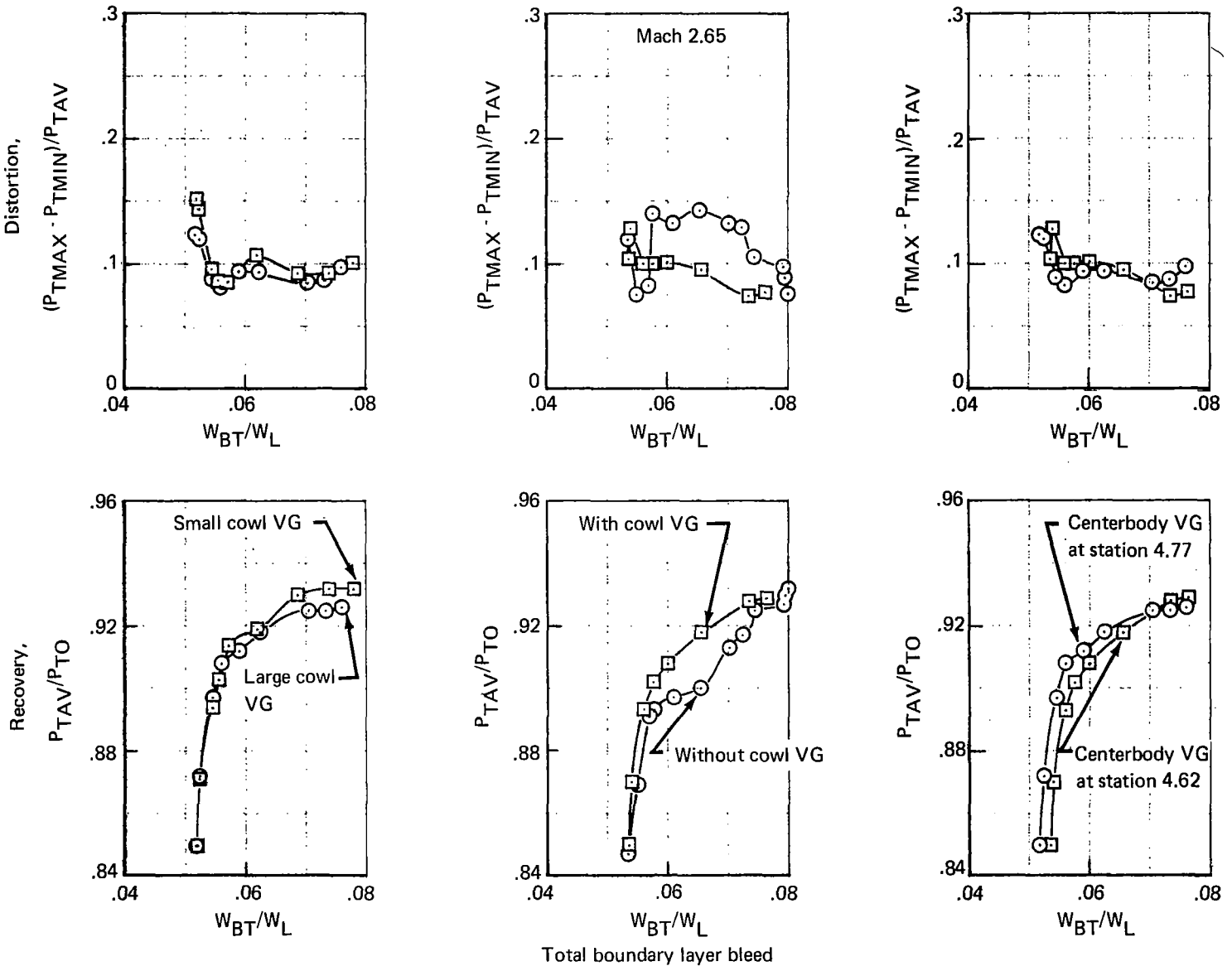

Figure 35.—Vortex Generator Evaluation

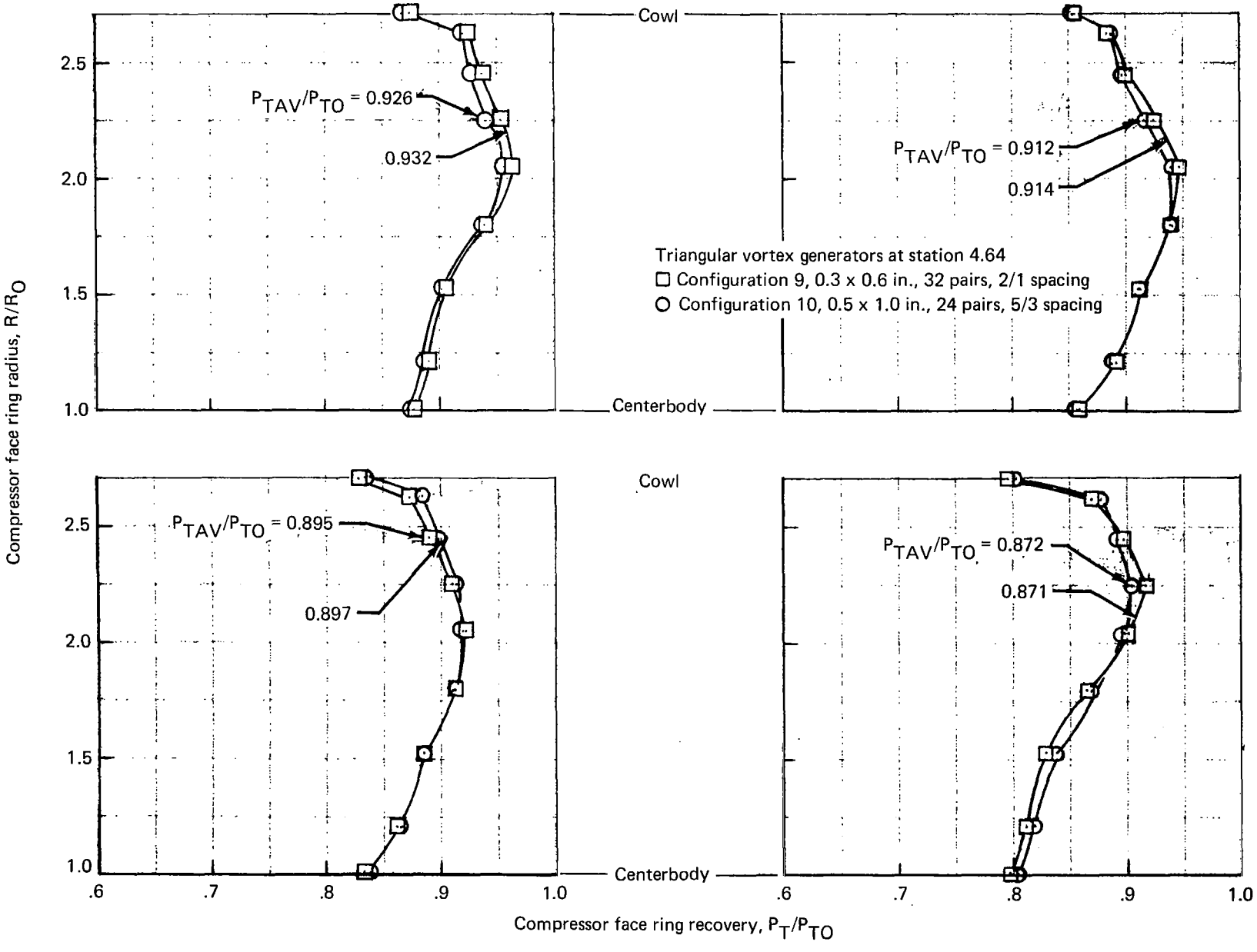

Figure–36.–Cowl Vortex Generator Evaluation, Mach 2.65, Small and Large Generators

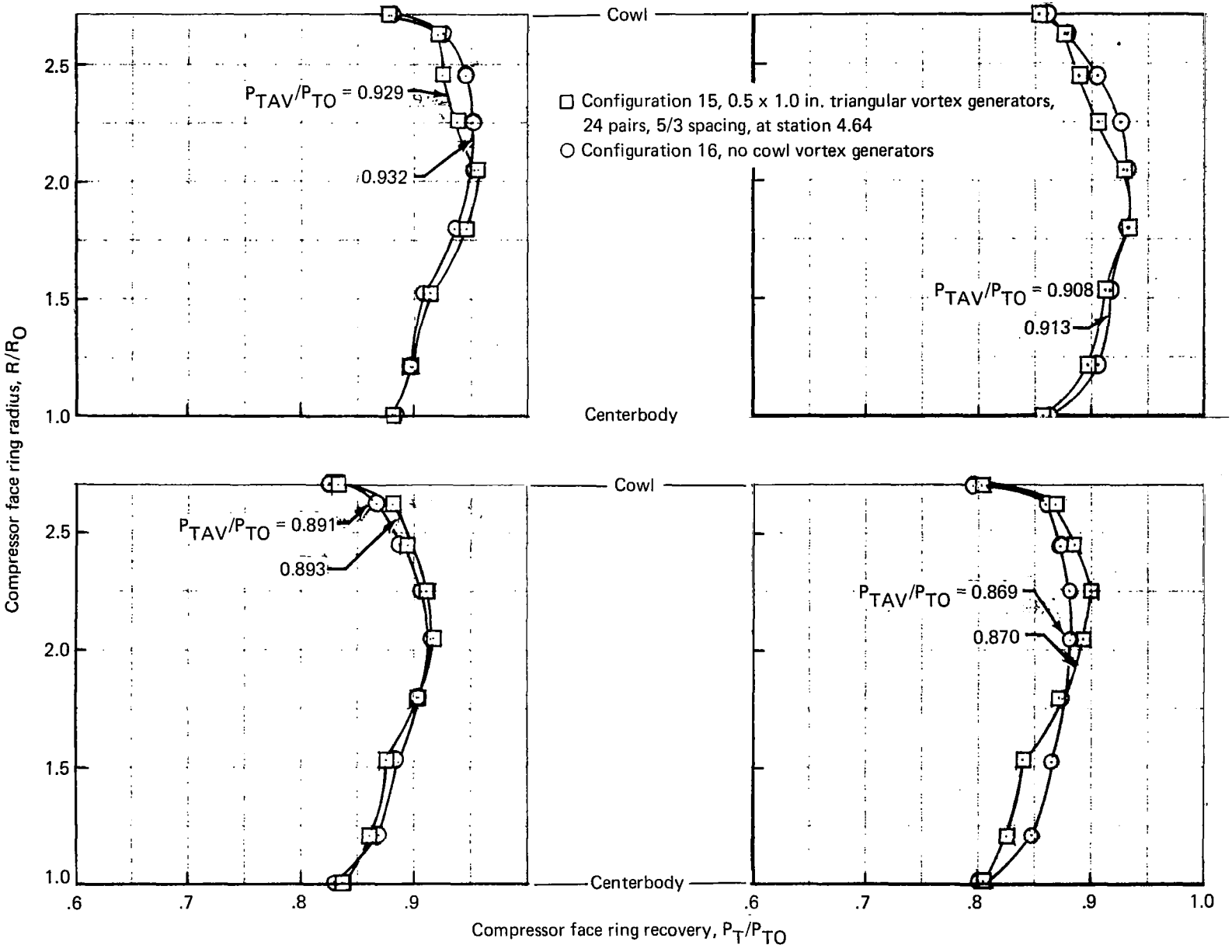

Figure 37.—Cowl Vortex Generator Evaluation, Mach 2.65, With and Without Generators

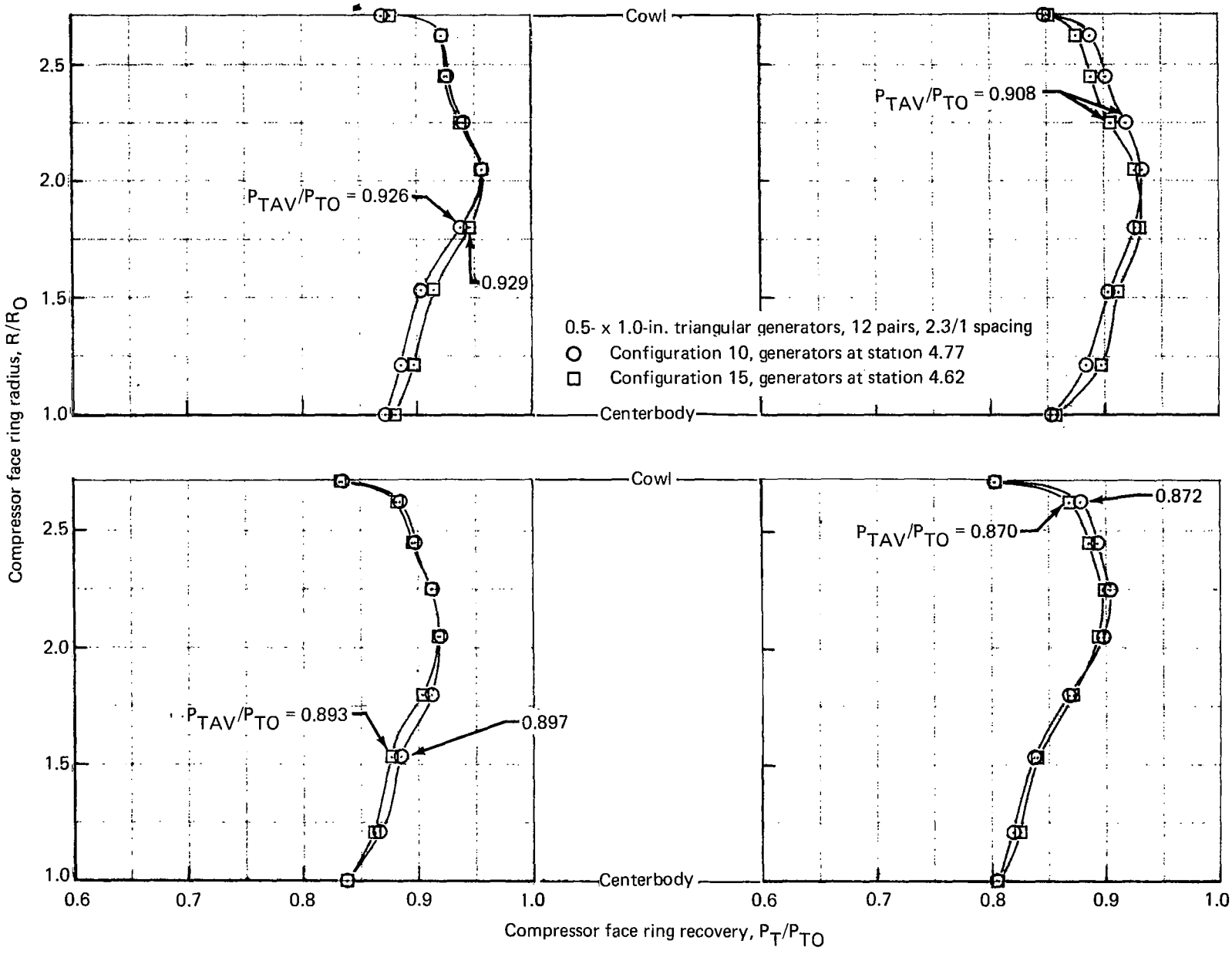

Figure 38.—Centerbody Vortex Generator Evaluation, Mach 2.65, Generators at Stations 4.77 and 4.62

Note: Transonic insert contours formed by rotating cruise contours about center shown.

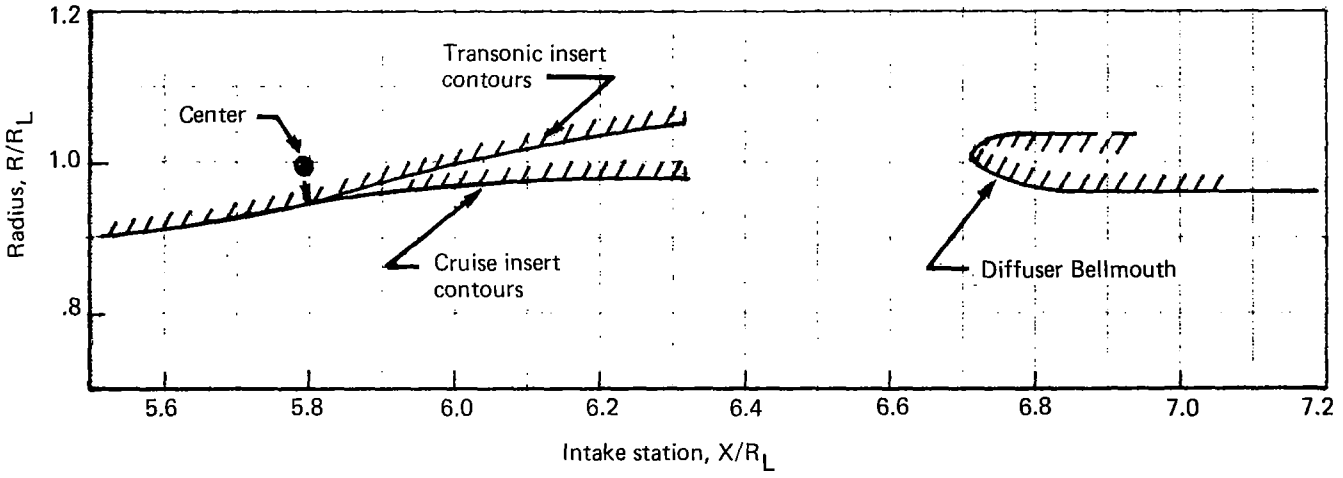

Figure 39.—Diffuser Insert Contours

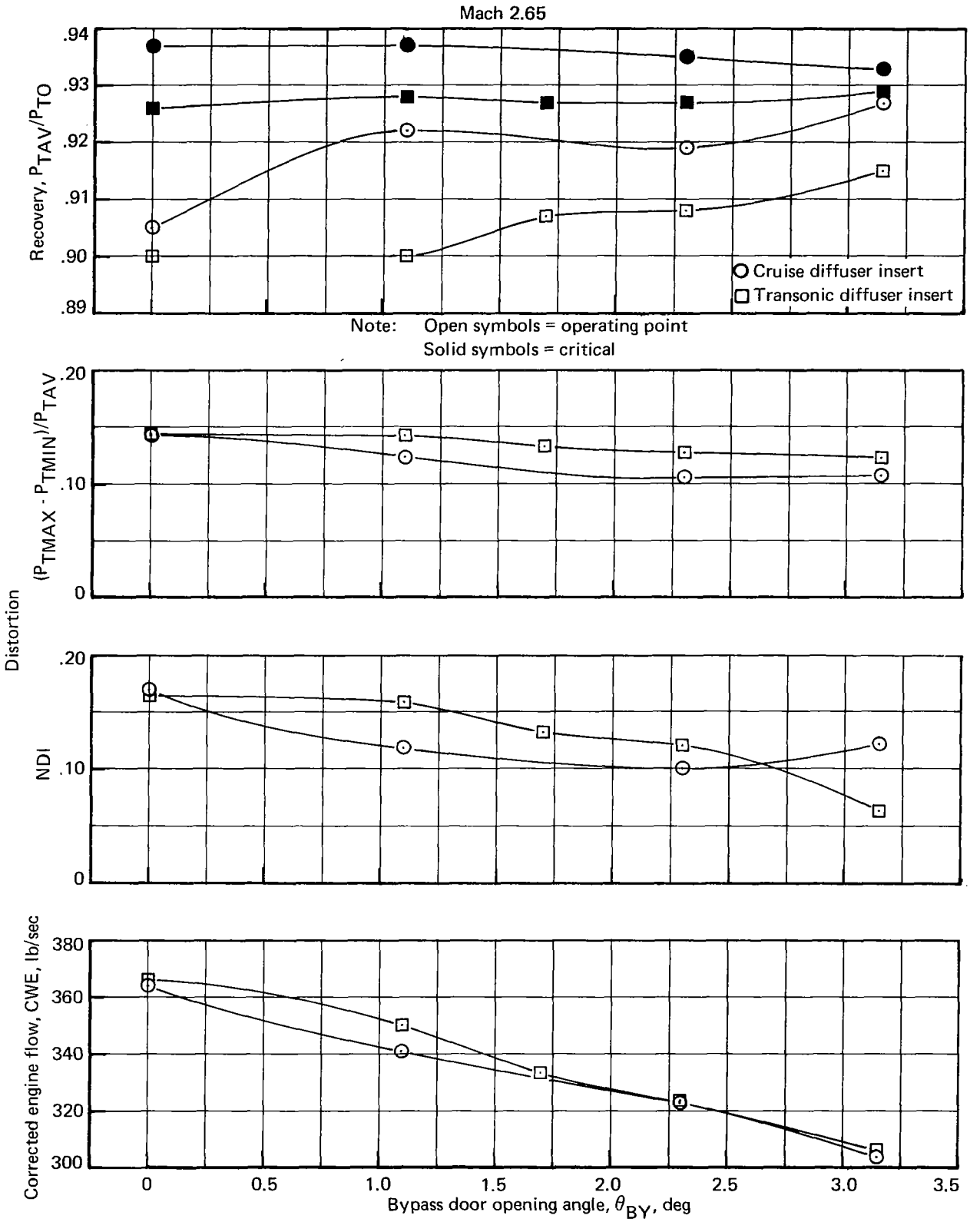

Figure 40.—Diffuser Insert Performance

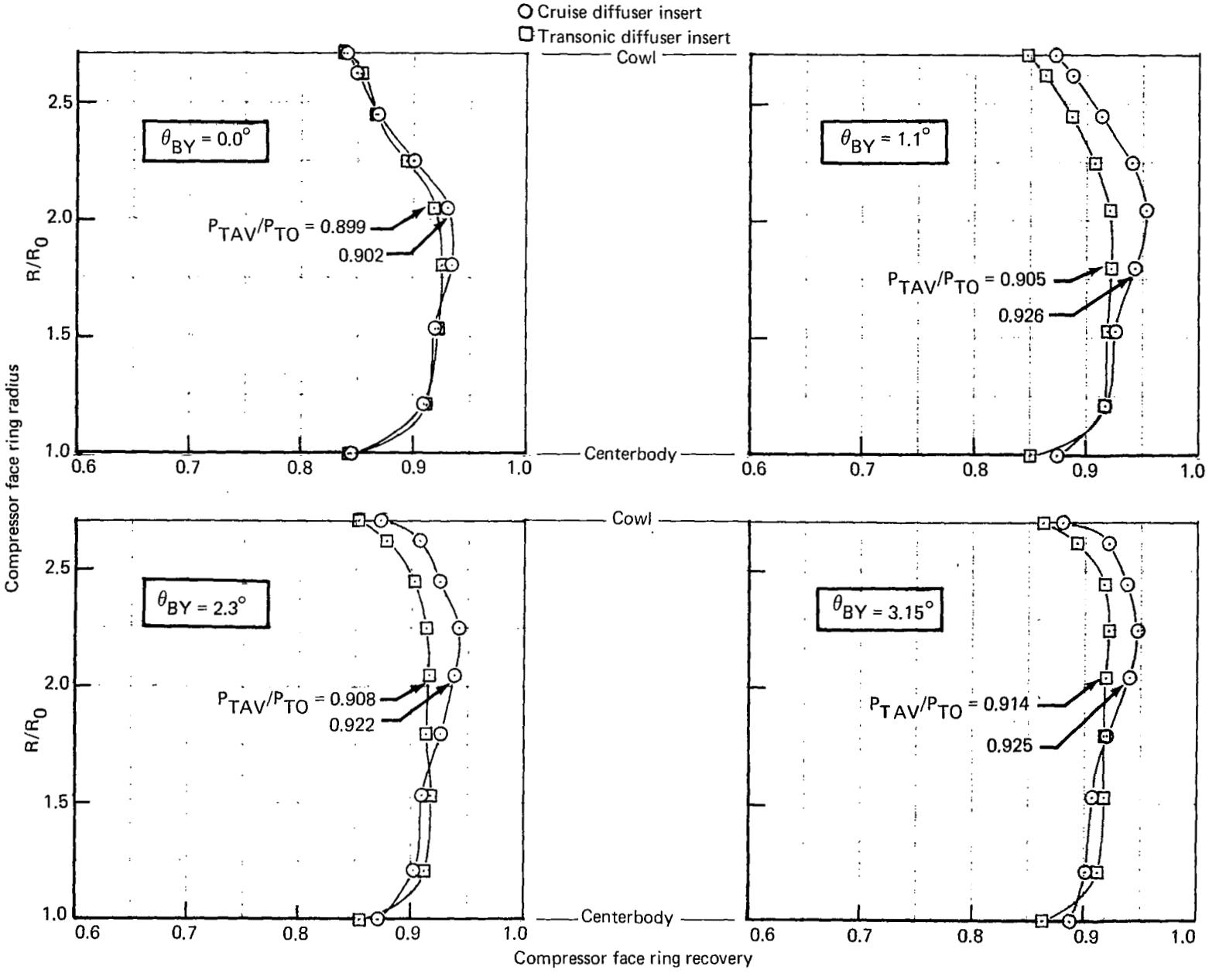

Figure 41.—Diffuser Insert Evaluation, Compressor Face Profiles Near the Operating Point

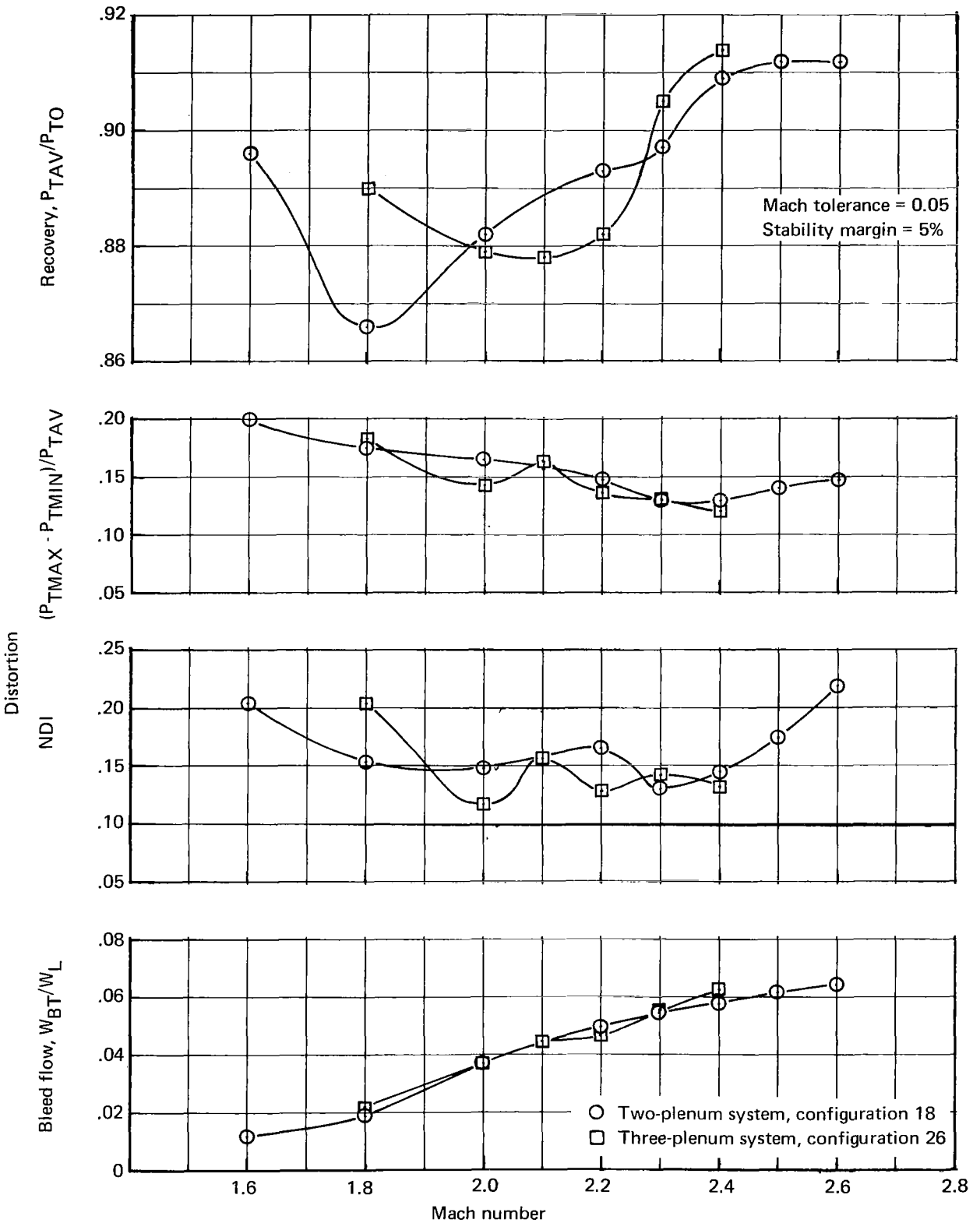

Figure 42.— Off-Design Started Intake Performance at Operating Point

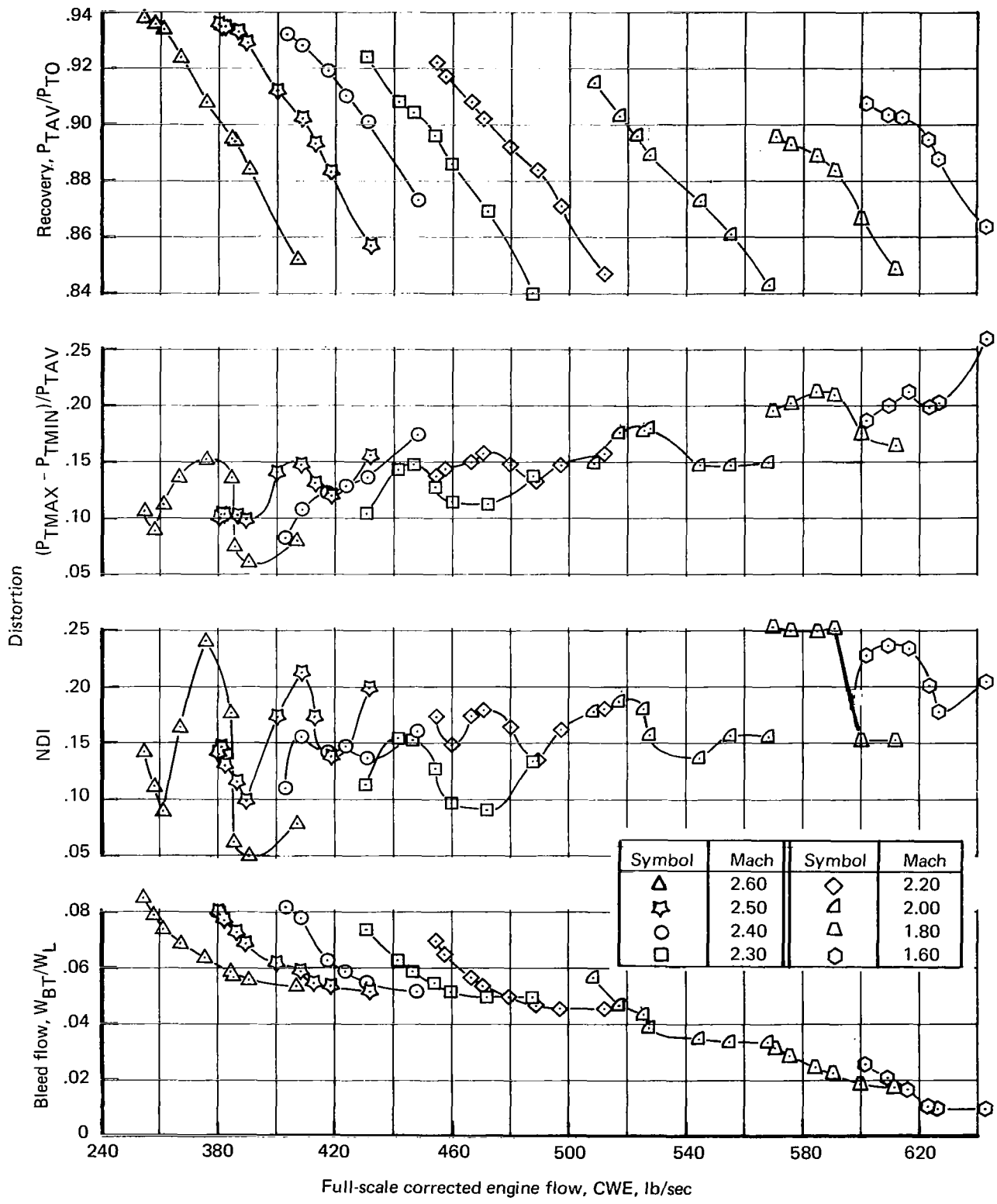

Figure 43.—Off-Design Intake Performance, Configuration 18

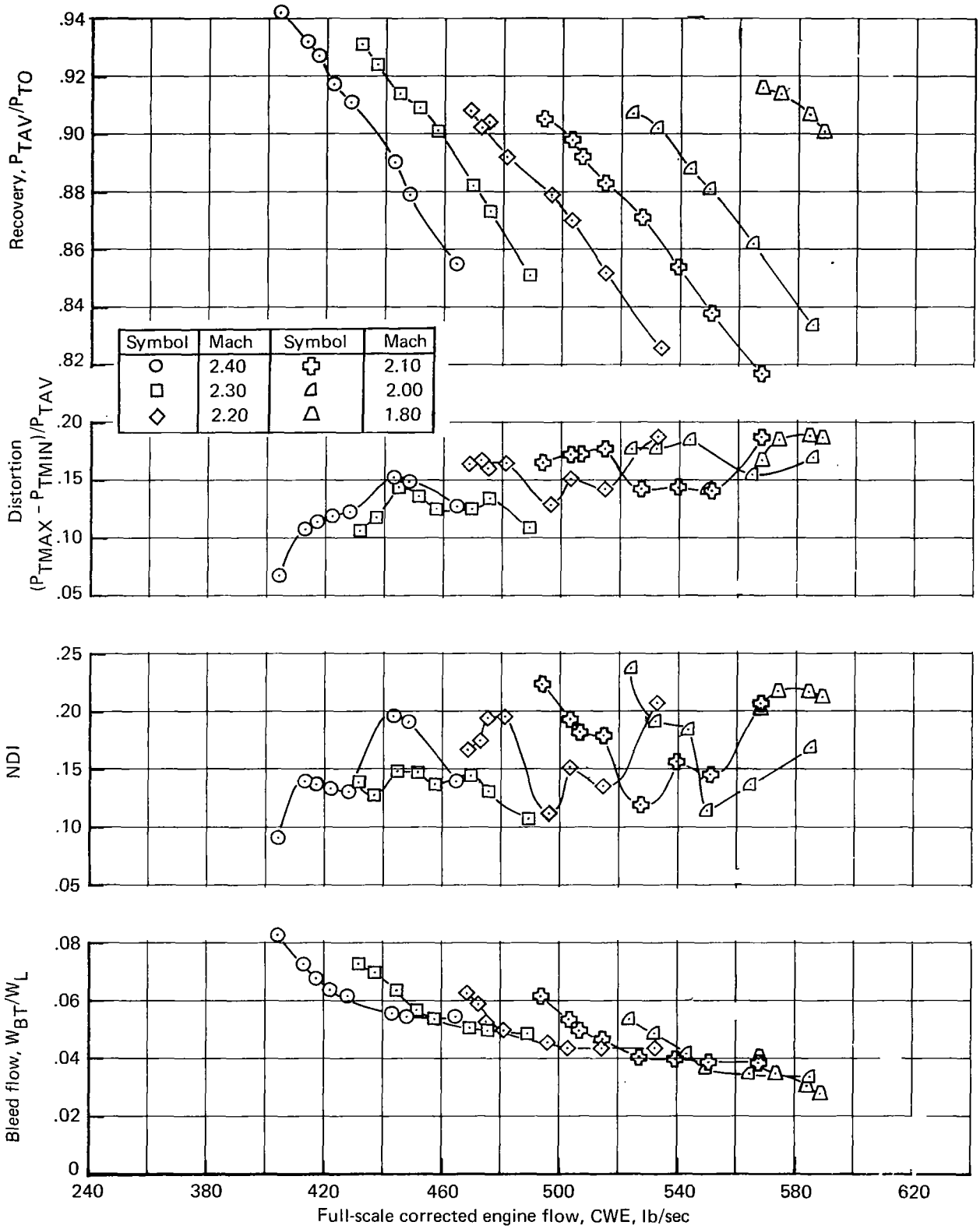

Figure 44.— Off-Design Intake Performance, Configuration 26

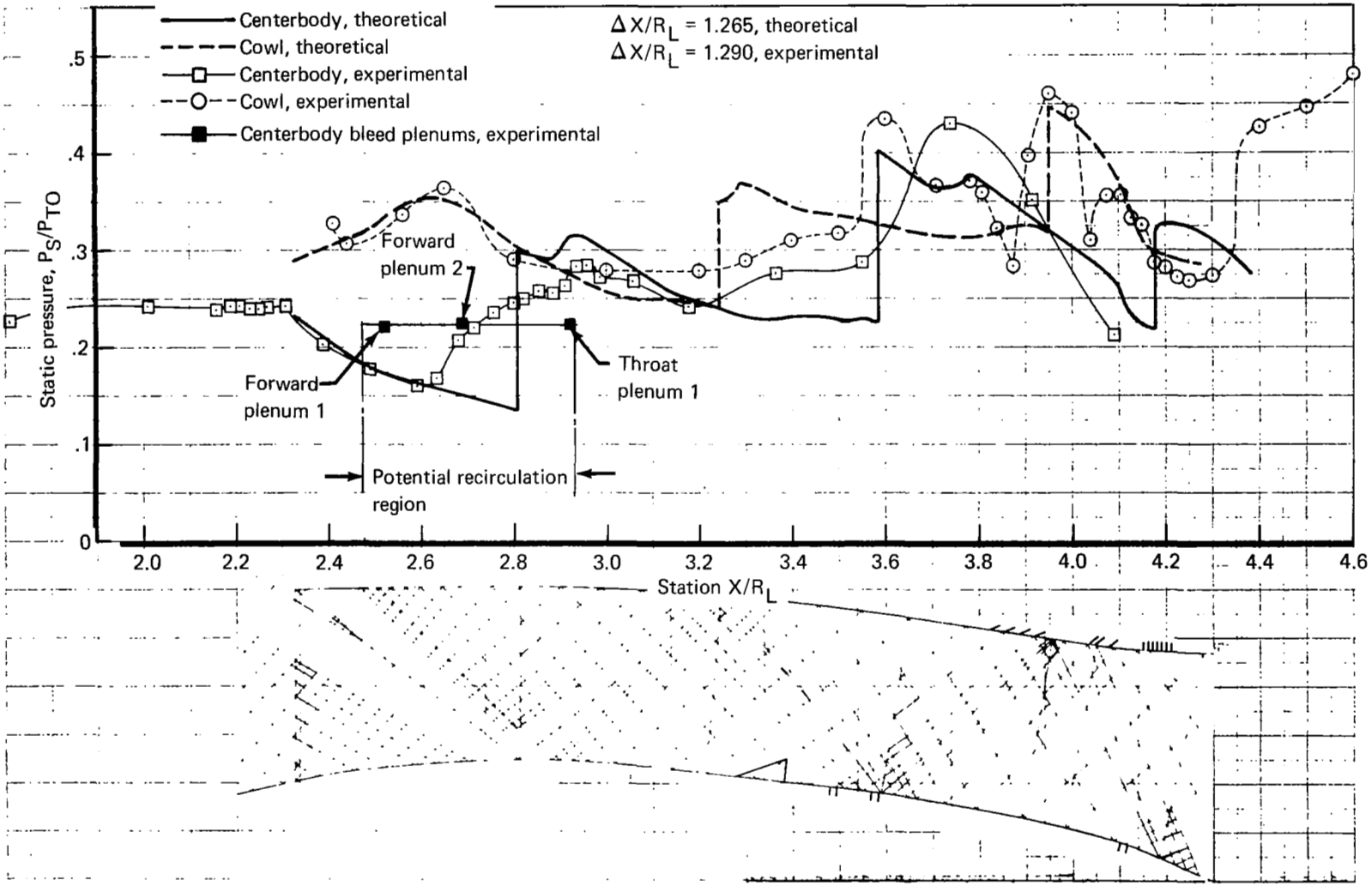

Figure 45.—Supersonic Diffuser Profile—Mach 1.80, Configuration 18

Figure 46.—Supersonic Diffuser Profile—Mach 1.80, Configuration 26

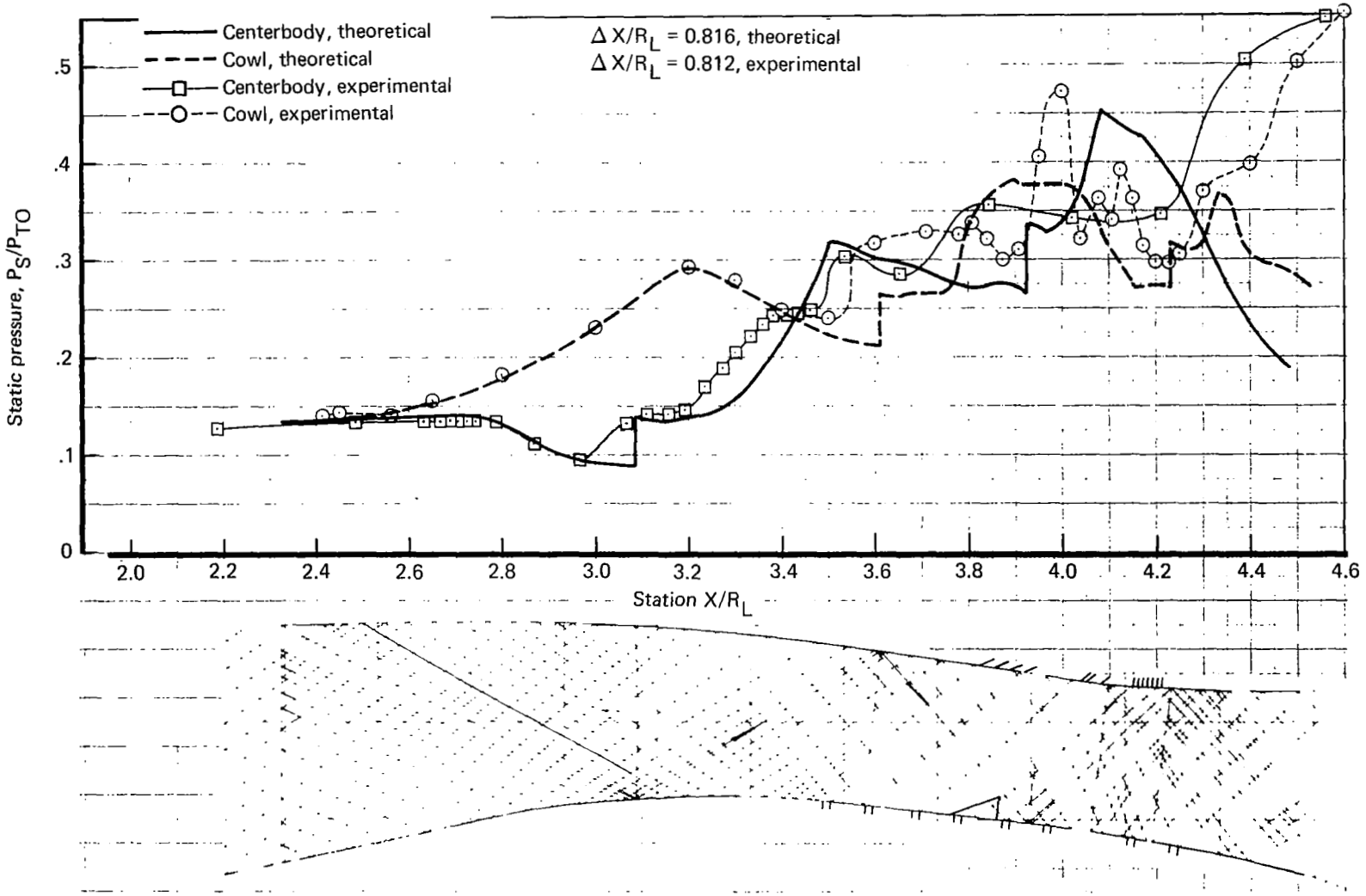

Figure 47.—Supersonic Diffuser Profile—Mach 2.20, Configuration 18

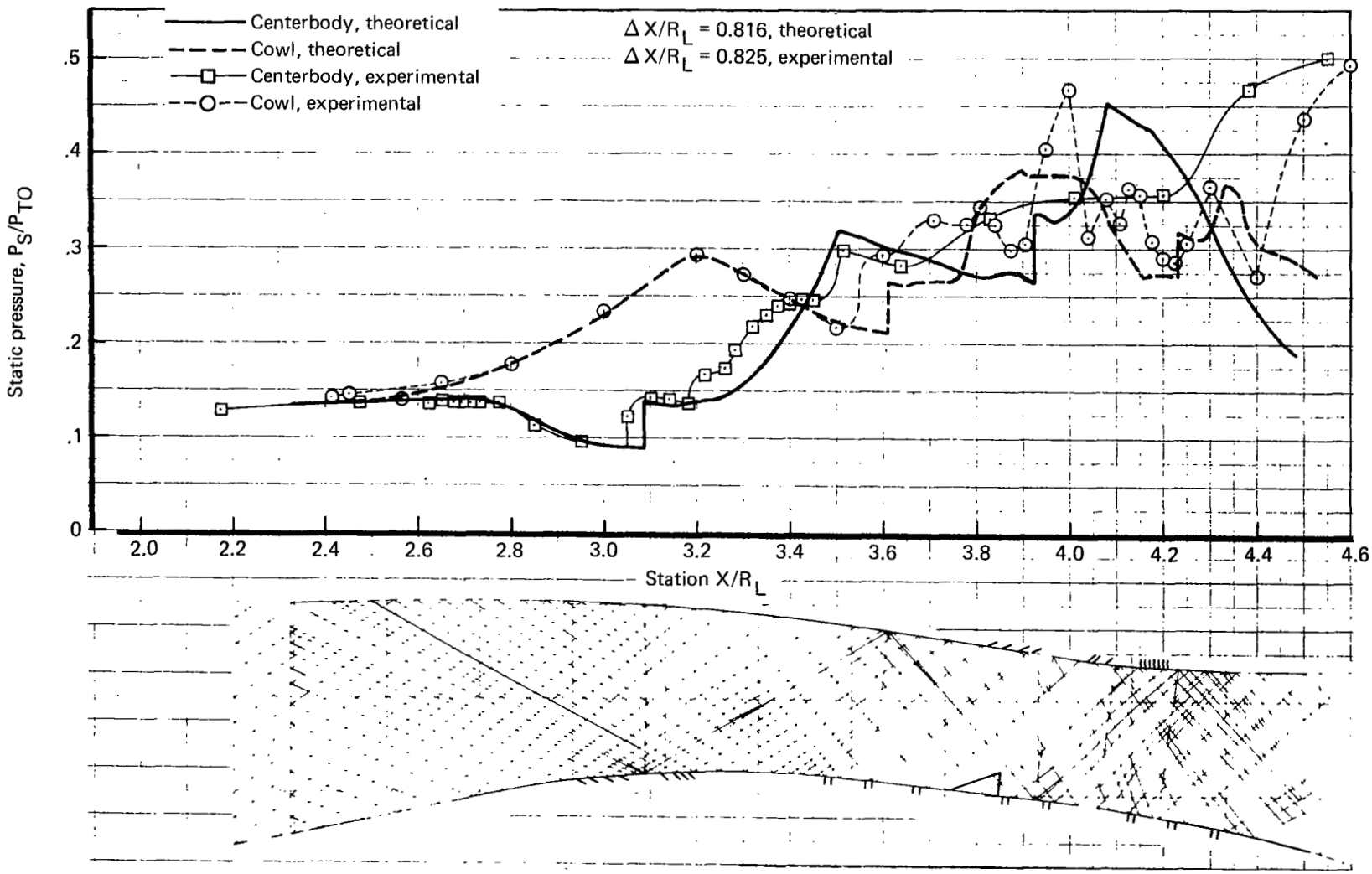

Figure 48.—Supersonic Diffuser Profile—Mach 2.20, Configuration 26

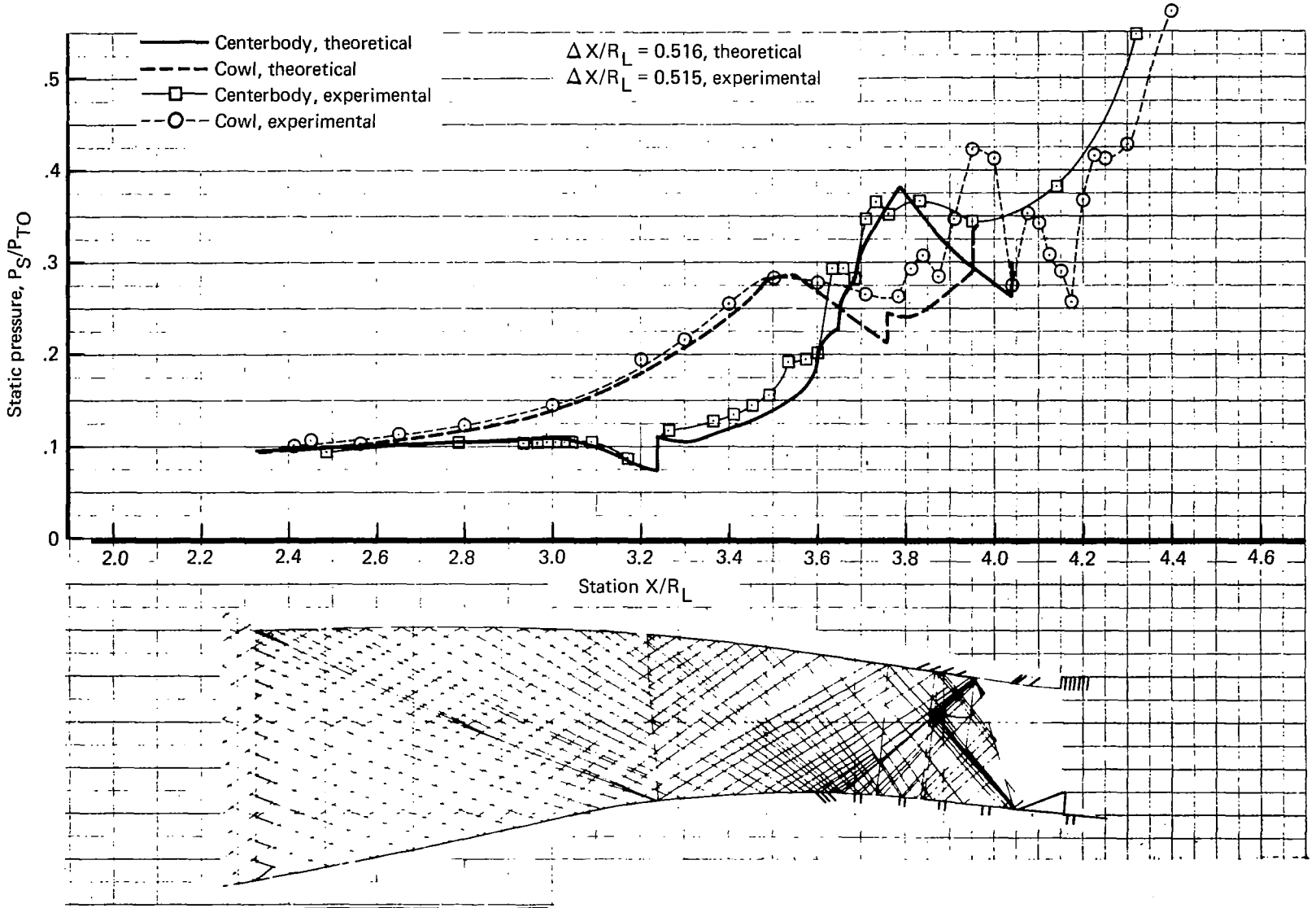

Figure 49.—Supersonic Diffuser Profile—Mach 2.40, Configuration 18

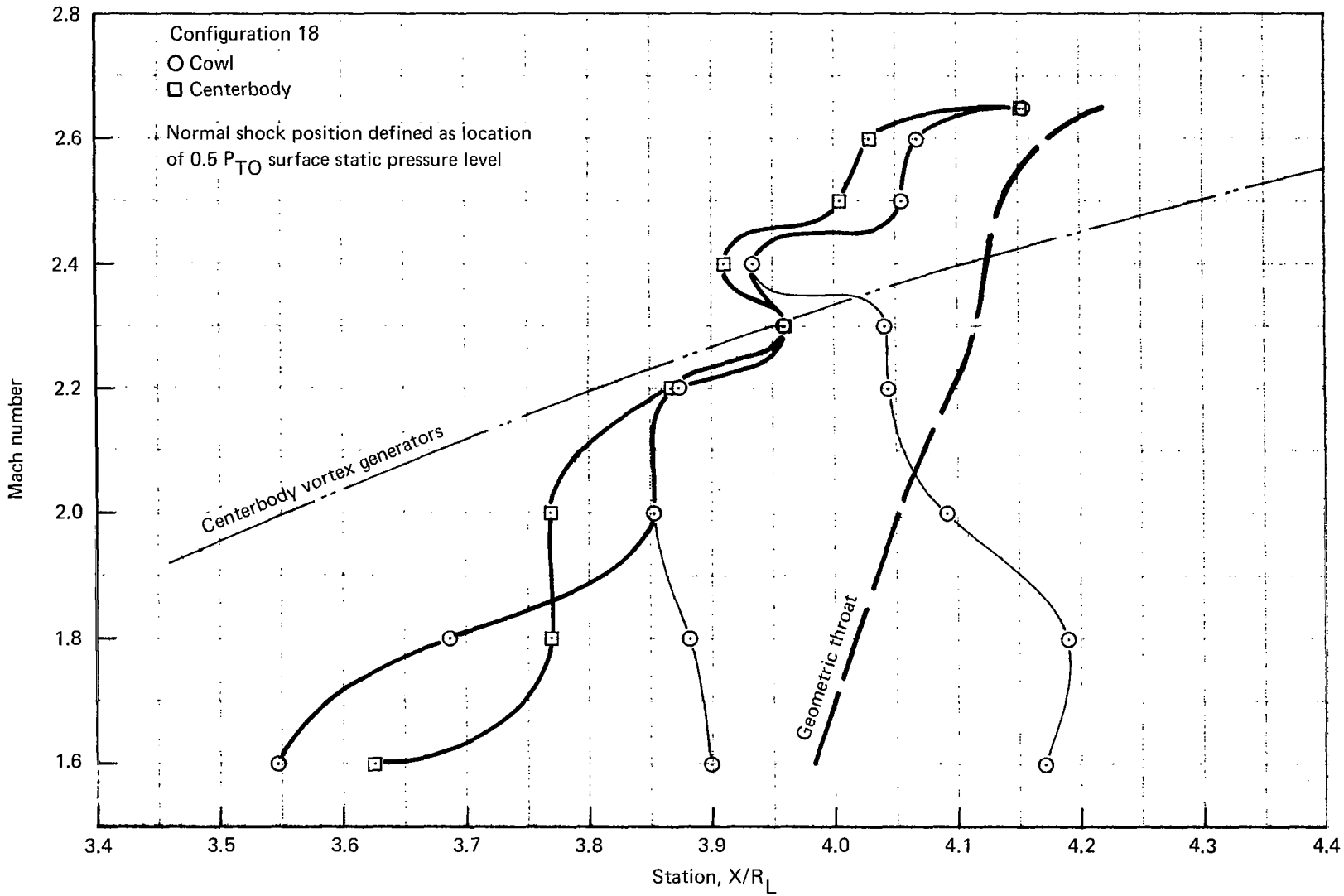

Figure 50.—Critical Normal Shock Positions

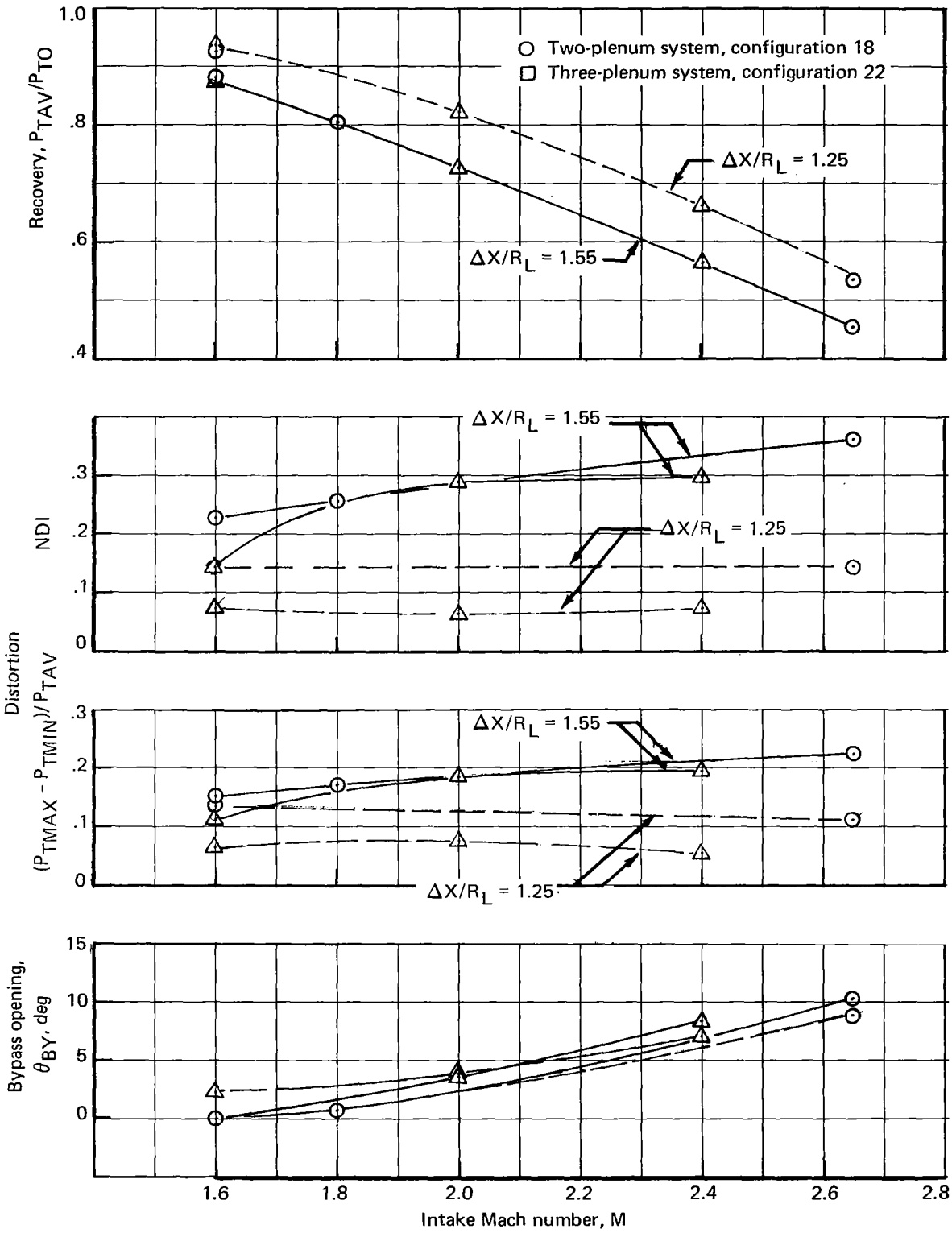

Figure 51.—Buzz Suppression Performance With Climb-Corrected Engine Flow

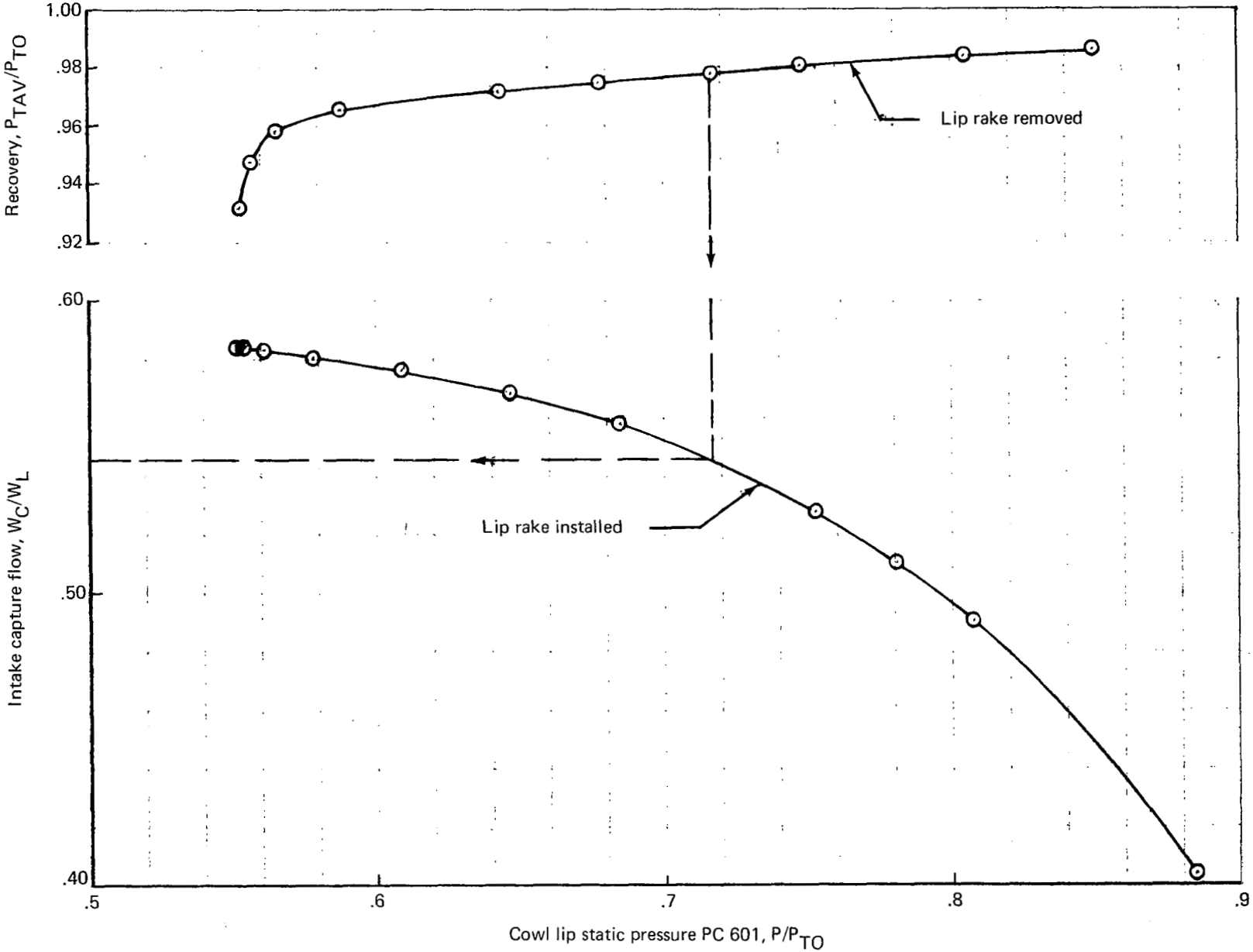

Figure 52.—Intake Capture Calibration, Mach 0.95 $\beta = 0°$, $\Delta X/R_L = 1.55$

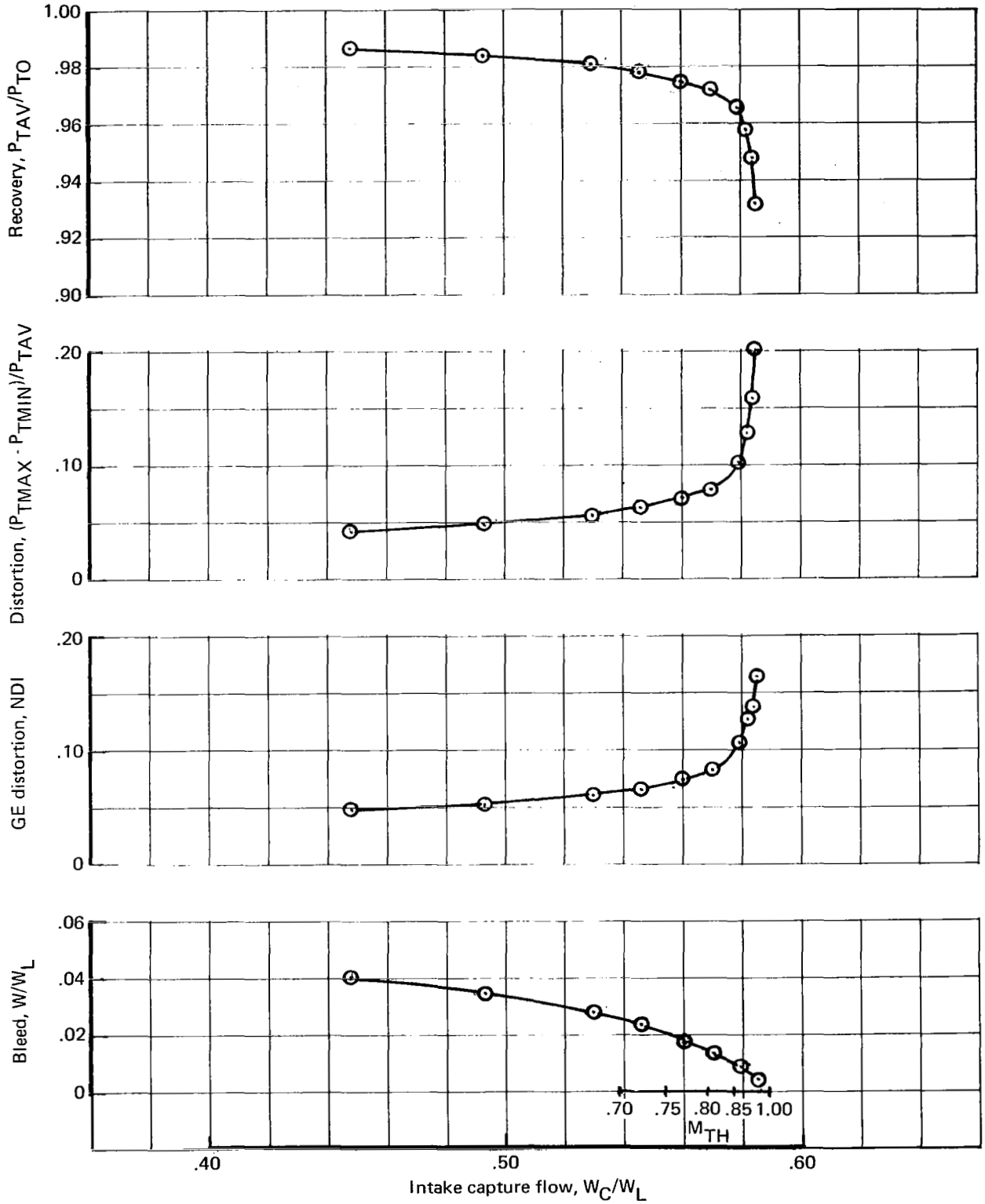

Figure 53.—Intake Performance, Mach 0.95, $\beta = 0°$, $\Delta X/R_L = 1.55$

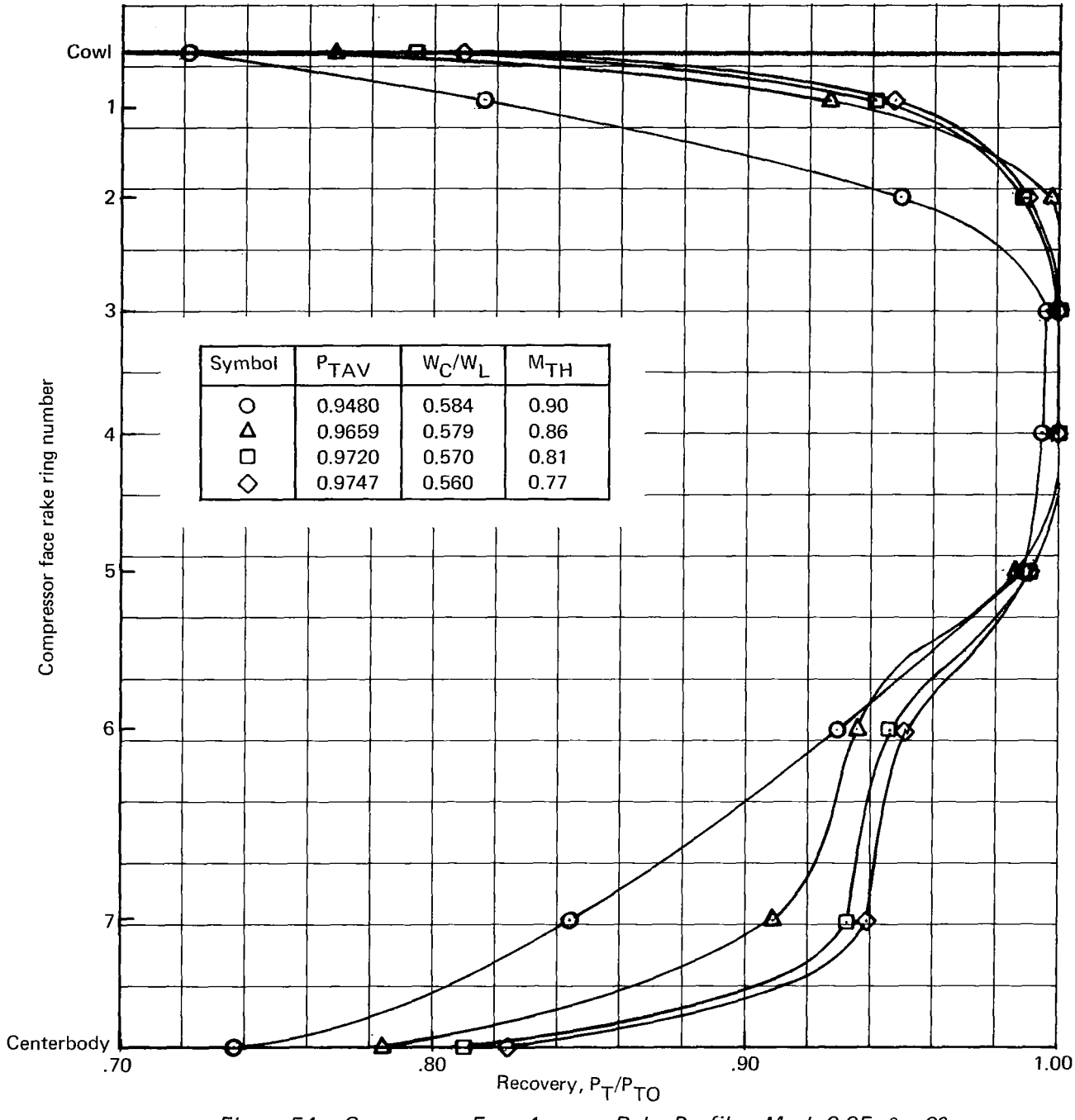

Figure 54.—Compressor Face Average Rake Profiles, Mach 0.95, $\beta = 0°$

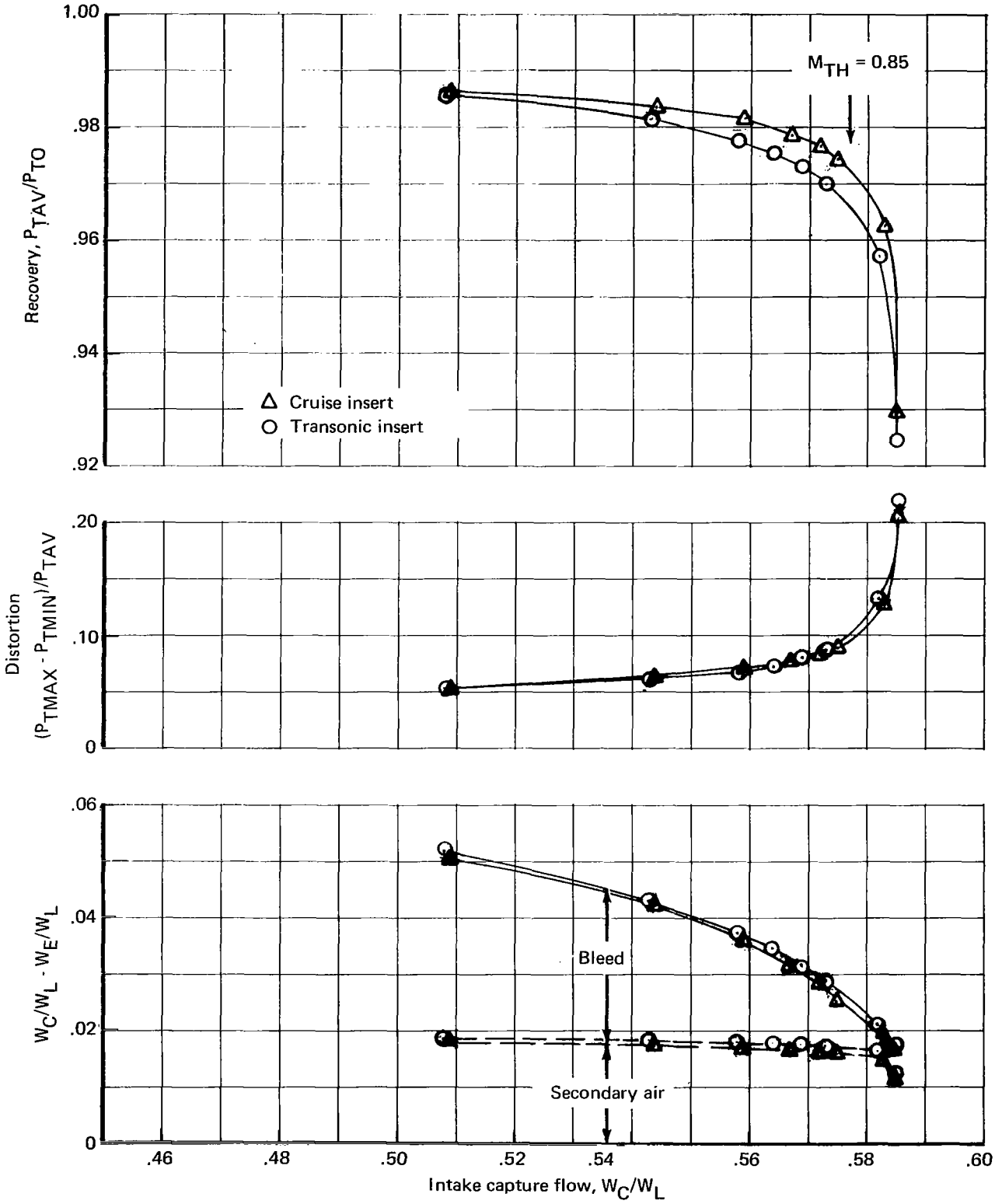

Figure 55.—Effect of Diffuser Insert, Mach 0.95, $\beta = 0°$, $\Delta X/R_L = 1.55$

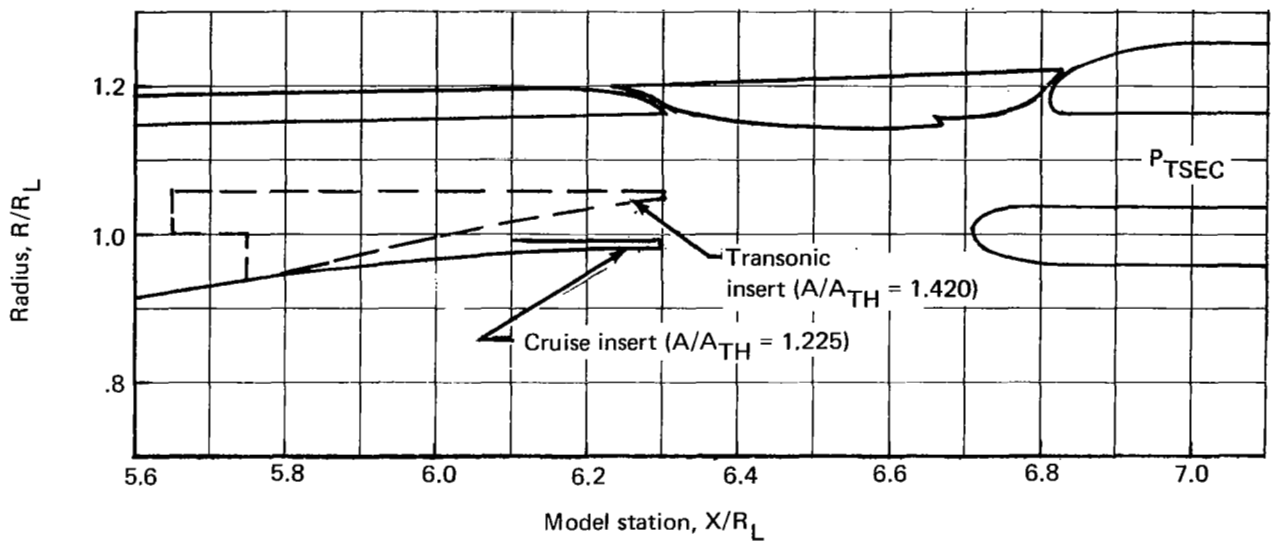

● ▲ One-dimensional, theoretical static pressure at diffuser trailing edge

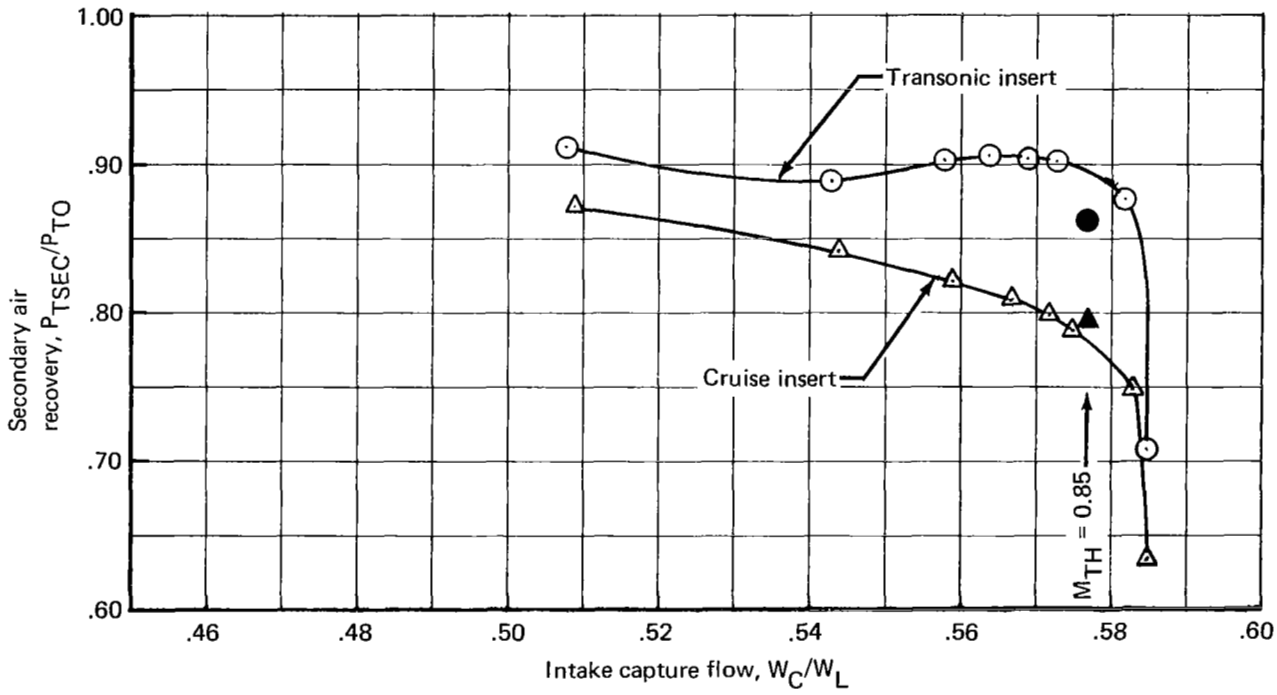

Figure 56.–Effect of Diffuser Contour on Secondary Air Recovery, Mach 0.95, $\beta = 0°$, $W_{SEC}/W_L = 0.017$

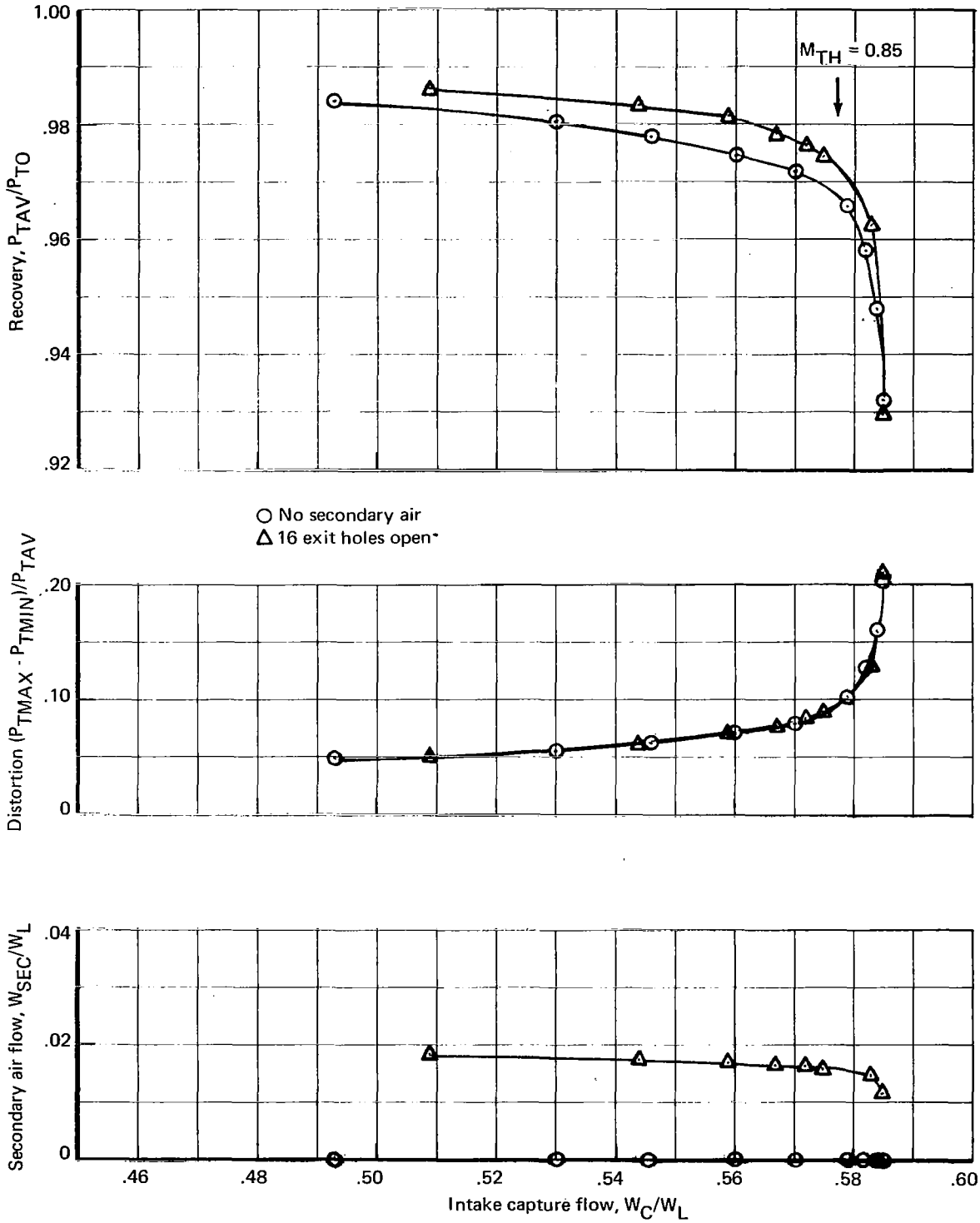

Figure 57.—Effect of Secondary Air on Intake Performance, Mach 0.95, $\beta = 0°$, $\Delta X/R_L = 1.55$, Cruise Insert

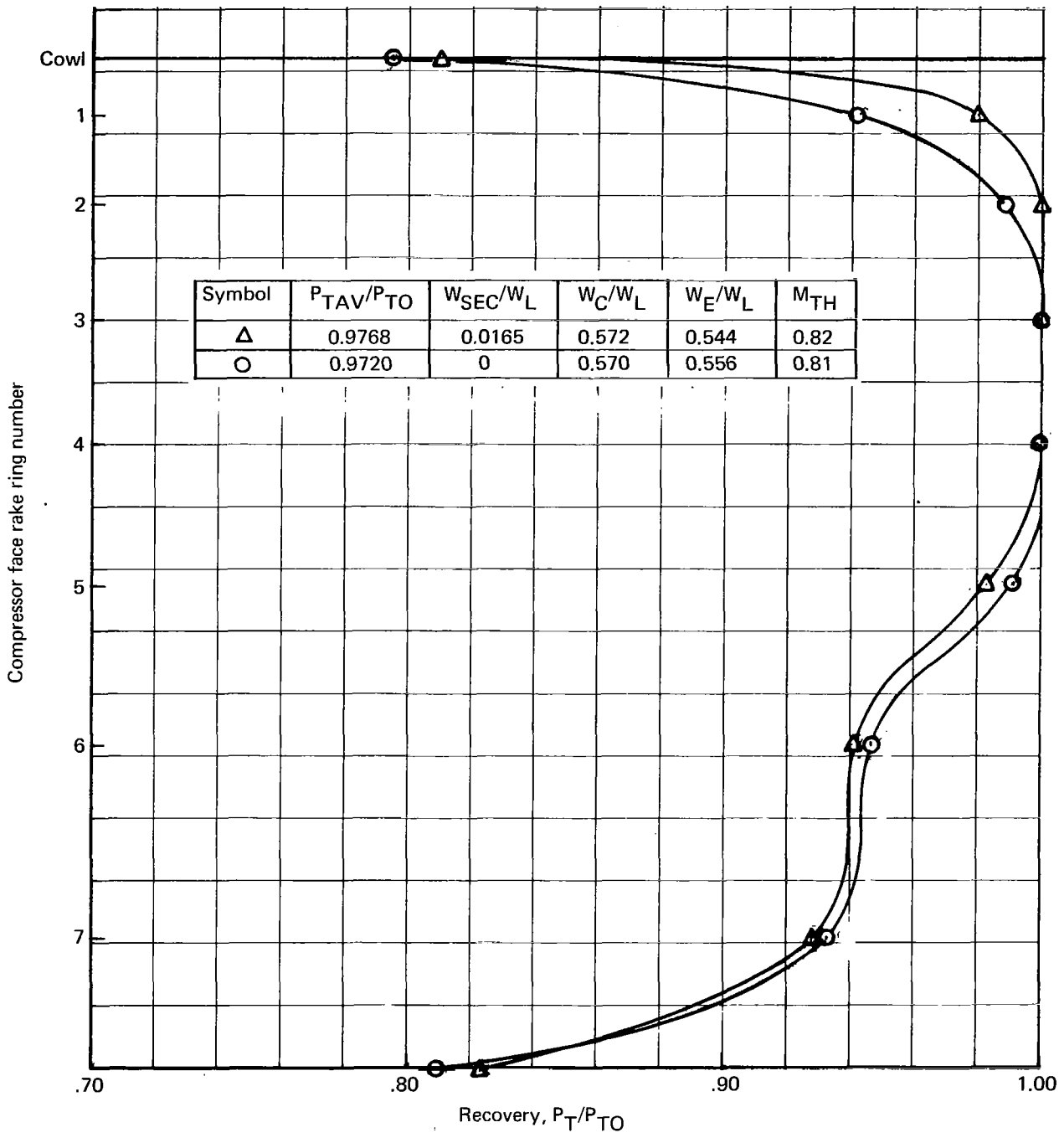

Figure 58.—Effect of Secondary Air on Compressor Face Rake Profiles, Mach 0.95, $\beta = 0°$, $\Delta X/R_L = 1.55$, Cruise Insert

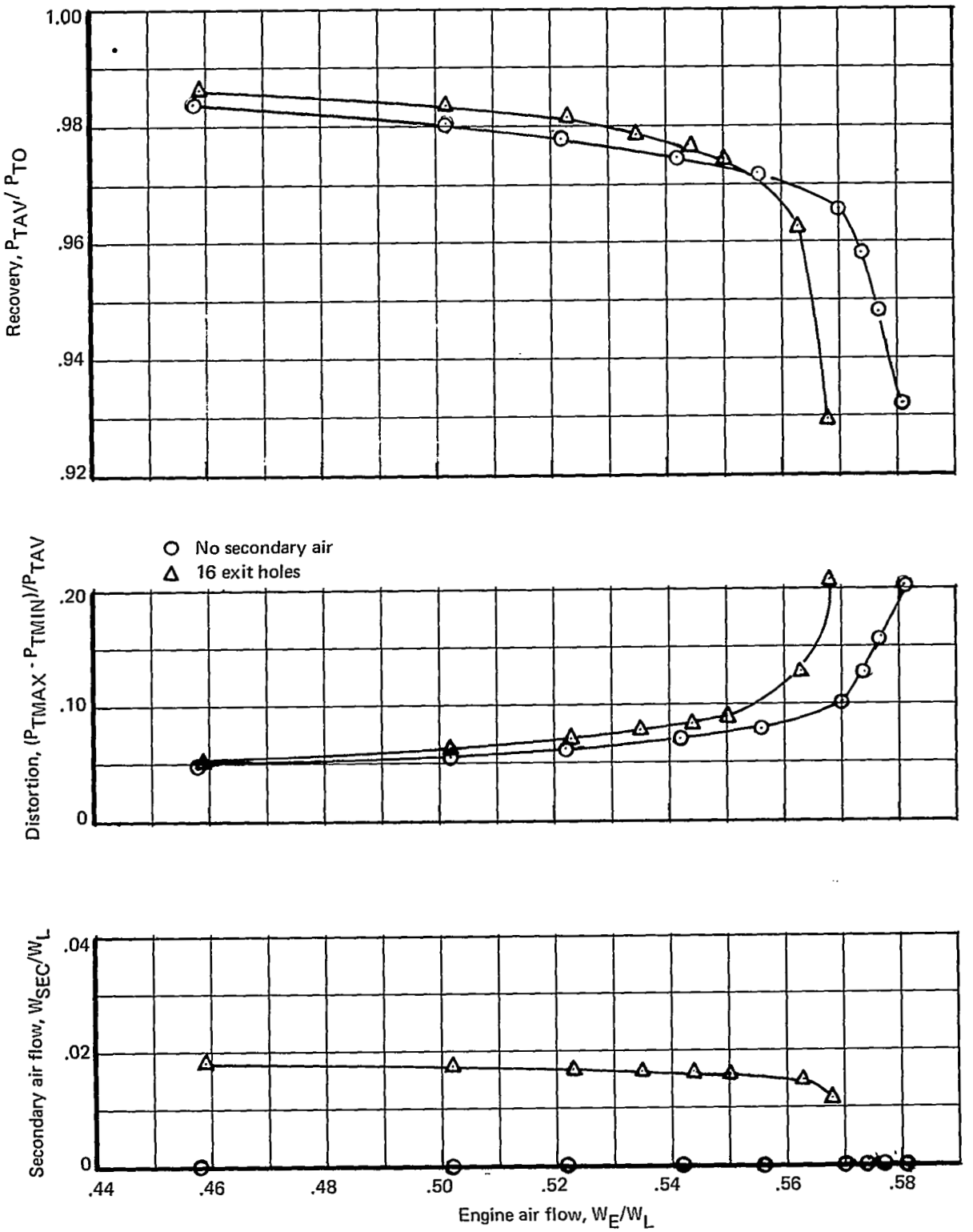

Figure 59.—Intake Performance Vs Engine Air Flow, Mach 0.95, $\beta = 0°, \Delta X/R_L = 1.55$, Cruise Insert

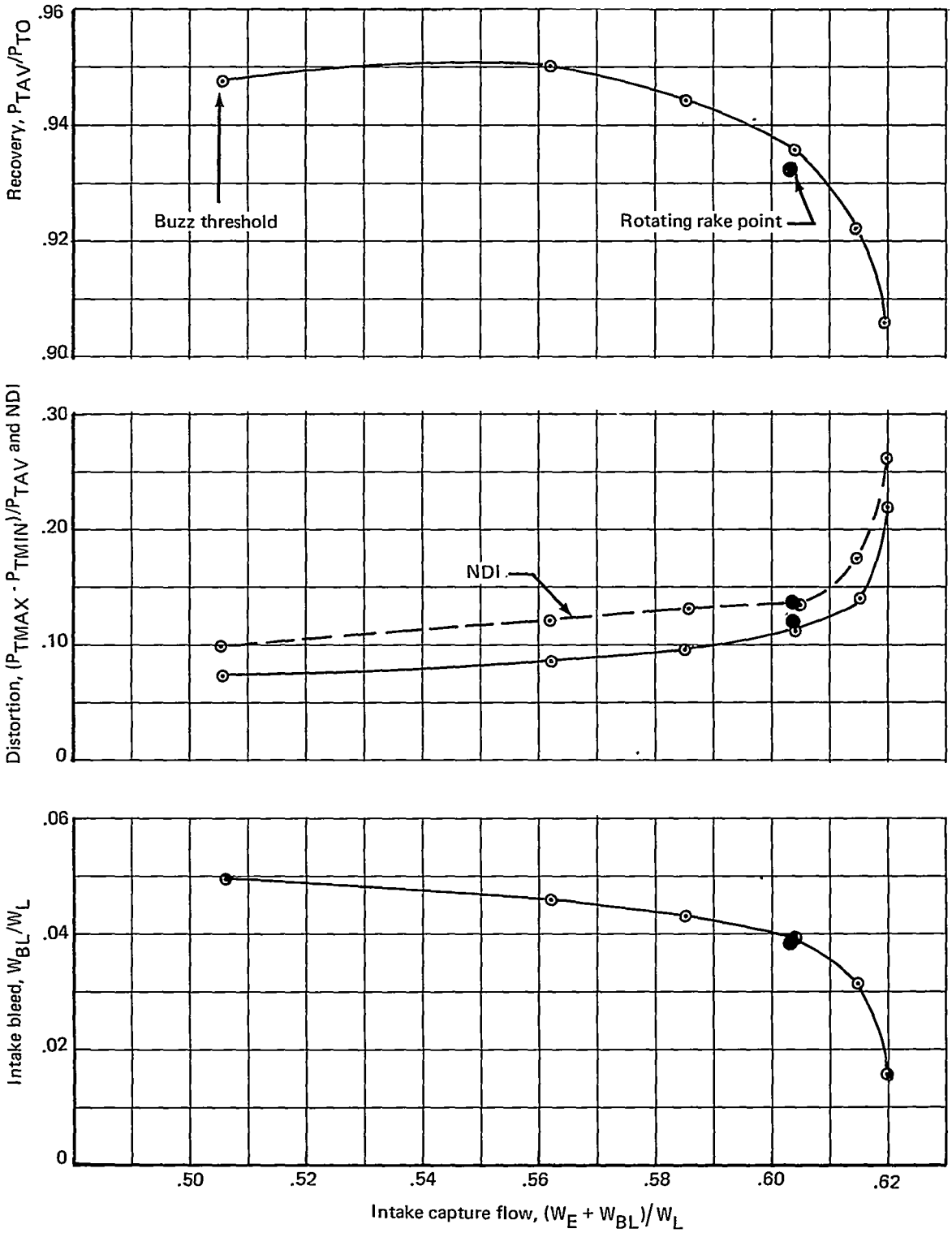

Figure 60.— Intake Performance, Mach 1.40, $\beta = 0°$, $\Delta X/R_L = 1.55$

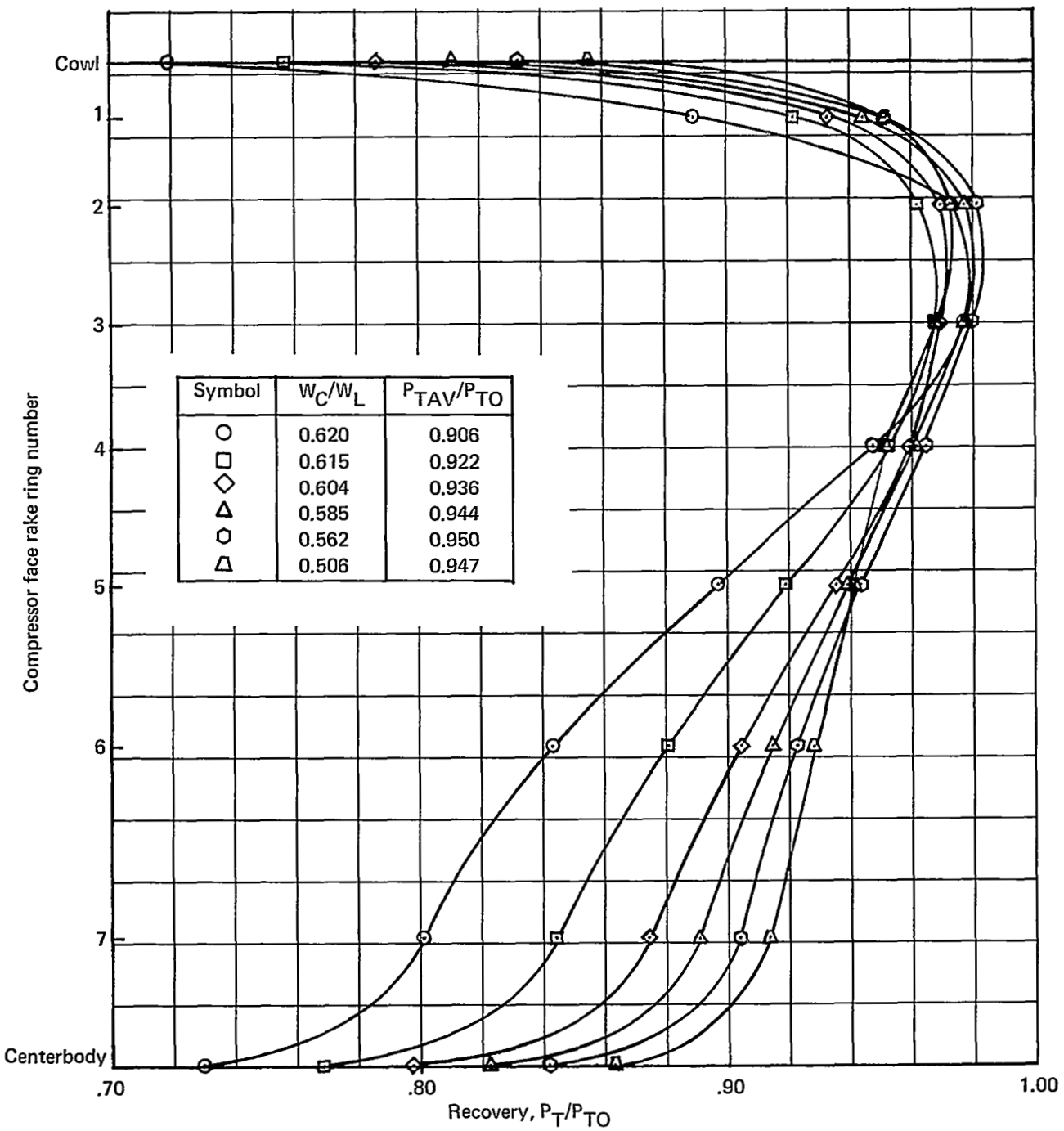

Figure 61.—Compressor Face Average Rake Profiles, Mach 1.40, $\beta = 0°$, $\Delta X/R_L = 1.55$

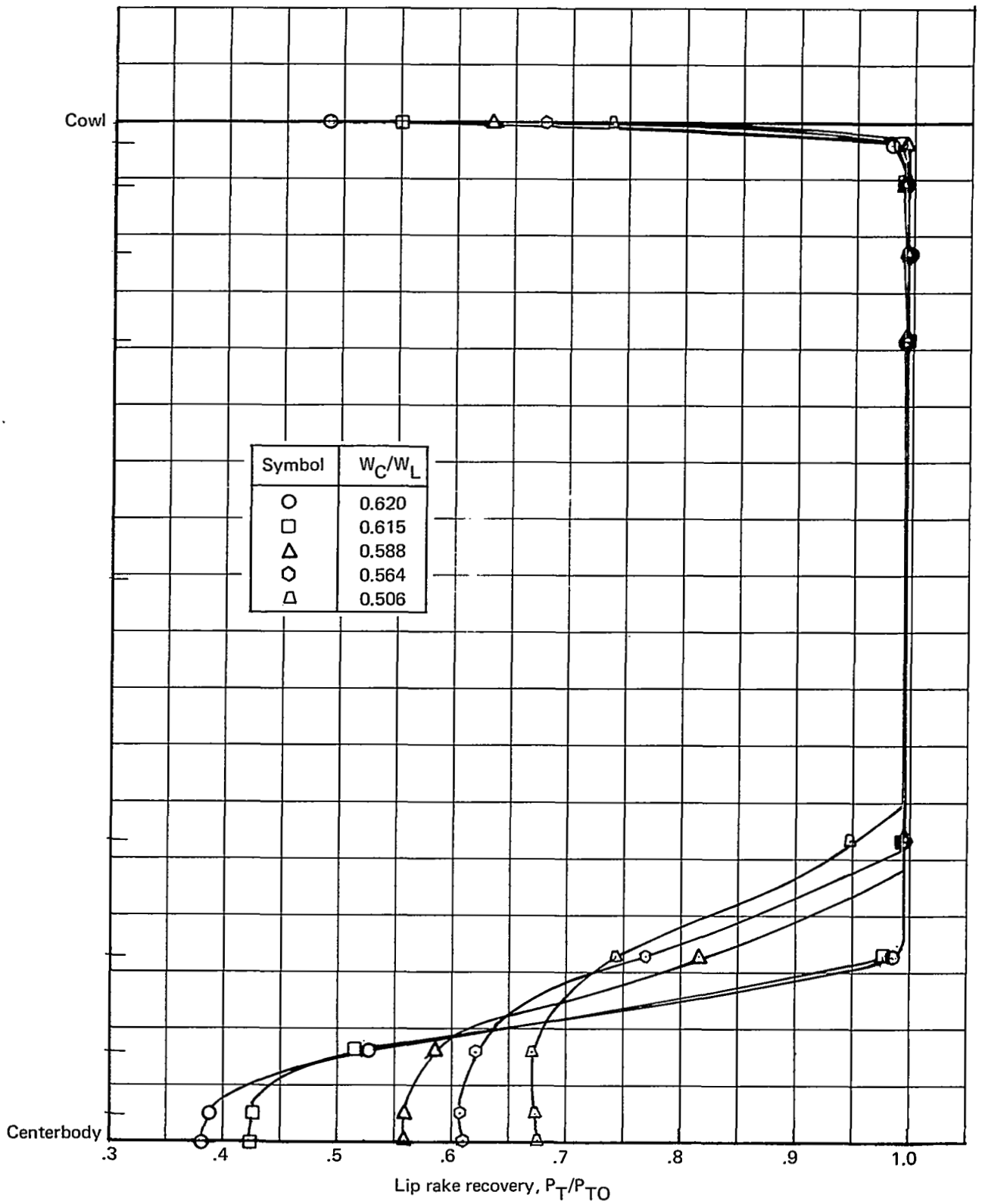

Figure 62.– Lip Rake Profiles, Station X/R_L = 2.565, Mach 1.40

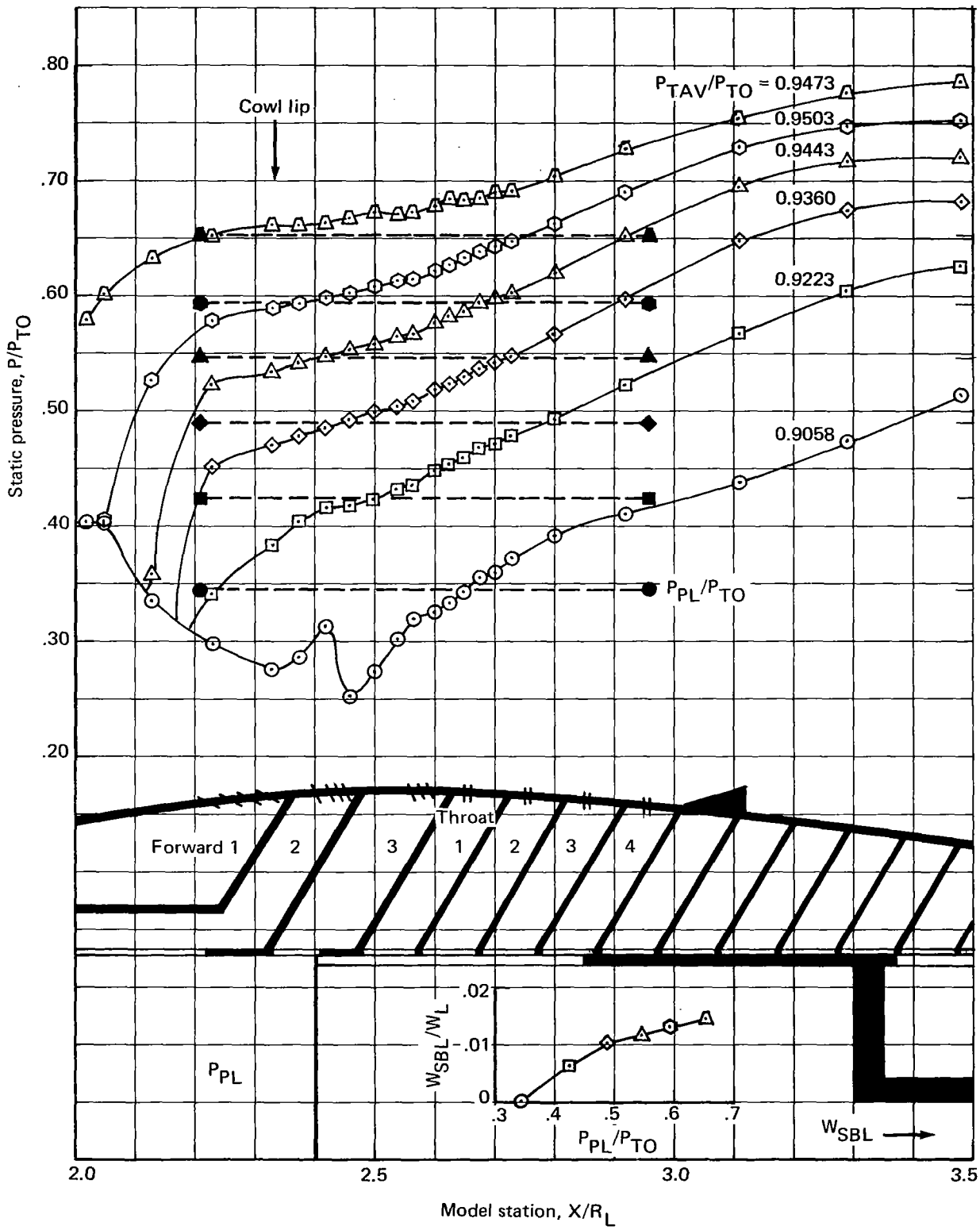

Figure 63.— Centerbody Static Pressure Profiles, Mach 1.40, $\beta = 0°$, $\Delta X/R_L = 1.55$

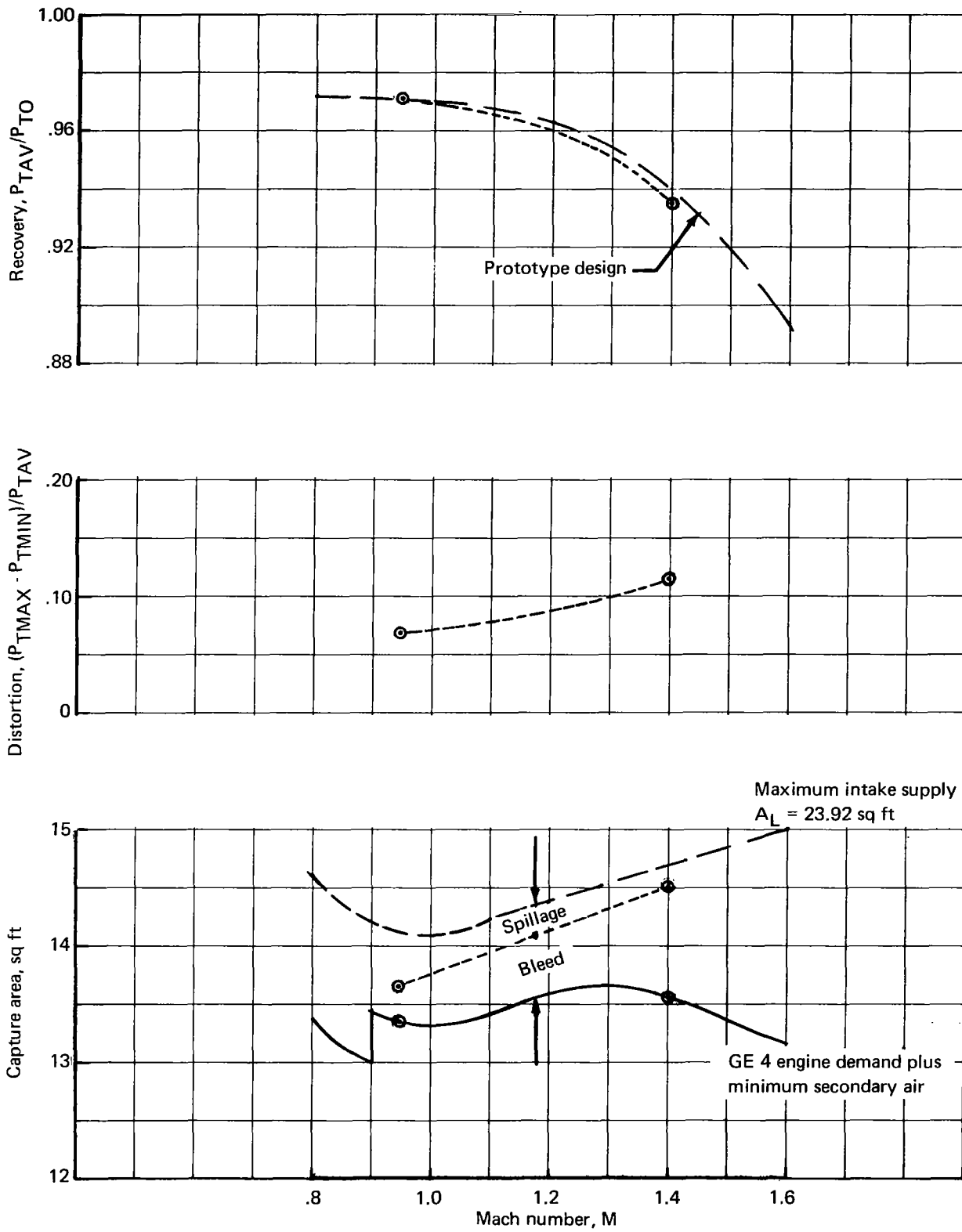

Figure 64.—Intake/GE4 Engine Matching, Standard Day, SST Prototype Design Recovery